



Test of CP invariance in vector-boson fusion production of the Higgs boson in the $H \rightarrow \tau\tau$ channel in proton–proton collisions at $\sqrt{s} = 13$ TeV with the ATLAS detector

The ATLAS Collaboration ^{*}

ARTICLE INFO

Article history:

Received 14 February 2020
 Received in revised form 26 March 2020
 Accepted 9 April 2020
 Available online 16 April 2020
 Editor: M. Doser

ABSTRACT

A test of CP invariance in Higgs boson production via vector-boson fusion is performed in the $H \rightarrow \tau\tau$ decay channel. This test uses the Optimal Observable method and is carried out using 36.1 fb^{-1} of $\sqrt{s} = 13$ TeV proton–proton collision data collected by the ATLAS experiment at the LHC. Contributions from CP-violating interactions between the Higgs boson and electroweak gauge bosons are described by an effective field theory, in which the parameter \tilde{d} governs the strength of CP violation. No sign of CP violation is observed in the distributions of the Optimal Observable, and \tilde{d} is constrained to the interval $[-0.090, 0.035]$ at the 68% confidence level (CL), compared to an expected interval of $\tilde{d} \in [-0.035, 0.033]$ based upon the Standard Model prediction. No constraints can be set on \tilde{d} at 95% CL, while an expected 95% CL interval of $\tilde{d} \in [-0.21, 0.15]$ for the Standard Model hypothesis was expected.

© 2020 The Author(s). Published by Elsevier B.V. This is an open access article under the CC BY license (<http://creativecommons.org/licenses/by/4.0/>). Funded by SCOAP³.

Contents

1. Introduction	1
2. Theoretical framework and methodology	2
3. ATLAS detector	3
4. Simulated event samples	4
5. Event selection	4
6. Background estimation	6
7. Systematic uncertainties	8
8. Fitting procedure	8
9. Results	9
10. Conclusion	11
Acknowledgements	11
References	12

1. Introduction

One of the central puzzles in physics today is the observed baryon asymmetry of the universe. The violation of invariance of fundamental interactions under the transformation of charge conjugation (C) and its combination with parity (CP) is one of the three necessary Sakharov conditions [1] to explain the dynamical generation of the baryon asymmetry. In the Standard Model (SM) of particle physics, CP violation (CPV) is introduced via the com-

plex phase in the quark mixing (CKM) matrix [2,3].¹ It is able to describe all observations of CPV in the K -, B -, and D -meson systems [4–15]. However, the measured size of the complex phase and the derived magnitude of CPV in the early universe are insufficient to explain the observed value of the baryon asymmetry within the SM [16–20] and, most probably, new sources of CPV beyond the SM need to be introduced.

¹ Effects of possible CPV in the neutrino sector and in the strong interaction are not considered in this statement.

^{*} E-mail address: atlas.publications@cern.ch.

The investigation of Higgs boson production and decay at the LHC offers a novel opportunity to search for new sources of CPV in the interaction of the Higgs boson with other SM particles. No observable effect of CPV is expected in the production or decay of the SM Higgs boson. Hence any observation of CP violation involving the observed Higgs boson [21,22] would be an unequivocal sign of physics beyond the SM.

The measured Higgs boson production cross sections, branching ratios, and derived constraints on coupling-strength modifiers, assuming the tensor structure of the SM, agree with the SM predictions within the current precision [23–25]. Investigations of spin and CP quantum numbers strongly indicate that the observed particle is of scalar nature and that the dominant coupling structure is CP-even and consistent with the SM expectation [26–28]. Various measurements have been used in the framework of effective field theories to derive limits on Wilson coefficients which multiply CP-even and CP-odd operators and modify the structure and strength of the coupling of the Higgs boson to gluons and electroweak gauge bosons. These include measurements of differential cross sections as functions of CP-even observables in the decay $H \rightarrow \gamma\gamma$ [29], measurements of event rates in specific event categories and phase-space regions in the decay $H \rightarrow ZZ^*$ [30], and measurements of the VH invariant mass in Higgs boson production in association with a weak gauge boson V ($V = W^\pm, Z$) [31]. These analyses use CP-even observables and event rate information and hence are not directly sensitive to possible interference between the CP-even SM operators and new CP-odd operators. The shapes of distributions of CP-odd and CP-even observables (without exploiting CP-even rate information) have been used to set limits on CP-odd and CP-even couplings of the Higgs boson to gauge bosons. This is done by investigating the decay $H \rightarrow VV^*$ ($V = W^\pm, Z$), using only information from the decay [27,32] and combining it with information from vector-boson fusion (VBF) or associated VH production [33,34]. Another analysis using the decay $H \rightarrow \tau\tau$ exploits information from VBF and VH production [35]. The shape of the distribution of a single CP-odd observable constructed from kinematic information in VBF production in $H \rightarrow \tau\tau$ candidate events has been previously used to set a limit on the parameter \tilde{d} [36], which governs the strength of CPV in an effective field theory ansatz as described in Section 2. This analysis constrained \tilde{d} to the interval $[-0.11, 0.05]$ at the 68% confidence level (CL) using ATLAS data collected at $\sqrt{s} = 8$ TeV in 2012, while a 68% CL interval of $\tilde{d} \in [-0.16, 0.16]$ was expected. No hints of CPV have been observed in these studies.

In this Letter, a direct test of CP invariance in Higgs boson production via VBF is presented in the $H \rightarrow \tau\tau$ channel, based on proton–proton collision data corresponding to an integrated luminosity of 36.1 fb^{-1} collected with the ATLAS detector at $\sqrt{s} = 13$ TeV in the years 2015 and 2016. A CP-odd Optimal Observable [37–39] is employed. The Optimal Observable combines the information from the multidimensional phase space in a single quantity calculated from leading-order matrix elements for VBF production, independent of the decay mode of the Higgs boson. VBF production provides a promising physics process to test CP invariance in the HVV vertex [40]. The decay mode $H \rightarrow \tau\tau$ allows the selection of signal events with a good signal-to-background ratio and the reconstruction of the four-momentum of the Higgs boson candidate with adequate precision.

In the present work a direct test of CP invariance is obtained through a measurement of the mean value of the CP-odd Optimal Observable, neglecting possible effects from rescattering by new light particles in loops [40]. A measurement of the parameter \tilde{d} is also performed. Limits on \tilde{d} are derived by analysing the shapes of distributions of the Optimal Observable measured in $H \rightarrow \tau\tau$ candidate events with two jets in the final state consistent with VBF production. The event selection, estimation of background contri-

butions, and systematic uncertainties closely follow the analysis employed for the observation of the $H \rightarrow \tau\tau$ decay [41]. In order to increase the signal-to-background ratio, the final event selection utilizes multivariate discriminants.

2. Theoretical framework and methodology

The effective Lagrangian \mathcal{L}_{eff} considered is the SM Lagrangian augmented with CP-odd operators of mass dimension six, involving the Higgs field and electroweak gauge fields. No CP-even dimension-six operators built from these fields are taken into account. All interactions between the Higgs boson and other SM particles (fermions and gluons) are assumed to be as predicted in the SM, i.e. the coupling structure in gluon–gluon fusion production and in the decay into a pair of τ -leptons is considered to be the same as in the SM. The theoretical ansatz considered and the methodology is the same as in Ref. [36], which contains further details. After electroweak symmetry breaking, the Lagrangian can be written in the mass basis of the Higgs boson H , photon A and weak gauge bosons W^\pm and Z as in Ref. [42]:

$$\mathcal{L}_{\text{eff}} = \mathcal{L}_{\text{SM}} + \tilde{g}_{HAA} H \tilde{A}_{\mu\nu} A^{\mu\nu} + \tilde{g}_{HAZ} H \tilde{A}_{\mu\nu} Z^{\mu\nu} + \tilde{g}_{HZZ} H \tilde{Z}_{\mu\nu} Z^{\mu\nu} + \tilde{g}_{HWW} H \tilde{W}_{\mu\nu}^+ W^{-\mu\nu},$$

where $V^{\mu\nu}$ and $\tilde{V}^{\mu\nu} = \epsilon^{\mu\nu\rho\sigma} V_{\rho\sigma}$ (with $V = W^\pm, Z, A$) denote the field strength and dual field strength tensors, respectively. Only two of the four couplings $\tilde{g}_{HVV'}$ are independent due to constraints imposed by $U(1)_Y$ and $SU(2)_{I_W, L}$ invariance. They can be expressed in terms of two dimensionless couplings \tilde{d} and \tilde{d}_B as in Refs. [43,44]:

$$\tilde{g}_{HAA} = \frac{g}{2m_W} (\tilde{d} \sin^2 \theta_W + \tilde{d}_B \cos^2 \theta_W)$$

$$\tilde{g}_{HAZ} = \frac{g}{2m_W} \sin 2\theta_W (\tilde{d} - \tilde{d}_B)$$

$$\tilde{g}_{HZZ} = \frac{g}{2m_W} (\tilde{d} \cos^2 \theta_W + \tilde{d}_B \sin^2 \theta_W)$$

$$\tilde{g}_{HWW} = \frac{g}{m_W} \tilde{d},$$

where g is the $SU(2)$ coupling constant and θ_W is the weak mixing angle. Adopting the arbitrary choice $\tilde{d} = \tilde{d}_B$ yields the following relations²:

$$\tilde{g}_{HAA} = \tilde{g}_{HZZ} = \frac{1}{2} \tilde{g}_{HWW} = \frac{g}{2m_W} \tilde{d} \quad \text{and} \quad \tilde{g}_{HAZ} = 0.$$

In an effective field theory (EFT), the coupling parameters are real valued. However, rescattering effects from new particles in loops, with masses lower than the scale of new physics assumed in the EFT, may introduce an imaginary part [40]. Such effects are not considered in the analysis presented here, as \tilde{d} is assumed to be real valued.

The strength of CP violation in VBF Higgs boson production is then described by a single parameter \tilde{d} . The corresponding matrix element \mathcal{M} for VBF production is the sum of a CP-even contribution \mathcal{M}_{SM} from the SM and a CP-odd contribution $\mathcal{M}_{\text{CP-odd}}$ from the dimension-six operators considered:

$$\mathcal{M} = \mathcal{M}_{\text{SM}} + \tilde{d} \cdot \mathcal{M}_{\text{CP-odd}},$$

where the dependence on \tilde{d} has explicitly been factored out. The squared matrix element has three contributions:

² The parameter \tilde{d} is related to the parameter $\hat{\kappa}_W = (\tilde{\kappa}_W/\kappa_{\text{SM}}) \tan \alpha$ used in the investigation of CP properties in the decay $H \rightarrow WW^*$ via $\tilde{d} = -\hat{\kappa}_W = -(\tilde{\kappa}_W/\kappa_{\text{SM}}) \tan \alpha$. The choice $\tilde{d} = \tilde{d}_B$ yields $\hat{\kappa}_W = \hat{\kappa}_Z$ as assumed in the combination of the $H \rightarrow WW^*$ and $H \rightarrow ZZ^*$ decay analyses [27].

$$|\mathcal{M}|^2 = |\mathcal{M}_{\text{SM}}|^2 + \tilde{d} \cdot 2 \operatorname{Re}(\mathcal{M}_{\text{SM}}^* \mathcal{M}_{\text{CP-odd}}) + \tilde{d}^2 \cdot |\mathcal{M}_{\text{CP-odd}}|^2.$$

The first term $|\mathcal{M}_{\text{SM}}|^2$ and third term $\tilde{d}^2 \cdot |\mathcal{M}_{\text{CP-odd}}|^2$ are both CP-even and hence are not a source of CPV. The second term $\tilde{d} \cdot 2 \operatorname{Re}(\mathcal{M}_{\text{SM}}^* \mathcal{M}_{\text{CP-odd}})$ stems from the interference of the two contributions to the matrix element and is CP-odd, representing a possible new source of CPV in the Higgs sector. The interference term integrated over a CP-symmetric part of phase space vanishes and therefore does not contribute to the total cross section and observed event yield after CP-symmetric selection criteria are applied. The third term increases the total cross section by an amount quadratic in \tilde{d} , but this is not exploited in the analysis presented here as the observed rate can also be influenced by additional CP-conserving new physics.

The final state consisting of the reconstructed decay of the Higgs boson and the two tagging jets corresponding to the VBF topology can be characterized by seven phase-space variables, by fixing the mass of the Higgs boson, neglecting jet masses, and exploiting momentum conservation in the plane transverse to the beam line. The concept of the Optimal Observable (\mathcal{O}_{opt}) combines the information from the seven-dimensional phase space into a single observable, which is shown to have the highest sensitivity to small values of the parameter of interest and neglects contributions proportional to \tilde{d}^2 in the matrix element.

The Optimal Observable for the determination of \tilde{d} is given by the ratio of the interference term in the matrix element to the SM contribution:

$$\mathcal{O}_{\text{opt}} = \frac{2 \operatorname{Re}(\mathcal{M}_{\text{SM}}^* \mathcal{M}_{\text{CP-odd}})}{|\mathcal{M}_{\text{SM}}|^2}.$$

In order to make an almost model-independent test of CP invariance, the mean value of the Optimal Observable can be measured. If no CPV is present in the HVV vertex, then the expectation value of the Optimal Observable vanishes: $\langle \mathcal{O}_{\text{opt}} \rangle = 0$, as the Optimal Observable is a CP-odd (and \hat{T} -odd³) variable. Since the initial state of VBF production of the Higgs boson is not CP-symmetric, this argument assumes that effects from rescattering are negligible [40]. Thus an observation of a non-vanishing mean value or an asymmetry in the Optimal Observable distribution would indicate physics beyond the SM, either stemming from CPV, or originating from rescattering effects (i.e. new particles being on the mass shell in loop corrections to the HVV vertex). Example distributions of the Optimal Observable for signal events after the full event selection, as described in Section 5, are shown for various values of \tilde{d} in Fig. 1. In the SM the distribution is symmetric and has a mean value of zero, whereas a non-vanishing value of \tilde{d} causes an asymmetry and a non-vanishing mean value of the Optimal Observable.

The values of the leading-order matrix elements (ME) needed for the calculation of the Optimal Observable are extracted from HAWK [45–47]. The evaluation requires the four-momenta of the Higgs boson and the two tagging jets (jj). The momentum fraction x_1 (x_2) of the initial-state parton from the proton moving in the positive (negative) z -direction (along the beam) can be derived by exploiting energy-momentum conservation from the Higgs boson and tagging jet four-momenta as

$$x_{1,2}^{\text{reco}} = \frac{m_{Hjj}}{\sqrt{s}} e^{\pm y_{Hjj}},$$

where m_{Hjj} (y_{Hjj}) is the invariant mass (rapidity) obtained from the vectorially summed four-momenta of the tagging jets and the Higgs boson. Since the flavour of the initial- and final-state partons

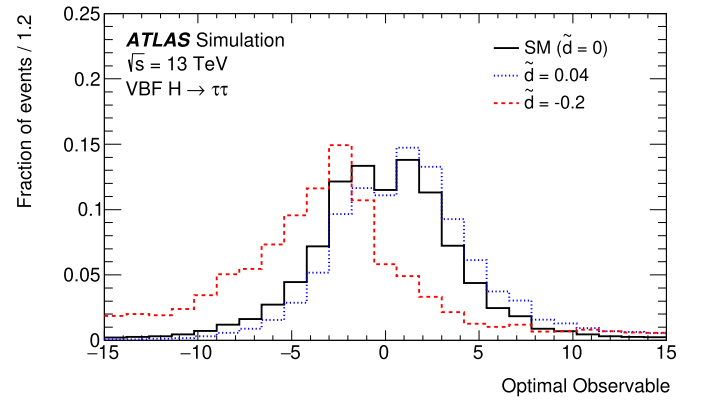


Fig. 1. Distribution of the Optimal Observable for signal events for three example values of \tilde{d} after event reconstruction and application of the full event selection used to define the signal region (see Section 5). Non-vanishing values of \tilde{d} cause an asymmetry and a non-vanishing mean value.

cannot be determined experimentally, the sum over all possible flavour configurations $ij \rightarrow klH$ weighted by the CT10 leading-order parton distribution functions (PDFs) [48] is calculated separately for the matrix elements in the numerator and denominator:

$$2 \operatorname{Re}(\mathcal{M}_{\text{SM}}^* \mathcal{M}_{\text{CP-odd}}) = \sum_{i,j,k,l} f_i(x_1) f_j(x_2) 2 \operatorname{Re}((\mathcal{M}_{\text{SM}}^{ij \rightarrow klH})^* \mathcal{M}_{\text{CP-odd}}^{ij \rightarrow klH})$$

$$|\mathcal{M}_{\text{SM}}|^2 = \sum_{i,j,k,l} f_i(x_1) f_j(x_2) |\mathcal{M}_{\text{SM}}^{ij \rightarrow klH}|^2.$$

The best estimate and confidence intervals for \tilde{d} in this analysis are determined by a fit of the predicted distribution of the Optimal Observable to that measured in data. It has been shown in Ref. [36] that the Optimal Observable yields a significantly higher sensitivity in the determination of \tilde{d} than the CP-odd signed difference in the azimuthal angle $\Delta\phi_{jj}$ between the two tagging jets, as suggested in Ref. [44].

3. ATLAS detector

The ATLAS experiment [49–51] at the LHC is a multipurpose particle detector with a forward-backward symmetric cylindrical geometry and a near 4π coverage in solid angle.⁴ It consists of an inner tracking detector surrounded by a thin superconducting solenoid providing a 2 T axial magnetic field, electromagnetic and hadron calorimeters, and a muon spectrometer. The inner tracking detector covers the pseudorapidity range $|\eta| < 2.5$. It consists of silicon pixel, silicon microstrip, and transition radiation tracking detectors. Lead/liquid-argon (LAr) sampling calorimeters provide electromagnetic (EM) energy measurements with high granularity. A steel/scintillator-tile hadron calorimeter covers the central pseudorapidity range ($|\eta| < 1.7$). The endcap and forward regions are instrumented with LAr calorimeters for both the EM and hadronic energy measurements up to $|\eta| = 4.9$. The muon spectrometer surrounds the calorimeters and is based on three large air-core toroidal superconducting magnets with eight coils each. The field integral of the toroids ranges between 2.0 and 6.0 Tm across most

³ \hat{T} denotes the naive time reversal according to Ref. [40], which inverts the directions of momenta and spins.

⁴ ATLAS uses a right-handed coordinate system with its origin at the nominal interaction point (IP) in the centre of the detector and the z -axis along the beam pipe. The x -axis points from the IP to the centre of the LHC ring, and the y -axis points upwards. Cylindrical coordinates (r, ϕ) are used in the transverse plane, ϕ being the azimuthal angle around the z -axis. The pseudorapidity is defined in terms of the polar angle θ as $\eta \equiv -\ln \tan(\theta/2)$. Angular distance is measured in units of $\Delta R \equiv \sqrt{(\Delta\eta)^2 + (\Delta\phi)^2}$.

Table 1
Overview of simulation tools used to generate signal and background processes and to model the UEPS. Details on the tunes used in the UEPS model can be found in Ref. [41]. The PDF sets are also summarized. All Higgs boson events were generated assuming $m_H = 125$ GeV. Alternative event generators and configurations used to estimate systematic uncertainties are shown in parentheses. The prediction order in the last column refers to the cross section used to normalize the event sample.

Process	Matrix element (alternative)	PDF set	UEPS model (alternative model)	Prediction order for total cross section
VBF H	POWHEG-Box v2 [59–63]	PDF4LHC15 NLO [64]	PYTHIA 8 [65] (Herwig 7 [67,68])	approx. NNLO QCD + NLO EW [45,46,66]
ggF H	POWHEG-Box v2 NNLOPS [73–75]	PDF4LHC15 NNLO	PYTHIA 8 (Herwig 7)	N ³ LO QCD + NLO EW [69–72]
VH	POWHEG-Box v2 [76]	PDF4LHC15 NLO	PYTHIA 8	$qq/qg \rightarrow VH$: NNLO QCD + NLO EW [77,78] $gg \rightarrow ZH$: NLO + NLL QCD [79,80]
$t\bar{t}H$	MG5_aMC@NLO 2.2.2 [81,82]	NNPDF3.0LO [83]	PYTHIA 8	NLO QCD + NLO EW [84–89]
W/Z +jets	SHERPA 2.2.1 [90] (MG5_aMC@NLO 2.2.2)	NNPDF3.0NNLO	SHERPA 2.2.1 [91] (PYTHIA 8)	NNLO [92,93]
Electroweak W/Zjj	SHERPA 2.2.1	NNPDF3.0NNLO	SHERPA 2.2.1	LO
$VV/V\gamma^*$	SHERPA 2.2.1	NNPDF3.0NNLO	SHERPA 2.2.1	NLO
$t\bar{t}$	POWHEG-Box v2 [94]	CT10 [48]	PYTHIA 6.428 [95]	NNLO+NNLL [96]
Wt	POWHEG-Box v1 [97]	CT10	PYTHIA 6.428	NLO [97]

of the detector. The muon spectrometer includes a system of precision tracking chambers and fast detectors for triggering. The integrated luminosity recorded by ATLAS is obtained with the LUCID-2 detector [52].

A two-level trigger system is used to select events [53]. The first-level trigger is implemented in hardware and uses a subset of the detector information to reduce the accepted rate to at most 100 kHz. This is followed by a software-based trigger that reduces the accepted event rate to 1 kHz on average depending on the data-taking conditions.

4. Simulated event samples

Samples of signal and background events were simulated using various Monte Carlo (MC) event generators. The generators and the PDF sets used for the hard-scattering process and the models used for the parton showers, hadronization, and underlying-event activity (UEPS) are summarized in Table 1. In addition, the order of the total cross-section calculation is given.

Only Higgs boson production via VBF is considered as signal, including the signals observed as $H \rightarrow \tau\tau$ decay and $H \rightarrow WW^* \rightarrow \ell\nu\ell\nu$ decay. The analysis is not sensitive to CPV in the $H \rightarrow WW^*$ decay vertex and the shape of the Optimal Observable is the same for the $H \rightarrow WW^* \rightarrow \ell\nu\ell\nu$ and $H \rightarrow \tau\tau \rightarrow \ell\ell 4\nu$ decay modes regardless of the value of \tilde{d} . The other Higgs boson production modes – gluon-gluon fusion (ggF H), VH , $t\bar{t}H$ – are considered as background in this analysis, and all couplings other than the HVV coupling were set to SM values. All SM signal and background samples used in this analysis are the same as those employed in Ref. [41], and the same normalization of those samples is used. The only exception is the normalization of the electroweak Zjj process. Here, the leading-order (LO) cross section calculated by the SHERPA 2.2.1 generator [54–57] is multiplied by a factor of 1.7 to match the cross-section value measured by the ATLAS experiment at $\sqrt{s} = 13$ TeV [58]. An uncertainty of 25% from the measured cross-section of the electroweak Zjj process is applied to the normalization.

To simulate the presence of non-vanishing values of \tilde{d} in the HVV vertex, a matrix-element reweighting method is applied to the VBF SM signal sample. The weight is defined as the ratio of the squared ME value of the VBF process associated with a specific amount of CP mixing (given in terms of \tilde{d}) to that obtained from the SM. To extract the weights, the leading-order MEs from HAWK are used for the $2 \rightarrow 2 + H$ and $2 \rightarrow 3 + H$ processes separately. The MEs are evaluated using the four-momenta and particle identification codes of the initial- and final-state partons and the Higgs boson of each event. The reweighting procedure has been validated [36] against samples generated with MAD-

GRAPH5_aMC@NLO [98] and proves to be a good approximation of a full NLO description of the process with non-vanishing values of \tilde{d} .

For all samples, a full simulation of the ATLAS detector response [99] using the GEANT4 program [100] was performed. The effect of multiple pp interactions in the same and neighbouring bunch crossings (pile-up) was included by overlaying minimum-bias events simulated with PYTHIA 8 using the MSTW2008LO PDF [101] and the A2 set [102] of tuned parameters on each generated signal and background event. The number of overlaid events was chosen such that the distribution of the average number of interactions per pp bunch crossing in the simulation matches that observed in data.

5. Event selection

In this analysis, events with at least two jets and a $H \rightarrow \tau\tau$ decay candidate in the final state are selected. Decays of the τ -leptons with all combinations of leptonic ($\tau \rightarrow \ell\nu\bar{\nu}$ with $\ell = e, \mu$) and hadronic ($\tau \rightarrow \text{hadrons}\nu$) final states are considered. In the following, the event preselection, which closely follows Ref. [41], is summarized and the analysis strategy using gradient boosted decision trees (BDTs) [103] is described. After data quality requirements [104], the integrated luminosity of the $\sqrt{s} = 13$ TeV dataset used is 36.1 fb^{-1} . The definition of the reconstructed objects as well as the triggers used in this analysis correspond to those used in Ref. [41], where more details are given.

Depending on the reconstructed decay modes of the two τ -leptons, events are separated into four analysis channels: the dileptonic same-flavour ($\tau_{\text{lep}}\tau_{\text{lep}}$ SF), the dileptonic different flavour ($\tau_{\text{lep}}\tau_{\text{lep}}$ DF), the semileptonic ($\tau_{\text{lep}}\tau_{\text{had}}$), and the fully hadronic ($\tau_{\text{had}}\tau_{\text{had}}$) channel. All channels require an exact number of identified and isolated τ -lepton decay candidates, i.e. electrons, muons, and visible products of hadronic τ decays ($\tau_{\text{had-vis}}$), as defined in Ref. [41], corresponding to their respective final state. Events with additional τ -lepton decay candidates are rejected. This ensures that the selected data samples in the four channels do not overlap. The two τ -lepton decay candidates are required to be of opposite electric charge and to fulfil the requirements on the transverse momentum given in Table 2.

The event selection for the four analysis channels is summarized in Table 2. In the $\tau_{\text{lep}}\tau_{\text{lep}}$ and $\tau_{\text{had}}\tau_{\text{had}}$ channels, only events with missing transverse momentum $E_{\text{T}}^{\text{miss}} > 20$ GeV are selected to reject events without neutrino candidates. To suppress the large background from $Z \rightarrow \ell\ell$ production in the $\tau_{\text{lep}}\tau_{\text{lep}}$ SF channel, the requirement on $E_{\text{T}}^{\text{miss}}$ is tightened. Furthermore, an additional requirement is imposed on the quantity $E_{\text{T}}^{\text{miss,hard}}$, obtained from

Table 2

Summary of the event selection requirements for the four analysis channels. In the case of the p_T requirements on the τ -lepton decay candidates, the asterisk marks the lowest p_T threshold, which varies depending on the trigger used. Details of this are given in Ref. [41]. The transverse momentum of the visible decay products of the τ -lepton candidate with the higher (lower) transverse momentum is denoted by $p_T^{\tau_1}$ ($p_T^{\tau_2}$). The input variables used for the BDT training and the $\text{BDT}_{\text{score}}$ threshold used to define the signal regions are also reported.

Channel	$\tau_{\text{lep}} \tau_{\text{lep}}$ SF	$\tau_{\text{lep}} \tau_{\text{lep}}$ DF	$\tau_{\text{lep}} \tau_{\text{had}}$	$\tau_{\text{had}} \tau_{\text{had}}$
Two isolated τ -lepton decay candidates with opposite electric charge				
Preselection	$p_T^{\tau_1} > 19^*/15^*$ GeV (μ/e) $p_T^{\tau_2} > 10/15^*$ GeV (μ/e) $m_{\tau\tau}^{\text{coll}} > m_Z - 25$ GeV $30 < m_{\ell\ell} < 75$ GeV $E_T^{\text{miss}} > 55$ GeV $E_T^{\text{miss,hard}} > 55$ GeV	$p_T^e > 18$ GeV $p_T^\mu > 14$ GeV $30 < m_{\ell\ell} < 100$ GeV $E_T^{\text{miss}} > 20$ GeV $N_{b\text{-jets}} = 0$	$p_T^{\tau_{\text{had}}} > 30$ GeV $p_T^{\tau_{\text{lep}}} > 21^*$ GeV $m_T < 70$ GeV	$p_T^{\tau_1} > 40$ GeV $p_T^{\tau_2} > 30$ GeV $0.8 < \Delta R_{\tau\tau} < 2.5$ $ \Delta\eta_{\tau\tau} < 1.5$ $E_T^{\text{miss}} > 20$ GeV
VBF topology		$N_{\text{jets}} \geq 2$, $p_T^{j_2} > 30$ GeV, $m_{jj} > 300$ GeV, $ \Delta\eta_{jj} > 3$ $p_T^{j_1} > 40$ GeV		$p_T^{j_1} > 70$ GeV, $ \eta_{j_1} < 3.2$
BDT input variables	$m_{\tau\tau}^{\text{vis}}$, $m_T^{\tau_1, E_T^{\text{miss}}}$, $p_T^{j_3}$	$m_{\tau\tau}^{\text{MMC}}$, m_{jj} , $\Delta R_{\tau\tau}$, $C_{jj}(\tau_1)$, $C_{jj}(\tau_2)$, p_T^{tot}	$C(\phi^{\text{miss}})/\sqrt{2}$	$p_T^{\tau_1, E_T^{\text{miss}}}$, $ \Delta\eta_{\tau\tau} $
Signal region		$E_T^{\text{miss}}/p_T^{\tau_1}$, $E_T^{\text{miss}}/p_T^{\tau_2}$	$m_{\tau\tau}^{\text{vis}}$, $ \Delta\eta_{\tau\tau} $	
		$\text{BDT}_{\text{score}} > 0.78$	$\text{BDT}_{\text{score}} > 0.86$	$\text{BDT}_{\text{score}} > 0.87$

an E_T^{miss} calculation considering only contributions from reconstructed objects and neglecting contributions from inner-detector tracks originating from the vertex of the hard-scattering process, but not associated with any of the reconstructed objects. In addition, a requirement on the invariant mass of the two light leptons, $m_{\ell\ell}$, is applied in the $\tau_{\text{lep}} \tau_{\text{lep}}$ channels. A requirement on the di- τ mass calculated in the collinear approximation [105] of $m_{\tau\tau}^{\text{coll}} > m_Z - 25$ GeV is introduced in the $\tau_{\text{lep}} \tau_{\text{lep}}$ channels to ensure orthogonality between this analysis and the analysis of $H \rightarrow WW^* \rightarrow \ell\nu\ell\nu$ [106], which has a similar final state. In the $\tau_{\text{lep}} \tau_{\text{lep}}$ and $\tau_{\text{lep}} \tau_{\text{had}}$ channels, the top quark background is suppressed by requiring that no jet with $p_T > 25$ GeV and $|\eta| < 2.5$ contains b -hadrons (b -jets). A multivariate algorithm [107,108] is used to identify and select b -jets with a working point corresponding to an average efficiency of 85%, as measured on a sample from top quark pair production. Low transverse mass⁵ ($m_T < 70$ GeV) is required in the $\tau_{\text{lep}} \tau_{\text{had}}$ channel to reject events with leptonic W decays. Requirements on the angular distance between the visible products of the two selected τ -lepton decays, $\Delta R_{\tau\tau}$, and their pseudorapidity difference, $|\Delta\eta_{\tau\tau}|$, are applied in the $\tau_{\text{had}} \tau_{\text{had}}$ channel to reject non-resonant background events.

To select Higgs boson events produced by VBF, all channels require at least two jets with transverse momentum of the leading jet $p_T^{j_1} > 40$ GeV and of the subleading jet $p_T^{j_2} > 30$ GeV, a large invariant mass of the two leading jets, $m_{jj} > 300$ GeV, and a pseudorapidity separation of $|\Delta\eta_{jj}| > 3$. In the $\tau_{\text{had}} \tau_{\text{had}}$ channel, the requirements on the leading jet are raised to $p_T^{j_1} > 70$ GeV and $|\eta_{j_1}| < 3.2$ to achieve a uniform trigger selection efficiency as a function of $p_T^{j_1}$. This selection is referred to as the VBF event selection in the following.

To construct a region enriched in VBF signal events, BDTs trained to discriminate between the VBF signal and the backgrounds are used in all channels. Kinematic variables used in the BDT training can be categorized as follows:

⁵ The transverse mass is defined as $m_T = \sqrt{2p_T^e E_T^{\text{miss}} \cdot (1 - \cos \Delta\phi)}$, where $\Delta\phi$ is the azimuthal separation between the directions of the lepton and the missing transverse momentum.

- Properties of the Higgs boson which discriminate against all background processes without a Higgs boson: the visible mass of the di- τ system, $m_{\tau\tau}^{\text{vis}}$, the transverse momentum of the $\tau\tau E_T^{\text{miss}}$ system, $p_T^{\tau\tau E_T^{\text{miss}}}$, and the reconstructed Higgs boson mass, $m_{\tau\tau}^{\text{MMC}}$, determined using the missing-mass calculator (MMC) [109].
- Properties of a resonant di- τ decay which discriminate against processes with jets that are misidentified as τ -decay candidates (referred to as ‘‘Misidentified τ ’’): the angular distance $\Delta R_{\tau\tau}$, the difference in pseudorapidity $|\Delta\eta_{\tau\tau}|$, and the difference in azimuth $\Delta\phi_{\tau\tau}$ between the two visible τ -leptons. In addition, the transverse momentum ratio $E_T^{\text{miss}}/p_T^{\tau_1}$ ($E_T^{\text{miss}}/p_T^{\tau_2}$) between the E_T^{miss} and the leading (subleading) τ -candidate as well as the transverse mass of the E_T^{miss} and the leading τ -candidate, $m_T^{\tau_1, E_T^{\text{miss}}}$, is used. Furthermore, the azimuthal centrality of E_T^{miss} , $C(\phi^{\text{miss}})/\sqrt{2}$, which quantifies the angular direction of the missing transverse momentum relative to the visible τ -decay products in the transverse plane, is constructed.⁶
- Properties of the VBF topology: m_{jj} , the total transverse momentum p_T^{tot} , which is defined as the transverse momentum of the system composed of all objects in a VBF event (τ_1 , τ_2 , j_1 , j_2 , E_T^{miss}), η -centralities, $C_{jj}(\tau_1)$ and $C_{jj}(\tau_2)$, of each τ -candidate relative to the pseudorapidity of the two leading jets,⁷ and the transverse momentum of the third leading jet $p_T^{j_3}$ which is set to zero for events with exactly two jets.

The most important variables in the training are $m_{\tau\tau}^{\text{MMC}}$, m_{jj} , and $C_{jj}(\tau_1)$. The resulting BDT score ($\text{BDT}_{\text{score}}$) distributions are shown in Fig. 2 for events surviving the VBF event selection

⁶ $C(\phi^{\text{miss}})$ is defined as $(A+B)/\sqrt{A^2+B^2}$, where $A = \sin(\phi_{E_T^{\text{miss}}} - \phi_{\tau_2})/\sin(\phi_{\tau_1} - \phi_{\tau_2})$ and $B = \sin(\phi_{\tau_1} - \phi_{E_T^{\text{miss}}})/\sin(\phi_{\tau_1} - \phi_{\tau_2})$.

⁷ $C_{jj}(\tau) = \exp\left[\frac{-4}{(\eta_{j_1} - \eta_{j_2})^2} \left(\eta_\tau - \frac{\eta_{j_1} + \eta_{j_2}}{2}\right)^2\right]$, where η_τ , η_{j_1} and η_{j_2} are the pseudorapidities of the τ -candidate and the two leading jets, respectively. This variable has a value of unity when the object is halfway in η between the two jets, $1/e$ when the object is aligned with one of the jets, and $< 1/e$ when the object is not between the jets in η .

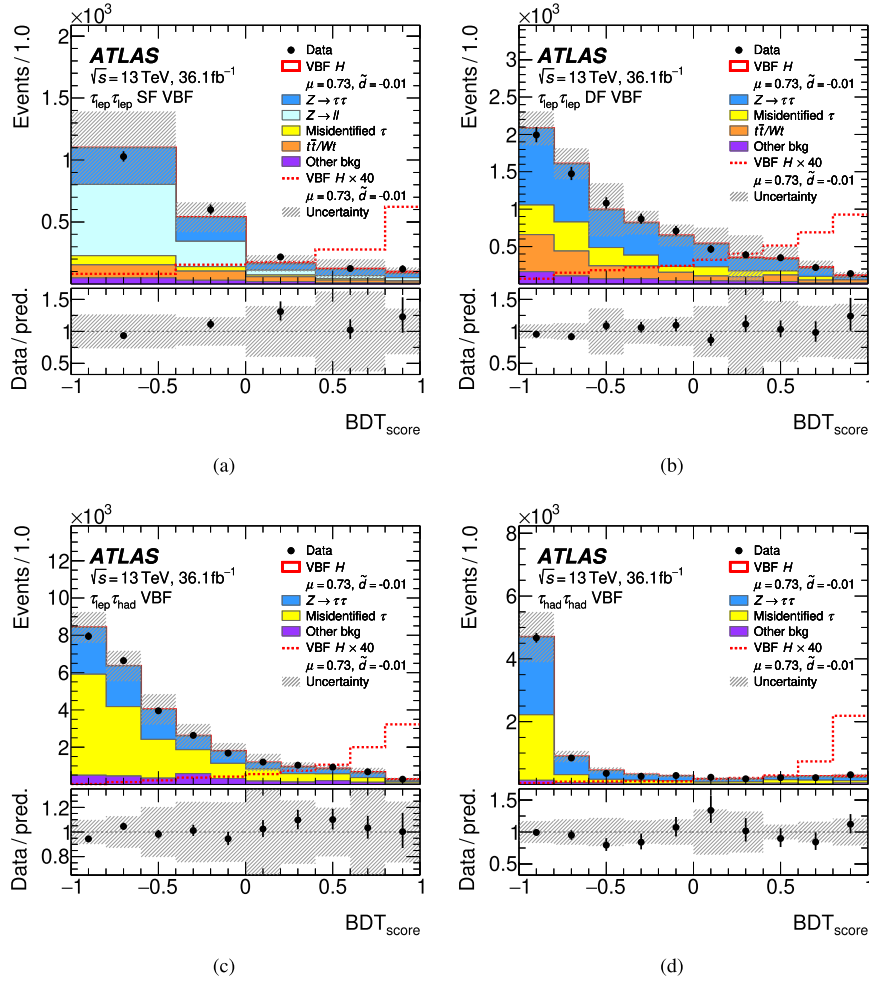


Fig. 2. Post-fit BDT_{score} distributions after the VBF event selection for the (a) $\tau_{lep}\tau_{lep}$ SF, (b) $\tau_{lep}\tau_{lep}$ DF, (c) $\tau_{lep}\tau_{had}$ and (d) $\tau_{had}\tau_{had}$ analysis channels. The ratios of the data to the prediction are shown in the lower panels. The observed VBF signal ($\mu = 0.73$, $\tilde{d} = -0.01$) is shown with the solid red line on the top of the histogram stack. “Other bkg” denotes all background contributions not listed explicitly in the legend. The dashed line shows the observed VBF signal scaled up by a factor of 40 and is not part of the histogram stack. The size of the combined statistical, experimental, and theoretical uncertainties in the background is indicated by the hatched bands.

and show the ability of the BDT to separate the signal process from background processes. All figures in this Letter use signal strength μ (defined as the ratio of the measured cross section times branching ratio to the SM prediction for the VBF signal process), background normalizations, and systematic uncertainties as fitted by the final statistical analysis discussed in Section 8 and referred to as *post-fit*. The signal purity increases at high values of BDT_{score} . A threshold value of BDT_{score} is used to define the final signal region (SR) in each channel. This threshold is chosen to yield a high signal significance and is given in Table 2 for each channel. The efficiency of the signal selection relative to the VBF event selection is 32% (27%) for the $\tau_{lep}\tau_{lep}$ SF ($\tau_{lep}\tau_{lep}$ DF) channel, 29% for the $\tau_{lep}\tau_{had}$ channel, and 49% for the $\tau_{had}\tau_{had}$ channel. The efficiency for the sum of background processes, on the other hand, is 1.5% (0.8%) for the $\tau_{lep}\tau_{lep}$ SF ($\tau_{lep}\tau_{lep}$ DF) channel, 0.4% for the $\tau_{lep}\tau_{had}$ channel, and 1.1% for the $\tau_{had}\tau_{had}$ channel. In each SR the Optimal Observable is then used to probe for CPV. No dependence of the mean values of the Optimal Observable on BDT_{score} is observed, confirming that the SR selection criteria do not introduce a CP asymmetry.

6. Background estimation

Several background processes contribute to the SR event yields in the four analysis channels. The dominant contributions in the

$\tau_{lep}\tau_{lep}$ DF, $\tau_{lep}\tau_{had}$, and $\tau_{had}\tau_{had}$ channels arise from $Z \rightarrow \tau\tau$ production and from light- and heavy-flavour jets that are misidentified as prompt leptonic or hadronic τ decays. The misidentified τ decays in the $\tau_{lep}\tau_{lep}$ and $\tau_{lep}\tau_{had}$ channels originate largely from W +jets production with smaller contributions from multijet and top quark production, while in the $\tau_{had}\tau_{had}$ channel the contribution from multijet production dominates. In the $\tau_{lep}\tau_{lep}$ SF channel the contribution from $Z \rightarrow \ell\ell$ production is dominant. Other background contributions in all analysis channels originate from top quark pair and associated Wt production (denoted by “ $t\bar{t}/Wt$ ” in the following), diboson production, and other Higgs boson production modes.

Background contributions with prompt leptonic or hadronic τ decays are estimated from simulation, while the estimation of the background contribution from misidentified τ decays is mostly data-driven [41]. Dedicated control regions (CR) are defined in data to normalize the predictions of the following background processes: $Z \rightarrow \tau\tau$ (for all channels), $t\bar{t}/Wt$ and $Z \rightarrow \ell\ell$ (only for the $\tau_{lep}\tau_{lep}$ channels), and the misidentified τ decays (only for the $\tau_{had}\tau_{had}$ channel). All other background processes with prompt τ decays (including other Higgs boson production modes) are normalized to their SM prediction.

To construct a CR for $Z \rightarrow \tau\tau$ production, the SR requirement on the BDT_{score} (given in Table 2) is inverted for each analysis channel. This CR is called the “low- BDT_{score} CR” in the follow-

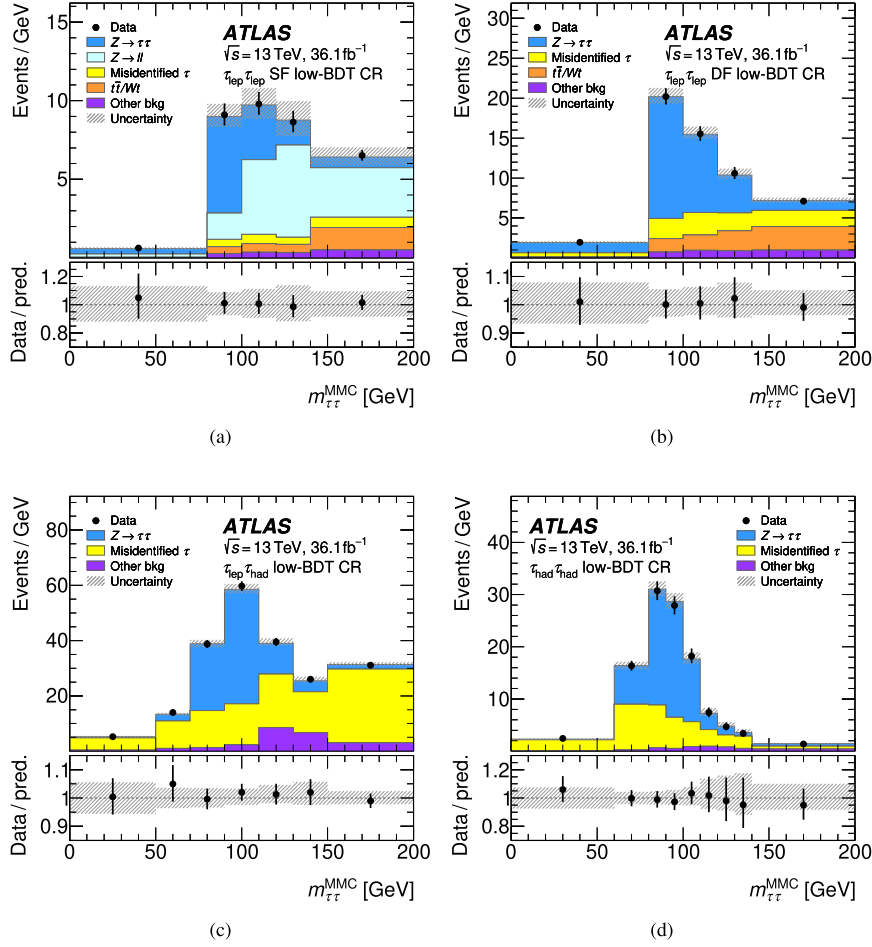


Fig. 3. Post-fit $m_{\tau\tau}^{\text{MMC}}$ distributions in the low-BDT_{score} CR for the (a) $\tau_{\text{lep}}\tau_{\text{lep}}$ SF, (b) $\tau_{\text{lep}}\tau_{\text{lep}}$ DF, (c) $\tau_{\text{lep}}\tau_{\text{had}}$ and (d) $\tau_{\text{had}}\tau_{\text{had}}$ analysis channels. The ratios of the data to the prediction are shown in the lower panels. The contamination of the CR by signal is negligible. “Other bkg” denotes all background contributions not listed explicitly in the legend. The size of the combined statistical, experimental, and theoretical uncertainties in the background is indicated by the hatched bands. The rightmost bins of each of the subfigures include event yields with $m_{\tau\tau}^{\text{MMC}}$ values larger than the shown range.

ing. Since the purity of $Z \rightarrow \tau\tau$ production in the low-BDT_{score} CR ranges from 30% to 54% depending on the analysis channel, $Z \rightarrow \tau\tau$ production is normalized to data in the Z boson mass peak of the $m_{\tau\tau}^{\text{MMC}}$ distributions, shown in Fig. 3. In the fit the $Z \rightarrow \tau\tau$ normalization is correlated across all analysis channels and the fit yields a normalization factor of 0.93 ± 0.08 . To ensure that the normalization is valid in the SR, the modelling of the Z -boson and jet kinematic properties was checked in a validation region which is composed of $Z \rightarrow \ell\ell$ events with kinematic properties similar to those of the $Z \rightarrow \tau\tau$ events in the VBF region of each analysis channel. This region is defined by selecting two same-flavour leptons of opposite charge with a dilepton mass of $m_{\ell\ell} > 80$ GeV and low missing transverse momentum ($E_{\text{T}}^{\text{miss}} < 55$ GeV). All VBF selection requirements given in Table 2 are applied as well. As in Ref. [41], a slight positive slope in the ratio of the data to the SHERPA simulation as a function of m_{jj} is observed. In this analysis, the simulated $Z \rightarrow \tau\tau$ and $Z \rightarrow \ell\ell$ events are reweighted to the observed m_{jj} distribution after the VBF event selection, which results in a small change in the acceptance of $Z \rightarrow \tau\tau$ and $Z \rightarrow \ell\ell$ events in the SR.

In each of the two $\tau_{\text{lep}}\tau_{\text{lep}}$ channels, a top quark CR is defined by inverting the veto on b -tagged jets and not applying the selection on the BDT_{score}. The normalization of $t\bar{t}/Wt$ production is constrained by the event yield in these CRs, corresponding to a normalization of 1.16 ± 0.06 from the combined fit to the data. Additionally, another CR is defined to normalize the $Z \rightarrow \ell\ell$ process for the $\tau_{\text{lep}}\tau_{\text{lep}}$ SF channel. Again, the selection on the BDT_{score}

is not applied, and the requirement on the dilepton invariant mass is changed to $80 < m_{\ell\ell} < 100$ GeV. The observed event yield in the $Z \rightarrow \ell\ell$ CR constrains the normalization of simulated $Z \rightarrow \ell\ell$ events in the $\tau_{\text{lep}}\tau_{\text{lep}}$ SF channel to 1.0 ± 0.4 .

In the $\tau_{\text{had}}\tau_{\text{had}}$ channel, the background from misidentified hadronic τ decays is dominated by multijet events. This background process is modelled using a template extracted from $\tau_{\text{had-vis}}$ candidates with one, two, or three associated tracks that pass all selection requirements, but fail the opposite-charge requirement. Before the final fit, the template is normalized to data by a fit of the $|\Delta\eta_{\tau\tau}|$ distribution after the preselection, but removing the requirement on $|\Delta\eta_{\tau\tau}|$. In the final fit the template is normalized to data in the $m_{\tau\tau}^{\text{MMC}}$ distribution of the low-BDT_{score} CR in the $\tau_{\text{had}}\tau_{\text{had}}$ channel. Then, the multijet background is normalized with a factor of 0.99 ± 0.09 relative to the pre-fit normalization.

The modelling of the Optimal Observable distribution for the background processes is validated in all CRs. Fig. 4 shows Optimal Observable distributions in the low-BDT_{score} CR for all analysis channels, where the background processes have been normalized to the result of the fit. Neither the observed nor the predicted distributions in any CR show hints of an asymmetry or non-vanishing mean values of the Optimal Observable caused by event reconstruction and selection within uncertainties. The data and the predicted distributions are observed to be compatible within uncertainties here as well as in the top quark and $Z \rightarrow \ell\ell$ CRs of the $\tau_{\text{lep}}\tau_{\text{lep}}$ channels.

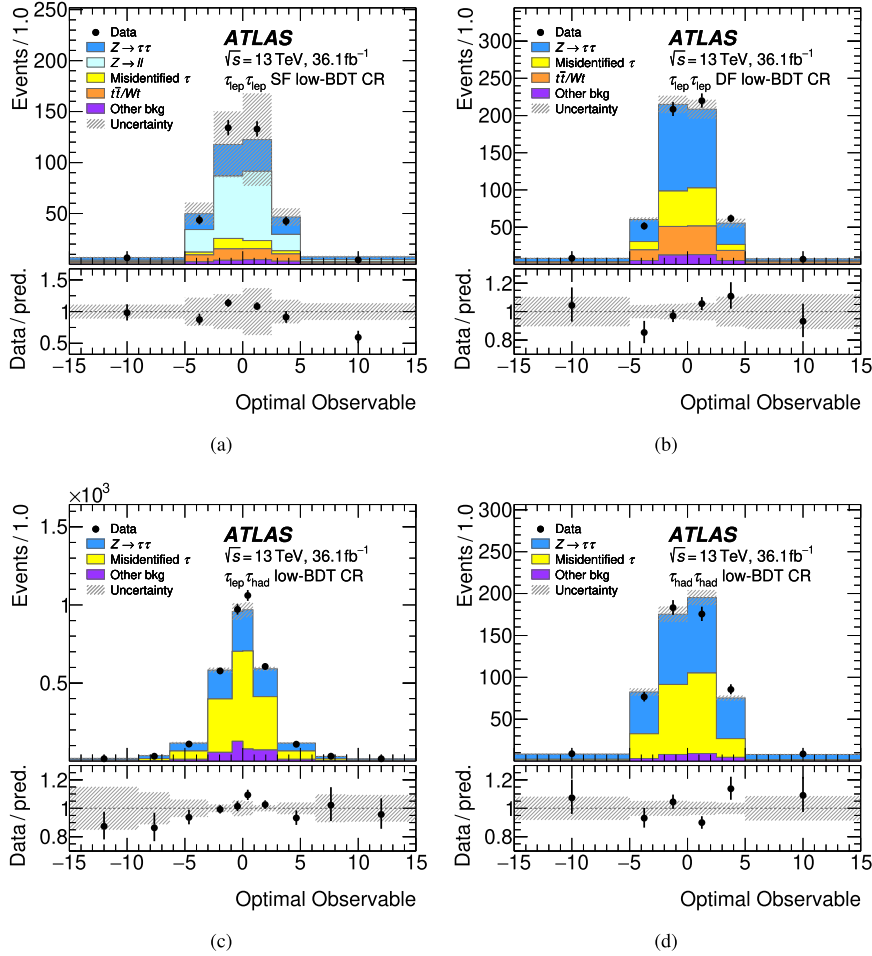


Fig. 4. Post-fit Optimal Observable distributions in the low- $\text{BDT}_{\text{score}}$ CR for the (a) $\tau_{\text{lep}}\tau_{\text{lep}}$ SF, (b) $\tau_{\text{lep}}\tau_{\text{lep}}$ DF, (c) $\tau_{\text{lep}}\tau_{\text{had}}$ and (d) $\tau_{\text{had}}\tau_{\text{had}}$ analysis channels. The ratios of the data to the prediction are shown in the lower panels. The contamination of the CR by signal is negligible. “Other bkg” denotes all background contributions not listed explicitly in the legend. The size of the combined statistical, experimental, and theoretical uncertainties in the background is indicated by the hatched bands.

7. Systematic uncertainties

The effects of the systematic uncertainties on the yields in both the SRs and CRs and on the shape of the Optimal Observable in the SRs, as well as the $m_{\tau\tau}^{\text{MMC}}$ distributions in the CRs, are evaluated following the procedures in Ref. [41]. No sources of systematic uncertainties introduce a significant asymmetry in the Optimal Observable distribution. The sources of uncertainty can be grouped into two categories: experimental and theoretical. The dominant experimental uncertainties stem from the determination of the jet energy resolution and scale [110], the $\tau_{\text{had-vis}}$ energy scale and resolution [111], and the $\tau_{\text{had-vis}}$ reconstruction and identification efficiencies [112]. Other sources of uncertainty are the electron (muon) energy (momentum) scale and resolution, lepton identification and isolation [113–115], missing transverse momentum reconstruction [116], b -tagging efficiency [107,117], modelling of pile-up, and luminosity measurement [118]. The luminosity uncertainty of 2.1% [118] is only applied to the VBF signal and to background processes normalized to theoretical predictions. Uncertainties in backgrounds from misidentified τ -leptons arise from the limited statistical precision of the data-driven templates and corrections used, from closure tests performed in regions where the τ -leptons are required to have the same charge, and from the subtraction of the electroweak contributions.

Theoretical uncertainties affecting the total cross section are evaluated for the Higgs boson production cross sections for ggF H , VH , and $t\bar{t}H$ production by varying the QCD factorization and

renormalization scales as well as the PDF model following the recommendations in Ref. [119]. Also, uncertainties in the $H \rightarrow \tau\tau$ and $H \rightarrow WW^*$ branching ratios are considered [119]. Theoretical uncertainties in the MC modelling are considered for the VBF and gluon-gluon fusion production of the Higgs boson as well as for $Z \rightarrow \tau\tau$ production. For all simulated background contributions other than $Z \rightarrow \tau\tau$, no theoretical uncertainties are considered, as their impact is negligible. Uncertainties in MC modelling are assessed by a comparison between nominal and alternative event generators and UEPS models, as indicated in Table 1. In addition, the effects of QCD factorization and renormalization scale variations, matching-scale variations (in the case of $Z \rightarrow \tau\tau$ only), and PDF model uncertainties are evaluated. As an additional uncertainty in the $Z \rightarrow \tau\tau$ and $Z \rightarrow \ell\ell$ processes, the full difference between the sample reweighted to the observed m_{jj} distribution and the sample without reweighting is applied to the full analysis. An uncertainty to account for the signal reweighting procedure described in Section 4 was considered and found to be negligible. The uncertainty due to limited MC sample size is evaluated for the sum of all MC-based background processes in each analysis bin.

8. Fitting procedure

The estimate of \tilde{d} is obtained using a binned maximum-likelihood fit (ML-fit) performed simultaneously on the SRs and all introduced CRs, which are included in order to constrain background normalizations and nuisance parameters describing

the systematic uncertainties. The ML-fit uses the distribution of the Optimal Observable in each of the four high-BDT_{score} SRs, one for each analysis channel. The $m_{\tau\tau}^{\text{MMC}}$ distributions in the low-BDT_{score} region for each channel are included in the ML-fit, and so are the event yields in the $Z \rightarrow \ell\ell$ ($\tau_{\text{lep}}\tau_{\text{lep}}$ SF) and top quark ($\tau_{\text{lep}}\tau_{\text{lep}}$ SF and DF) CRs.

The inclusion of the $m_{\tau\tau}^{\text{MMC}}$ distributions in the low-BDT_{score} regions provides the main constraint on the $Z \rightarrow \tau\tau$ normalization, which is free to float in the ML-fit. The $Z \rightarrow \ell\ell$ background in the $\tau_{\text{lep}}\tau_{\text{lep}}$ SF channel and top quark backgrounds in the $\tau_{\text{lep}}\tau_{\text{lep}}$ SF and DF channels are also free to float, and their contributions are constrained by the inclusion of CRs in the ML-fit.

The normalization of the signal is not constrained in the ML-fit, so that the analysis only exploits the shape of the distribution of the Optimal Observable in the estimation of \tilde{d} . Any possible model-dependence of the cross section on CP-mixing scenarios is not exploited. The relative contribution of the two Higgs boson decay modes ($H \rightarrow \tau\tau$ and $H \rightarrow WW^*$) to the signal (relevant only for the $\tau_{\text{lep}}\tau_{\text{lep}}$ channel) is assumed to be correctly predicted by the SM. All other Higgs boson production modes for these decays are considered as background and are normalized to their SM predicted yields.

The ML-fit uses a binned likelihood function $\mathcal{L}(\mathbf{x}; \mu, \theta)$, which is a function of the data \mathbf{x} , the free-floating signal strength μ , and nuisance parameters θ corresponding to the systematic uncertainties mentioned in Section 7. The likelihood function is evaluated for each \tilde{d} hypothesis using the relevant reweighted signal templates defined in Section 4, with the background model unchanged, and a negative log-likelihood (NLL) curve can then be constructed as a function of \tilde{d} .

The parameter of interest, \tilde{d} , is obtained at the point where the NLL curve reaches a minimum. Central confidence intervals are obtained by reading off the points on the NLL curve which exceed the minimum value by a certain amount.

9. Results

For a CP-even Higgs boson, the mean value of the Optimal Observable for the signal and background processes is expected to be zero if any effects from the rescattering of new particles in loops can be neglected. However, CP-violating effects could result in the mean value of the Optimal Observable in data deviating from zero, allowing an almost model-independent test for CP-violating effects in this measurement.

The observed values for the mean of the Optimal Observable in data, along with their statistical uncertainties, are summarized in Table 3 for the four channels in this analysis, as well as their combination. The combined mean is obtained by weighting the mean value of each individual channel by the inverse of its respective variance. These values are fully consistent with zero, so no evidence of CPV is observed.

To extract confidence intervals for the CP-mixing parameter \tilde{d} , the ML-fit described in Section 8 is carried out. The post-fit distributions of the Optimal Observable in the various analysis channels are shown in Fig. 5. Here the value of the parameter of interest \tilde{d} , the values of the nuisance parameters, and the normalizations of the signal and background processes have been adjusted within their allowed constraints to minimize the NLL curve. Values of the NLL are evaluated in steps of $\Delta\tilde{d} = 0.01$, and the smallest value of the NLL is observed at $\tilde{d} = -0.01$. This is the value of \tilde{d} that is used for the post-fit distributions and event yields. Based upon interpolations between the discrete evaluations of the various NLL values as a function of \tilde{d} , the best estimator for \tilde{d} is $-0.013_{-0.077}^{+0.048}$. This value is consistent with the SM expectation of zero, and no evidence of CPV is observed using this approach. The best-fit signal strength from the ML-fit is $\mu = 0.73 \pm 0.47$.

Table 3

Mean values of the Optimal Observable with statistical uncertainties that are observed in data for the four analysis channel SRs and their combination.

Channel	(Optimal observable)
$\tau_{\text{lep}}\tau_{\text{lep}}$ SF	-0.54 ± 0.72
$\tau_{\text{lep}}\tau_{\text{lep}}$ DF	0.71 ± 0.81
$\tau_{\text{lep}}\tau_{\text{had}}$	0.74 ± 0.78
$\tau_{\text{had}}\tau_{\text{had}}$	-1.13 ± 0.65
Combined	-0.19 ± 0.37

While the predicted background distributions for the Optimal Observable are not perfectly symmetric, they are statistically consistent with a symmetric distribution. This slight asymmetry causes the expected confidence intervals for \tilde{d} to also be asymmetric.

Tables 4 and 5 display the fitted event yields of the signal ($\mu = 0.73$, $\tilde{d} = -0.01$) and various background processes for the SRs of each channel, along with the corresponding number of events observed in data. For reference, the signal yields for the SM expectation ($\mu = 1$, $\tilde{d} = 0$) are also shown.

The observed and expected ΔNLL curves are shown in Fig. 6(a) as a function of \tilde{d} . The expected curves are obtained in a two-step process: firstly, nuisance parameters and background normalization factors are constrained via a ML-fit to all analysis CRs, excluding the SRs; then another fit is performed in all SRs and CRs to pseudo-data which were created with the best-fit parameter values from the first step. This two-step process ensures that the nuisance parameters and the background normalization factors for the expected sensitivity are set to values that are consistent with the observed data in the analysis CRs. The expected ΔNLL curve is shown for $\tilde{d} = 0$ and $\mu = 1$ and represents the best estimate of the sensitivity of the analysis based on SM expectations. Another ΔNLL curve with $\tilde{d} = 0$ and the signal strength μ set to the observed value of 0.73 is also shown in order to demonstrate the decrease in sensitivity due to the lower than expected event yields (see Tables 4 and 5). Also shown for comparison in Fig. 6(a) is the pre-fit expected ΔNLL curve, which is obtained using a pseudo-dataset where the event yields and distributions in the SRs and CRs are set to the SM expectations for both the signal (with $\tilde{d} = 0$ and $\mu = 1$) and background processes. This demonstrates that the preferred values of the nuisance parameters and normalization factors based on the observed data in the background CRs in the expected ΔNLL curve result in a decrease in sensitivity to \tilde{d} when compared with the pre-fit expected curve.

The effect of systematic uncertainties on the sensitivity to \tilde{d} can be seen in Fig. 6(b). Here, the expected ΔNLL curves are shown for $\tilde{d} = 0$ and $\mu = 1$, with and without the effect of systematic uncertainties. To assess the impact of systematic uncertainties stemming from jet reconstruction, τ -lepton identification, and MC sample size, expected ΔNLL curves are also shown where the nuisance parameters corresponding to the systematic uncertainties in question have been removed from the likelihood function. It is evident that the experimental uncertainties related to jet reconstruction have the largest effect on the sensitivity of this analysis to \tilde{d} .

To obtain insight into the preferred values of \tilde{d} obtained for the individual Optimal Observable distributions in the different analysis channels, ΔNLL curves for each individual channel are shown in Fig. 6(c), and compared with the combined result. For these individual ΔNLL curves, only event yield information from the other three signal regions that are not being featured is used, so that the distribution of events in the Optimal Observable in these other signal regions is not exploited in the ML-fit. For these individual channel ΔNLL curves, the signal strength is constrained to be positive so that the ML-fit is stable and insensitive to event yield fluctuations in the individual channel SRs that arise from smaller

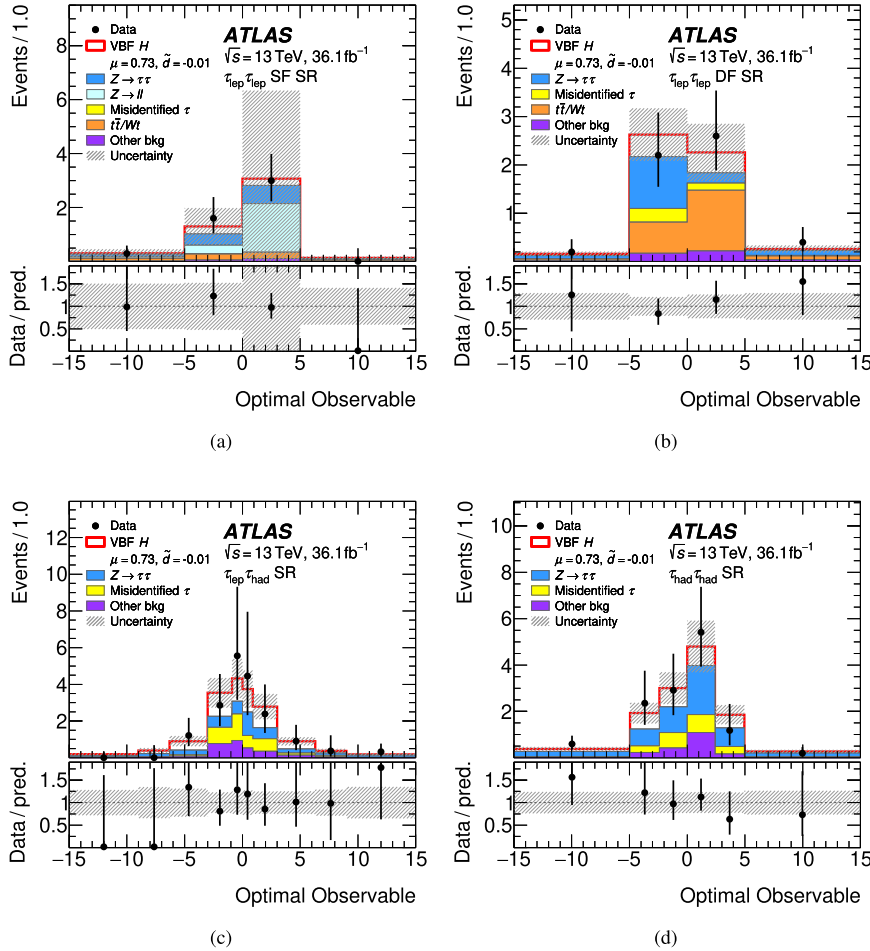


Fig. 5. Post-fit distributions of the event yields (divided by the bin width) as a function of the Optimal Observable in the SRs for the (a) $\tau_{lep}\tau_{lep}$ SF, (b) $\tau_{lep}\tau_{lep}$ DF, (c) $\tau_{lep}\tau_{had}$ and (d) $\tau_{had}\tau_{had}$ analysis channels. The values of \tilde{d} , the signal strength μ , the normalization of background processes, and nuisance parameters for the event yield prediction are set to those which minimize the NLL. The ratios of the data to the prediction are shown in the lower panels. The size of the combined statistical, experimental and theoretical uncertainties in the predicted event yields is indicated by the hatched bands.

Table 4

Post-fit event yields in the SRs for the $\tau_{lep}\tau_{lep}$ SF and $\tau_{lep}\tau_{lep}$ DF analysis channels. The $Z \rightarrow \ell\ell$ and diboson backgrounds are grouped together in a single background category for the $\tau_{lep}\tau_{lep}$ DF channel. For comparison, the expected signal yields for the SM expectation ($\mu = 1$, $\tilde{d} = 0$) are also shown.

Process	$\tau_{lep}\tau_{lep}$ SF	$\tau_{lep}\tau_{lep}$ DF
Data	26	30
VBF $H \rightarrow \tau\tau$ / WW ($\mu = 0.73$, $\tilde{d} = -0.01$)	3.3 ± 2.1	5.1 ± 3.1
VBF $H \rightarrow \tau\tau$ / WW ($\mu = 1$, $\tilde{d} = 0$)	4.5 ± 2.9	6.9 ± 4.4
$Z \rightarrow \tau\tau$	6.6 ± 3.7	8.2 ± 3.8
Fake lepton	0.02 ± 0.20	2.3 ± 0.7
$t\bar{t}$ + single top	3.8 ± 2.3	10.6 ± 5.5
$Z \rightarrow \ell\ell$	11 ± 18	1.8 ± 1.1
Diboson	0.70 ± 0.59	1.8 ± 1.1
ggF $H / VH / t\bar{t}H$, $H \rightarrow \tau\tau$ / WW	0.49 ± 0.48	0.70 ± 0.30
Sum of backgrounds	23 ± 17	23.6 ± 6.1

samples. This constraint is responsible for the plateau in the Δ NLL curve occurring at negative values in the $\tau_{lep}\tau_{had}$ channel.

An observed 68% CL interval of $\tilde{d} \in [-0.090, 0.035]$ is obtained from the observed Δ NLL curve using Optimal Observable distributions in all SRs. The corresponding expected interval, based upon the expected Δ NLL curve for $\tilde{d} = 0$ and $\mu = 1$ in Fig. 6(a) is

Table 5

Post-fit event yields in the SRs for the $\tau_{lep}\tau_{had}$ and $\tau_{had}\tau_{had}$ analysis channels. The line “Other backgrounds” includes top quark ($t\bar{t}$ and single top), diboson, and $Z \rightarrow \ell\ell$ backgrounds. Backgrounds from $W(\rightarrow \tau_{had}\nu)$ +jets production in the $\tau_{had}\tau_{had}$ channel are also included in “Other backgrounds”. For comparison, the expected signal yields for the SM expectation ($\mu = 1$, $\tilde{d} = 0$) are also shown.

Process	$\tau_{lep}\tau_{had}$	$\tau_{had}\tau_{had}$
Data	30	37
VBF $H \rightarrow \tau\tau$ ($\mu = 0.73$, $\tilde{d} = -0.01$)	11.8 ± 7.4	8.9 ± 5.6
VBF $H \rightarrow \tau\tau$ ($\mu = 1$, $\tilde{d} = 0$)	16 ± 10	12.3 ± 7.7
$Z \rightarrow \tau\tau$	7.8 ± 3.5	15.5 ± 5.2
Fake lepton/ τ	6.2 ± 1.0	5.4 ± 2.7
ggF $H / VH / t\bar{t}H$, $H \rightarrow \tau\tau$	2.1 ± 1.5	2.8 ± 1.4
Other backgrounds	2.8 ± 3.1	2.3 ± 0.8
Sum of backgrounds	19.0 ± 5.5	26.0 ± 6.6

$\tilde{d} \in [-0.035, 0.033]$. This represents an improvement on the confidence interval for \tilde{d} set in Ref. [36]. While no observed 95% CL interval for \tilde{d} can be quoted, the corresponding expected interval is $\tilde{d} \in [-0.21, 0.15]$ at 95% CL. The asymmetry in these expected intervals stems from the slightly asymmetric Optimal Observable distribution of the background estimates in the SRs, caused by the limited sample sizes for the background predictions.

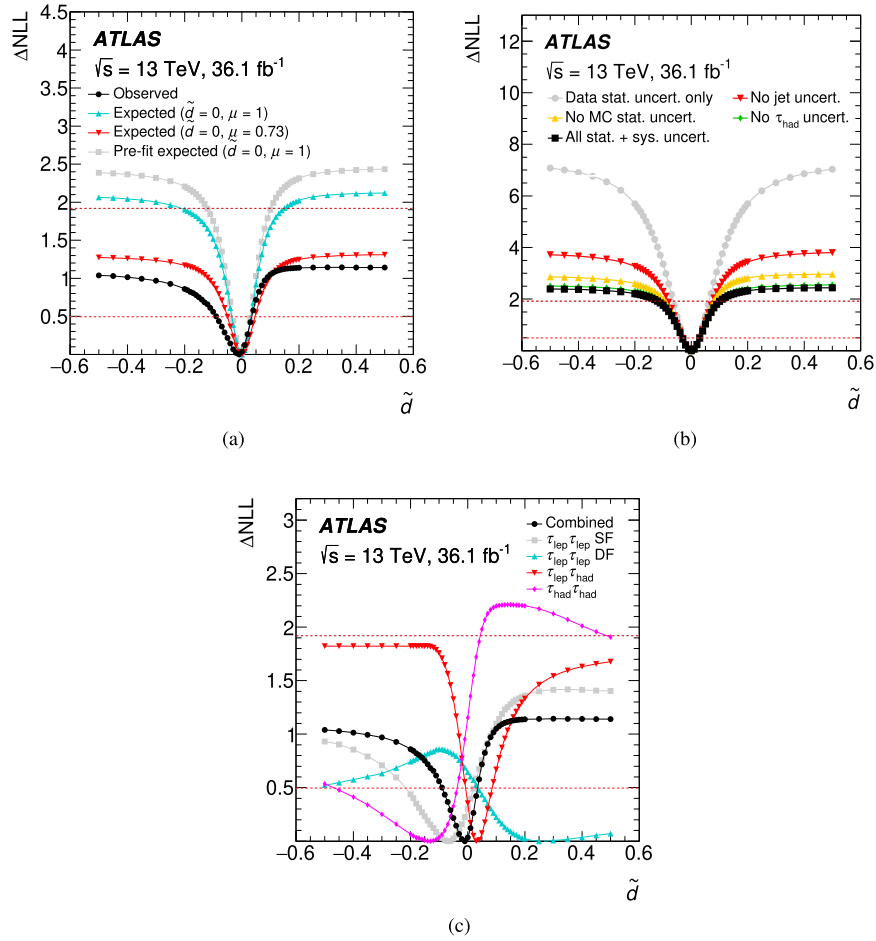


Fig. 6. (a) The observed ΔNLL curve as a function of \tilde{d} values. For comparison, expected ΔNLL curves are also shown. The constraints on the nuisance parameters and normalization factors are first determined in a CR-only fit, and then a fit to pseudo-data corresponding to these nuisance parameters, normalization factors, and to $\tilde{d} = 0, \mu = 1$ or $\tilde{d} = 0, \mu = 0.73$ is performed to obtain these ΔNLL curves. A pre-fit expected ΔNLL is also shown, using pseudo-data corresponding to $\tilde{d} = 0$ and $\mu = 1$ in the signal and control regions. (b) The expected ΔNLL curves ($\tilde{d} = 0, \mu = 1$) comparing the sensitivity of the fit with and without systematic uncertainties. For comparison, other curves are shown which remove the effect of jet-based systematic uncertainties, τ -based systematic uncertainties, and MC statistical uncertainties. (c) The observed ΔNLL curves for each analysis channel as a function of \tilde{d} , compared with the combined result. For the individual analysis channel ΔNLL curves, only event yield information in the other SRs is used, ensuring that the Optimal Observable distributions in the other SRs do not influence the preferred value of \tilde{d} . The signal strength is constrained to be positive in these individual channel ΔNLL curves. For all figures, the dashed horizontal lines show the values of ΔNLL used to define the 68% and 95% confidence intervals.

The intervals based upon the pre-fit expected ΔNLL curve in Fig. 6(a), where the nuisance parameters and background normalization factors do not take into account the observed data in the CRs, are $\tilde{d} \in [-0.032, 0.031]$ at 68% CL and $\tilde{d} \in [-0.12, 0.10]$ at 95% CL.

10. Conclusion

The CP invariance of the Higgs boson coupling to vector bosons has been tested in the VBF $H \rightarrow \tau\tau$ process in 36.1 fb^{-1} of $\sqrt{s} = 13$ TeV proton–proton collision data obtained with the ATLAS detector at the LHC. In this analysis, an Optimal Observable was used and confidence intervals were set on the CP-mixing parameter \tilde{d} .

Since the mean of the Optimal Observable observed in data is consistent with zero, and the obtained confidence intervals for \tilde{d} are consistent with the Standard Model value $\tilde{d} = 0$, no evidence of CP violation is observed from this analysis. Due to lower than expected signal yields in data, no constraints on \tilde{d} can be set at 95% CL, while the corresponding Standard Model expectation is $\tilde{d} \in [-0.21, 0.15]$. An observed 68% CL interval of $\tilde{d} \in [-0.090, 0.035]$ is obtained, while the corresponding interval based on the expectation is $\tilde{d} \in [-0.035, 0.033]$.

Declaration of competing interest

The authors declare that they have no known competing financial interests or personal relationships that could have appeared to influence the work reported in this paper.

Acknowledgements

We thank CERN for the very successful operation of the LHC, as well as the support staff from our institutions without whom ATLAS could not be operated efficiently.

We acknowledge the support of ANPCyT, Argentina; YerPhI, Armenia; ARC, Australia; BMWFW and FWF, Austria; ANAS, Azerbaijan; SSTC, Belarus; CNPq and FAPESP, Brazil; NSERC, NRC and CFI, Canada; CERN; CONICYT, Chile; CAS, MOST and NSFC, China; COLCIENCIAS, Colombia; MSMT CR, MPO CR and VSC CR, Czech Republic; DNRF and DNSRC, Denmark; IN2P3-CNRS and CEA-DRF/IRFU, France; SRNSFG, Georgia; BMBF, HGF and MPG, Germany; GSRT, Greece; RGC and Hong Kong SAR, China; ISF and Benozziyo Center, Israel; INFN, Italy; MEXT and JSPS, Japan; CNRST, Morocco; NWO, Netherlands; RCN, Norway; MNiSW and NCN, Poland; FCT, Portugal; MNE/IFA, Romania; MES of Russia and NRC KI, Russia Federation; JINR; MESTD, Serbia; MSSR, Slovakia; ARRS and MIZŠ, Slovenia; DST/NRF, South Africa; MINECO, Spain; SRC and Wallen-

berg Foundation, Sweden; SERI, SNSF and Cantons of Bern and Geneva, Switzerland; MOST, Taiwan; TAEK, Turkey; STFC, United Kingdom; DOE and NSF, United States of America. In addition, individual groups and members have received support from BCKDF, Canarie, Compute Canada and CRC, Canada; ERC, ERDF, Horizon 2020, Marie Skłodowska-Curie Actions and COST, European Union; Investissements d'Avenir Labex, Investissements d'Avenir IDEX and ANR, France; DFG and AvH Foundation, Germany; Herakleitos, Thales and Aristeia programmes co-financed by EU-ESF and the Greek NSRF, Greece; BSF-NSF and GIF, Israel; CERCA Programme Generalitat de Catalunya and PROMETEO Programme Generalitat Valenciana, Spain; Göran Gustafssons Stiftelse, Sweden; The Royal Society and Leverhulme Trust, United Kingdom.

The crucial computing support from all WLCG partners is acknowledged gratefully, in particular from CERN, the ATLAS Tier-1 facilities at TRIUMF (Canada), NDGF (Denmark, Norway, Sweden), CC-IN2P3 (France), KIT/GridKA (Germany), INFN-CNAF (Italy), NL-T1 (Netherlands), PIC (Spain), ASGC (Taiwan), RAL (UK) and BNL (USA), the Tier-2 facilities worldwide and large non-WLCG resource providers. Major contributors of computing resources are listed in Ref. [120].

References

- [1] A.D. Sakharov, Violation of CP invariance, C asymmetry, and baryon asymmetry of the universe, *Pisma Zh. Eksp. Teor. Fiz.* 5 (1967) 32.
- [2] N. Cabibbo, Unitary symmetry and leptonic decays, *Phys. Rev. Lett.* 10 (1963) 531.
- [3] M. Kobayashi, T. Maskawa, CP-violation in the renormalizable theory of weak interaction, *Prog. Theor. Phys.* 49 (1973) 652.
- [4] J.H. Christenson, J.W. Cronin, V.L. Fitch, R. Turlay, Evidence for the 2π decay of the K_S^0 meson, *Phys. Rev. Lett.* 13 (1964) 138.
- [5] KTeV Collaboration, Observation of direct CP violation in $K_{S,L} \rightarrow \pi\pi$ decays, *Phys. Rev. Lett.* 83 (1999) 22, arXiv:hep-ex/9905060.
- [6] NA48 Collaboration, A precise measurement of the direct CP violation parameter $\text{Re}(\epsilon'/\epsilon)$, *Eur. Phys. J. C* 22 (2001) 231, arXiv:hep-ex/0110019.
- [7] BaBar Collaboration, Observation of CP violation in the B^0 meson system, *Phys. Rev. Lett.* 87 (2001) 091801, arXiv:hep-ex/0107013.
- [8] Belle Collaboration, Observation of large CP violation in the neutral B meson system, *Phys. Rev. Lett.* 87 (2001) 091802, arXiv:hep-ex/0107061.
- [9] BaBar Collaboration, Direct CP violating asymmetry in $B^0 \rightarrow K^+\pi^-$ decays, *Phys. Rev. Lett.* 93 (2004) 131801, arXiv:hep-ex/0407057.
- [10] Belle Collaboration, Evidence for direct CP violation in $B^0 \rightarrow K^+\pi^-$ decays, *Phys. Rev. Lett.* 93 (2004) 191802, arXiv:hep-ex/0408100.
- [11] LHCb Collaboration, First observation of CP violation in the decays of B_S^0 mesons, *Phys. Rev. Lett.* 110 (2013) 221601, arXiv:1304.6173 [hep-ex].
- [12] LHCb Collaboration, Observation of CP violation in $B^\pm \rightarrow DK^\pm$ decays, *Phys. Lett. B* 712 (2012) 203, arXiv:1203.3662 [hep-ex], Erratum: *Phys. Lett. B* 713 (2012) 351.
- [13] LHCb Collaboration, Observation of CP violation in charm decays, *Phys. Rev. Lett.* 122 (2019) 211803, arXiv:1903.08726 [hep-ex].
- [14] J. Charles, et al., Current status of the standard model CKM fit and constraints on $\Delta F = 2$ new physics, *Phys. Rev. D* 91 (2015) 073007, arXiv:1501.05013 [hep-ph].
- [15] C. Alpigiani, et al., Unitarity triangle analysis in the standard model and beyond, in: *Proceedings of the 5th Large Hadron Collider Physics Conference*, 2017, arXiv:1710.09644 [hep-ph].
- [16] P. Huet, E. Sather, Electroweak baryogenesis and standard model CP violation, *Phys. Rev. D* 51 (1995) 379, arXiv:hep-ph/9404302.
- [17] M.B. Gavela, P. Hernández, J. Orloff, O. Pène, Standard model CP-violation and baryon asymmetry, *Mod. Phys. Lett. A* 9 (1994) 795, arXiv:hep-ph/9312215.
- [18] A.G. Cohen, D.B. Kaplan, A.E. Nelson, Progress in electroweak baryogenesis, *Annu. Rev. Nucl. Part. Sci.* 43 (1993) 27, arXiv:hep-ph/9302210.
- [19] A. Riotto, M. Trodden, Recent progress in baryogenesis, *Annu. Rev. Nucl. Part. Sci.* 49 (1999) 35, arXiv:hep-ph/9901362.
- [20] W.-S. Hou, Source of CP violation for the baryon asymmetry of the universe, *Chin. J. Phys.* 47 (2009) 134, arXiv:0803.1234 [hep-ph].
- [21] ATLAS Collaboration, Observation of a new particle in the search for the Standard Model Higgs boson with the ATLAS detector at the LHC, *Phys. Lett. B* 716 (2012) 1, arXiv:1207.7214 [hep-ex].
- [22] CMS Collaboration, Observation of a new boson at a mass of 125 GeV with the CMS experiment at the LHC, *Phys. Lett. B* 716 (2012) 30, arXiv:1207.7235 [hep-ex].
- [23] ATLAS and CMS Collaborations, Measurements of the Higgs boson production and decay rates and constraints on its couplings from a combined ATLAS and CMS analysis of the LHC pp collision data at $\sqrt{s} = 7$ and 8 TeV, *J. High Energy Phys.* 08 (2016) 045, arXiv:1606.02266 [hep-ex].
- [24] ATLAS Collaboration, Combined measurements of Higgs boson production and decay using up to 80 fb^{-1} of proton-proton collision data at $\sqrt{s} = 13$ TeV collected with the ATLAS experiment, *Phys. Rev. D* 101 (2020) 012002, arXiv:1909.02845 [hep-ex].
- [25] CMS Collaboration, Combined measurements of Higgs boson couplings in proton-proton collisions at $\sqrt{s} = 13$ TeV, *Eur. Phys. J. C* 79 (2019) 421, arXiv:1809.10733 [hep-ex].
- [26] ATLAS Collaboration, Evidence for the spin-0 nature of the Higgs boson using ATLAS data, *Phys. Lett. B* 726 (2013) 120, arXiv:1307.1432 [hep-ex].
- [27] ATLAS Collaboration, Study of the spin and parity of the Higgs boson in di-boson decays with the ATLAS detector, *Eur. Phys. J. C* 75 (2015) 476, arXiv:1506.05669 [hep-ex], Erratum: *Eur. Phys. J. C* 76 (2016) 152.
- [28] CMS Collaboration, Study of the mass and spin-parity of the Higgs boson candidate via its decays to Z boson pairs, *Phys. Rev. Lett.* 110 (2013) 081803, arXiv:1212.6639 [hep-ex].
- [29] ATLAS Collaboration, Measurements of Higgs boson properties in the diphoton decay channel with 36 fb^{-1} of pp collision data at $\sqrt{s} = 13$ TeV with the ATLAS detector, *Phys. Rev. D* 98 (2018) 052005, arXiv:1802.04146 [hep-ex].
- [30] ATLAS Collaboration, Measurement of the Higgs boson coupling properties in the $H \rightarrow ZZ^* \rightarrow 4\ell$ decay channel at $\sqrt{s} = 13$ TeV with the ATLAS detector, *J. High Energy Phys.* 03 (2018) 095, arXiv:1712.02304 [hep-ex].
- [31] CMS Collaboration, Combined search for anomalous pseudoscalar HVV couplings in $VH(H \rightarrow b\bar{b})$ production and $H \rightarrow VV$ decay, *Phys. Lett. B* 759 (2016) 672, arXiv:1602.04305 [hep-ex].
- [32] CMS Collaboration, Constraints on the spin-parity and anomalous HVV couplings of the Higgs boson in proton collisions at 7 and 8 TeV, *Phys. Rev. D* 92 (2015) 012004, arXiv:1411.3441 [hep-ex].
- [33] CMS Collaboration, Constraints on anomalous Higgs boson couplings using production and decay information in the four-lepton final state, *Phys. Lett. B* 775 (2017) 1, arXiv:1707.00541 [hep-ex].
- [34] CMS Collaboration, Measurements of the Higgs boson width and anomalous HVV couplings from on-shell and off-shell production in the four-lepton final state, *Phys. Rev. D* 99 (2019) 112003, arXiv:1901.00174 [hep-ex].
- [35] CMS Collaboration, Constraints on anomalous HVV couplings from the production of Higgs bosons decaying to τ lepton pairs, *Phys. Rev. D* 100 (2019) 112002, arXiv:1903.06973 [hep-ex].
- [36] ATLAS Collaboration, Test of CP invariance in vector-boson fusion production of the Higgs boson using the Optimal Observable method in the ditau decay channel with the ATLAS detector, *Eur. Phys. J. C* 76 (2016) 658, arXiv:1602.04516 [hep-ex].
- [37] D. Atwood, A. Soni, Analysis for magnetic moment and electric dipole moment form-factors of the top quark via $e^+e^- \rightarrow t\bar{t}$, *Phys. Rev. D* 45 (1992) 2405.
- [38] M. Davier, L. Duflot, F. Le Diberder, A. Rouge, The optimal method for the measurement of tau polarization, *Phys. Lett. B* 306 (1993) 411.
- [39] M. Diehl, O. Nachtmann, Optimal observables for the measurement of three gauge boson couplings in $e^+e^- \rightarrow W^+W^-$, *Z. Phys. C* 62 (1994) 397.
- [40] J. Brehmer, F. Kling, T. Plehn, T.M.P. Tait, Better Higgs-CP tests through information geometry, *Phys. Rev. D* 97 (2018) 095017, arXiv:1712.02350 [hep-ph].
- [41] ATLAS Collaboration, Cross-section measurements of the Higgs boson decaying into a pair of τ -leptons in proton-proton collisions at $\sqrt{s} = 13$ TeV with the ATLAS detector, *Phys. Rev. D* 99 (2019) 072001, arXiv:1811.08856 [hep-ex].
- [42] L3 Collaboration, Search for anomalous couplings in the Higgs sector at LEP, *Phys. Lett. B* 589 (2004) 89, arXiv:hep-ex/0403037.
- [43] W. Buchmüller, D. Wyler, Effective lagrangian analysis of new interactions and flavor conservation, *Nucl. Phys. B* 268 (1986) 621.
- [44] V. Hankele, G. Klämke, D. Zeppenfeld, T. Figy, Anomalous Higgs boson couplings in vector boson fusion at the CERN LHC, *Phys. Rev. D* 74 (2006) 095001, arXiv:hep-ph/0609075.
- [45] M. Ciccolini, A. Denner, S. Dittmaier, Strong and electroweak corrections to the production of a Higgs boson + 2 jets via weak interactions at the Large Hadron Collider, *Phys. Rev. Lett.* 99 (2007) 161803, arXiv:0707.0381 [hep-ph].
- [46] M. Ciccolini, A. Denner, S. Dittmaier, Electroweak and QCD corrections to Higgs production via vector-boson fusion at the LHC, *Phys. Rev. D* 77 (2008) 013002, arXiv:0710.4749 [hep-ph].
- [47] A. Denner, S. Dittmaier, S. Kallweit, A. Mück, HAWK 2.0: a Monte Carlo program for Higgs production in vector-boson fusion and Higgs strahlung at hadron colliders, *Comput. Phys. Commun.* 195 (2015) 161, arXiv:1412.5390 [hep-ph].
- [48] H.-L. Lai, et al., New parton distributions for collider physics, *Phys. Rev. D* 82 (2010) 074024, arXiv:1007.2241 [hep-ph].
- [49] ATLAS Collaboration, The ATLAS experiment at the CERN Large Hadron Collider, *J. Instrum.* 3 (2008) S08003.
- [50] ATLAS Collaboration, ATLAS Insertable B-Layer Technical Design Report, ATLAS-TDR-19, <https://cds.cern.ch/record/1291633>, 2010, ATLAS Insertable B-Layer Technical Design Report Addendum, ATLAS-TDR-19-ADD-1, <https://cds.cern.ch/record/1451888>, 2012.

- [51] B. Abbott, et al., Production and integration of the ATLAS Insertable B-Layer, *J. Instrum.* 13 (2018) T05008, arXiv:1803.00844 [physics.ins-det].
- [52] G. Avoni, et al., The new LUCID-2 detector for luminosity measurement and monitoring in ATLAS, *J. Instrum.* 13 (2018) P07017.
- [53] ATLAS Collaboration, Performance of the ATLAS trigger system in 2015, *Eur. Phys. J. C* 77 (2017) 317, arXiv:1611.09661 [hep-ex].
- [54] T. Gleisberg, S. Höche, F. Krauss, M. Schönherr, S. Schumann, et al., Event generation with SHERPA 1.1, *J. High Energy Phys.* 02 (2009) 007, arXiv:0811.4622 [hep-ph].
- [55] T. Gleisberg, S. Höche, Comix, a new matrix element generator, *J. High Energy Phys.* 12 (2008) 039, arXiv:0808.3674 [hep-ph].
- [56] F. Cascioli, P. Maierhöfer, S. Pozzorini, Scattering amplitudes with open loops, *Phys. Rev. Lett.* 108 (2012) 111601, arXiv:1111.5206 [hep-ph].
- [57] S. Höche, F. Krauss, S. Schumann, F. Siegert, QCD matrix elements and truncated showers, *J. High Energy Phys.* 05 (2009) 053, arXiv:0903.1219 [hep-ph].
- [58] ATLAS Collaboration, Measurement of the cross-section for electroweak production of dijets in association with a Z boson in pp collisions at $\sqrt{s} = 13$ TeV with the ATLAS detector, *Phys. Lett. B* 775 (2017) 206, arXiv:1709.10264 [hep-ex].
- [59] P. Nason, A new method for combining NLO QCD with shower Monte Carlo algorithms, *J. High Energy Phys.* 11 (2004) 040, arXiv:hep-ph/0409146.
- [60] S. Frixione, P. Nason, C. Oleari, Matching NLO QCD computations with parton shower simulations: the POWHEG method, *J. High Energy Phys.* 11 (2007) 070, arXiv:0709.2092 [hep-ph].
- [61] S. Alioli, P. Nason, C. Oleari, E. Re, A general framework for implementing NLO calculations in shower Monte Carlo programs: the POWHEG BOX, *J. High Energy Phys.* 06 (2010) 043, arXiv:1002.2581 [hep-ph].
- [62] K. Hamilton, P. Nason, G. Zanderighi, MINLO: multi-scale improved NLO, *J. High Energy Phys.* 10 (2012) 155, arXiv:1206.3572 [hep-ph].
- [63] P. Nason, C. Oleari, NLO Higgs boson production via vector-boson fusion matched with shower in POWHEG, *J. High Energy Phys.* 02 (2010) 037, arXiv:0911.5299 [hep-ph].
- [64] J. Butterworth, et al., PDF4LHC recommendations for LHC Run II, *J. Phys. G* 43 (2016) 023001, arXiv:1510.03865 [hep-ph].
- [65] T. Sjöstrand, et al., An introduction to PYTHIA 8.2, *Comput. Phys. Commun.* 191 (2015) 159, arXiv:1410.3012 [hep-ph].
- [66] P. Bolzoni, F. Maltoni, S.-O. Moch, M. Zaro, Higgs boson production via vector-boson fusion at next-to-next-to-leading order in QCD, *Phys. Rev. Lett.* 105 (2010) 011801, arXiv:1003.4451 [hep-ph].
- [67] M. Bahr, et al., Herwig++ physics and manual, *Eur. Phys. J. C* 58 (2008) 639, arXiv:0803.0883 [hep-ph].
- [68] J. Bellm, et al., Herwig 7.0/Herwig++ 3.0 release note, *Eur. Phys. J. C* 76 (2016) 196, arXiv:1512.01178 [hep-ph].
- [69] C. Anastasiou, C. Duhr, F. Dulat, F. Herzog, B. Mistlberger, Higgs boson gluon-fusion production in QCD at three loops, *Phys. Rev. Lett.* 114 (2015) 212001, arXiv:1503.06056 [hep-ph].
- [70] C. Anastasiou, et al., High precision determination of the gluon fusion Higgs boson cross-section at the LHC, *J. High Energy Phys.* 05 (2016) 058, arXiv:1602.00695 [hep-ph].
- [71] S. Actis, G. Passarino, C. Sturm, S. Uccirati, NLO electroweak corrections to Higgs boson production at hadron colliders, *Phys. Lett. B* 670 (2008) 12, arXiv:0809.1301 [hep-ph].
- [72] C. Anastasiou, R. Boughezal, F. Petriello, Mixed QCD-electroweak corrections to Higgs boson production in gluon fusion, *J. High Energy Phys.* 04 (2009) 003, arXiv:0811.3458 [hep-ph].
- [73] J.M. Campbell, et al., NLO Higgs boson production plus one and two jets using the POWHEG BOX, MadGraph4 and MCFM, *J. High Energy Phys.* 07 (2012) 092, arXiv:1202.5475 [hep-ph].
- [74] K. Hamilton, P. Nason, E. Re, G. Zanderighi, NNLO simulation of Higgs boson production, *J. High Energy Phys.* 10 (2013) 222, arXiv:1309.0017 [hep-ph].
- [75] K. Hamilton, P. Nason, G. Zanderighi, Finite quark-mass effects in the NNLO POWHEG+MiNLO Higgs generator, *J. High Energy Phys.* 05 (2015) 140, arXiv:1501.04637 [hep-ph].
- [76] G. Luisoni, P. Nason, C. Oleari, F. Tramontano, $HW^\pm/HZ + 0$ and 1 jet at NLO with the POWHEG BOX interfaced to GoSam and their merging within MiNLO, *J. High Energy Phys.* 10 (2013) 083, arXiv:1306.2542 [hep-ph].
- [77] O. Brein, A. Djouadi, R. Harlander, NNLO QCD corrections to the Higgs-strahlung processes at hadron colliders, *Phys. Lett. B* 579 (2004) 149, arXiv:hep-ph/0307206.
- [78] A. Denner, S. Dittmaier, S. Kallweit, A. Mück, Electroweak corrections to Higgs-strahlung off W/Z bosons at the Tevatron and the LHC with Hawk, *J. High Energy Phys.* 03 (2012) 075, arXiv:1112.5142 [hep-ph].
- [79] L. Altenkamp, S. Dittmaier, R.V. Harlander, H. Rzehak, T.J.E. Zirke, Gluon-induced Higgs-strahlung at next-to-leading order QCD, *J. High Energy Phys.* 02 (2013) 078, arXiv:1211.5015 [hep-ph].
- [80] R.V. Harlander, A. Kulesza, V. Theeuwes, T. Zirke, Soft gluon resummation for gluon-induced Higgs Strahlung, *J. High Energy Phys.* 11 (2014) 082, arXiv:1410.0217 [hep-ph].
- [81] J. Alwall, et al., The automated computation of tree-level and next-to-leading order differential cross sections, and their matching to parton shower simulations, *J. High Energy Phys.* 07 (2014) 079, arXiv:1405.0301 [hep-ph].
- [82] R. Frederix, S. Frixione, Merging meets matching in MC@NLO, *J. High Energy Phys.* 12 (2012) 061, arXiv:1209.6215 [hep-ph].
- [83] R.D. Ball, et al., Parton distributions for the LHC Run II, *J. High Energy Phys.* 04 (2015) 040, arXiv:1410.8849 [hep-ph].
- [84] W. Beenakker, et al., Higgs radiation off top quarks at the Tevatron and the LHC, *Phys. Rev. Lett.* 87 (2001) 201805, arXiv:hep-ph/0107081.
- [85] W. Beenakker, et al., NLO QCD corrections to $t\bar{t}H$ production in hadron collisions, *Nucl. Phys. B* 653 (2003) 151, arXiv:hep-ph/0211352.
- [86] S. Dawson, L.H. Orr, L. Reina, D. Wackerroth, Next-to-leading order QCD corrections to $pp \rightarrow t\bar{t}H$ at the CERN Large Hadron Collider, *Phys. Rev. D* 67 (2003) 071503, arXiv:hep-ph/0211438.
- [87] S. Dawson, C. Jackson, L.H. Orr, L. Reina, D. Wackerroth, Associated Higgs boson production with top quarks at the CERN Large Hadron Collider: NLO QCD corrections, *Phys. Rev. D* 68 (2003) 034022, arXiv:hep-ph/0305087.
- [88] Y. Zhang, W.-G. Ma, R.-Y. Zhang, C. Chen, L. Guo, QCD NLO and EW NLO corrections to $t\bar{t}H$ production with top quark decays at hadron collider, *Phys. Lett. B* 738 (2014) 1, arXiv:1407.1110 [hep-ph].
- [89] S. Frixione, V. Hirschi, D. Pagani, H.-S. Shao, M. Zaro, Electroweak and QCD corrections to top-pair hadroproduction in association with heavy bosons, *J. High Energy Phys.* 06 (2015) 184, arXiv:1504.03446 [hep-ph].
- [90] S. Höche, F. Krauss, M. Schönherr, F. Siegert, QCD matrix elements + parton showers. The NLO case, *J. High Energy Phys.* 04 (2013) 027, arXiv:1207.5030 [hep-ph].
- [91] S. Schumann, F. Krauss, A parton shower algorithm based on Catani-Seymour dipole factorisation, *J. High Energy Phys.* 03 (2008) 038, arXiv:0709.1027 [hep-ph].
- [92] K. Melnikov, F. Petriello, Electroweak gauge boson production at hadron colliders through $O(\alpha_s^2)$, *Phys. Rev. D* 74 (2006) 114017, arXiv:hep-ph/0609070.
- [93] C. Anastasiou, L. Dixon, K. Melnikov, F. Petriello, High precision QCD at hadron colliders: electroweak gauge boson rapidity distributions at next-to-next-to-leading order, *Phys. Rev. D* 69 (2004) 094008, arXiv:hep-ph/0312266.
- [94] S. Alioli, S.-O. Moch, P. Uwer, Hadronic top-quark pair-production with one jet and parton showering, *J. High Energy Phys.* 01 (2012) 137, arXiv:1110.5251 [hep-ph].
- [95] T. Sjöstrand, S. Mrenna, P.Z. Skands, PYTHIA 6.4 physics and manual, *J. High Energy Phys.* 05 (2006) 026, arXiv:hep-ph/0603175.
- [96] M. Czakon, P. Fiedler, A. Mitov, Total top-quark pair-production cross section at hadron colliders through $O(\alpha_s^3)$, *Phys. Rev. Lett.* 110 (2013) 252004, arXiv:1303.6254 [hep-ph].
- [97] E. Re, Single-top Wt-channel production matched with parton showers using the POWHEG method, *Eur. Phys. J. C* 71 (2011) 1547, arXiv:1009.2450 [hep-ph].
- [98] F. Maltoni, K. Mawatari, M. Zaro, Higgs characterisation via vector-boson fusion and associated production: NLO and parton-shower effects, *Eur. Phys. J. C* 74 (2014) 2710, arXiv:1311.1829 [hep-ph].
- [99] ATLAS Collaboration, The ATLAS simulation infrastructure, *Eur. Phys. J. C* 70 (2010) 823, arXiv:1005.4568 [physics.ins-det].
- [100] S. Agostinelli, et al., Geant4—a simulation toolkit, *Nucl. Instrum. Methods Phys. Res., Sect. A* 506 (2003) 250.
- [101] A.D. Martin, W.J. Stirling, R.S. Thorne, G. Watt, Parton distributions for the LHC, *Eur. Phys. J. C* 63 (2009) 189, arXiv:0901.0002 [hep-ph].
- [102] ATLAS Collaboration, Summary of ATLAS Pythia 8 tunes, ATL-PHYS-PUB-2012-003, <https://cds.cern.ch/record/1474107>, 2012.
- [103] J.H. Friedman, Greedy function approximation: a gradient boosting machine, *Ann. Stat.* 29 (2001) 1189.
- [104] ATLAS Collaboration, ATLAS data quality operations and performance for 2015–2018 data-taking, arXiv:1911.04632 [hep-ex], 2019.
- [105] R.K. Ellis, I. Hinchliffe, M. Soldate, J.J. Van Der Bij, Higgs decay to $\tau^+\tau^-$: a possible signature of intermediate mass Higgs bosons at high energy hadron colliders, *Nucl. Phys. B* 297 (1988) 221.
- [106] ATLAS Collaboration, Observation and measurement of Higgs boson decays to WW^* with the ATLAS detector, *Phys. Rev. D* 92 (2015) 012006, arXiv:1412.2641 [hep-ex].
- [107] ATLAS Collaboration, Performance of b-jet identification in the ATLAS experiment, *J. Instrum.* 11 (2016) P04008, arXiv:1512.01094 [hep-ex].
- [108] ATLAS Collaboration, Optimisation of the ATLAS b-tagging performance for the 2016 LHC Run, ATL-PHYS-PUB-2016-012, <https://cds.cern.ch/record/2160731>, 2016.
- [109] A. Elagin, P. Murat, A. Pranko, A. Safonov, A new mass reconstruction technique for resonances decaying to $\tau\tau$, *Nucl. Instrum. Methods Phys. Res., Sect. A* 654 (2011) 481, arXiv:1012.4686 [hep-ex].
- [110] ATLAS Collaboration, Jet energy scale measurements and their systematic uncertainties in proton–proton collisions at $\sqrt{s} = 13$ TeV with the ATLAS detector, *Phys. Rev. D* 96 (2017) 072002, arXiv:1703.09665 [hep-ex].
- [111] ATLAS Collaboration, Reconstruction, energy calibration, and identification of hadronically decaying tau leptons in the ATLAS experiment for Run-2 of the LHC, ATL-PHYS-PUB-2015-045, <https://cds.cern.ch/record/2064383>, 2015.
- [112] ATLAS Collaboration, Measurement of the tau lepton reconstruction and identification performance in the ATLAS experiment using pp collisions at $\sqrt{s} = 13$ TeV, ATLAS-CONF-2017-029, <https://cds.cern.ch/record/2261772>, 2017.

- [113] ATLAS Collaboration, Electron and photon energy calibration with the ATLAS detector using 2015–2016 LHC proton–proton collision data, *J. Instrum.* **14** (2019) P03017, arXiv:1812.03848 [hep-ex].
- [114] ATLAS Collaboration, Electron reconstruction and identification in the ATLAS experiment using the 2015 and 2016 LHC proton–proton collision data at $\sqrt{s} = 13$ TeV, *Eur. Phys. J. C* **79** (2019) 639, arXiv:1902.04655 [hep-ex].
- [115] ATLAS Collaboration, Muon reconstruction performance of the ATLAS detector in proton–proton collision data at $\sqrt{s} = 13$ TeV, *Eur. Phys. J. C* **76** (2016) 292, arXiv:1603.05598 [hep-ex].
- [116] ATLAS Collaboration, Performance of missing transverse momentum reconstruction with the ATLAS detector using proton–proton collisions at $\sqrt{s} = 13$ TeV, *Eur. Phys. J. C* **78** (2018) 903, arXiv:1802.08168 [hep-ex].
- [117] ATLAS Collaboration, Measurement of b -tagging efficiency of c -jets in $t\bar{t}$ events using a likelihood approach with the ATLAS detector, ATLAS-CONF-2018-001, <https://cds.cern.ch/record/2306649>, 2018.
- [118] ATLAS Collaboration, Luminosity determination in pp collisions at $\sqrt{s} = 13$ TeV using the ATLAS detector at the LHC, ATLAS-CONF-2019-021, <https://cds.cern.ch/record/2677054>, 2019.
- [119] LHC Higgs Cross Section Working Group, Handbook of LHC Higgs cross sections: 4. Deciphering the nature of the Higgs sector, arXiv:1610.07922 [hep-ph], 2016.
- [120] ATLAS Collaboration, ATLAS computing acknowledgements, ATL-GEN-PUB-2016-002, <https://cds.cern.ch/record/2202407>.

The ATLAS Collaboration

G. Aad¹⁰², B. Abbott¹²⁹, D.C. Abbott¹⁰³, A. Abed Abud³⁶, K. Abeling⁵³, D.K. Abhayasinghe⁹⁴, S.H. Abidi¹⁶⁷, O.S. AbouZeid⁴⁰, N.L. Abraham¹⁵⁶, H. Abramowicz¹⁶¹, H. Abreu¹⁶⁰, Y. Abulaiti⁶, B.S. Acharya^{67a,67b,n}, B. Achkar⁵³, S. Adachi¹⁶³, L. Adam¹⁰⁰, C. Adam Bourdarios⁵, L. Adamczyk^{84a}, L. Adamek¹⁶⁷, J. Adelman¹²¹, M. Adersberger¹¹⁴, A. Adiguzel^{12c}, S. Adorni⁵⁴, T. Adye¹⁴⁴, A.A. Affolder¹⁴⁶, Y. Afik¹⁶⁰, C. Agapopoulou⁶⁵, M.N. Agaras³⁸, A. Aggarwal¹¹⁹, C. Agheorghiesei^{27c}, J.A. Aguilar-Saavedra^{140f,140a,af}, F. Ahmadov⁸⁰, W.S. Ahmed¹⁰⁴, X. Ai¹⁸, G. Aielli^{74a,74b}, S. Akatsuka⁸⁶, T.P.A. Åkesson⁹⁷, E. Akilli⁵⁴, A.V. Akimov¹¹¹, K. Al Khoury⁶⁵, G.L. Alberghi^{23b,23a}, J. Albert¹⁷⁶, M.J. Alconada Verzini¹⁶¹, S. Alderweireldt³⁶, M. Aleksa³⁶, I.N. Aleksandrov⁸⁰, C. Alexa^{27b}, T. Alexopoulos¹⁰, A. Alfonsi¹²⁰, F. Alfonsi^{23b,23a}, M. Alhroob¹²⁹, B. Ali¹⁴², M. Aliev¹⁶⁶, G. Alimonti^{69a}, C. Allaire⁶⁵, B.M.M. Allbrooke¹⁵⁶, B.W. Allen¹³², P.P. Allport²¹, A. Aloisio^{70a,70b}, F. Alonso⁸⁹, C. Alpigiani¹⁴⁸, A.A. Alshehri⁵⁷, E. Alunno Camelia^{74a,74b}, M. Alvarez Estevez⁹⁹, M.G. Alvigi^{70a,70b}, Y. Amaral Coutinho^{81b}, A. Ambler¹⁰⁴, L. Ambroz¹³⁵, C. Amelung²⁶, D. Amidei¹⁰⁶, S.P. Amor Dos Santos^{140a}, S. Amoroso⁴⁶, C.S. Amrouche⁵⁴, F. An⁷⁹, C. Anastopoulos¹⁴⁹, N. Andari¹⁴⁵, T. Andeen¹¹, C.F. Anders^{61b}, J.K. Anders²⁰, A. Andreazza^{69a,69b}, V. Andrei^{61a}, C.R. Anelli¹⁷⁶, S. Angelidakis³⁸, A. Angerami³⁹, A.V. Anisenkov^{122b,122a}, A. Annovi^{72a}, C. Antel⁵⁴, M.T. Anthony¹⁴⁹, E. Antipov¹³⁰, M. Antonelli⁵¹, D.J.A. Antrim¹⁷¹, F. Anulli^{73a}, M. Aoki⁸², J.A. Aparisi Pozo¹⁷⁴, L. Aperio Bella^{15a}, J.P. Araque^{140a}, V. Araujo Ferraz^{81b}, R. Araujo Pereira^{81b}, C. Arcangeletti⁵¹, A.T.H. Arce⁴⁹, F.A. Arduh⁸⁹, J.-F. Arguin¹¹⁰, S. Argyropoulos⁵², J.-H. Arling⁴⁶, A.J. Armbruster³⁶, A. Armstrong¹⁷¹, O. Arnaez¹⁶⁷, H. Arnold¹²⁰, Z.P. Arrubarrena Tame¹¹⁴, G. Artoni¹³⁵, S. Artz¹⁰⁰, S. Asai¹⁶³, T. Asawatavonvanich¹⁶⁵, N. Asbah⁵⁹, E.M. Asimakopoulou¹⁷², L. Asquith¹⁵⁶, J. Assahsah^{35d}, K. Assamagan²⁹, R. Astalos^{28a}, R.J. Atkin^{33a}, M. Atkinson¹⁷³, N.B. Atlay¹⁹, H. Atmani⁶⁵, K. Augsten¹⁴², G. Avolio³⁶, M.K. Ayoub^{15a}, G. Azuelos^{110,ao}, H. Bachacou¹⁴⁵, K. Bachas^{68a,68b}, M. Backes¹³⁵, F. Backman^{45a,45b}, P. Bagnaia^{73a,73b}, M. Bahmani⁸⁵, H. Bahrasemani¹⁵², A.J. Bailey¹⁷⁴, V.R. Bailey¹⁷³, J.T. Baines¹⁴⁴, C. Bakalis¹⁰, O.K. Baker¹⁸³, P.J. Bakker¹²⁰, D. Bakshi Gupta⁸, S. Balaji¹⁵⁷, E.M. Baldin^{122b,122a}, P. Balek¹⁸⁰, F. Balli¹⁴⁵, W.K. Balunas¹³⁵, J. Balz¹⁰⁰, E. Banas⁸⁵, A. Bandyopadhyay²⁴, Sw. Banerjee^{181,i}, A.A.E. Bannoura¹⁸², L. Barak¹⁶¹, W.M. Barbe³⁸, E.L. Barberio¹⁰⁵, D. Barberis^{55b,55a}, M. Barbero¹⁰², G. Barbour⁹⁵, T. Barillari¹¹⁵, M.-S. Barisits³⁶, J. Barkeloo¹³², T. Barklow¹⁵³, R. Barnea¹⁶⁰, B.M. Barnett¹⁴⁴, R.M. Barnett¹⁸, Z. Barnovska-Blenessy^{60a}, A. Baroncelli^{60a}, G. Barone²⁹, A.J. Barr¹³⁵, L. Barranco Navarro^{45a,45b}, F. Barreiro⁹⁹, J. Barreiro Guimarães da Costa^{15a}, S. Barsov¹³⁸, R. Bartoldus¹⁵³, G. Bartolini¹⁰², A.E. Barton⁹⁰, P. Bartos^{28a}, A. Basalae⁴⁶, A. Basan¹⁰⁰, A. Bassalat^{65,ak}, M.J. Basso¹⁶⁷, R.L. Bates⁵⁷, S. Batlamous^{35e}, J.R. Batley³², B. Batool¹⁵¹, M. Battaglia¹⁴⁶, M. Bauce^{73a,73b}, F. Bauer¹⁴⁵, K.T. Bauer¹⁷¹, H.S. Bawa³¹, J.B. Beacham⁴⁹, T. Beau¹³⁶, P.H. Beauchemin¹⁷⁰, F. Becherer⁵², P. Bechtel²⁴, H.C. Beck⁵³, H.P. Beck^{20,r}, K. Becker¹⁷⁸, C. Becot⁴⁶, A. Beddall^{12d}, A.J. Beddall^{12a}, V.A. Bednyakov⁸⁰, M. Bedognetti¹²⁰, C.P. Bee¹⁵⁵, T.A. Beermann¹⁸², M. Begalli^{81b}, M. Begel²⁹, A. Behera¹⁵⁵, J.K. Behr⁴⁶, F. Beisiegel²⁴, A.S. Bell⁹⁵, G. Bella¹⁶¹, L. Bellagamba^{23b}, A. Bellerive³⁴, P. Bellos⁹, K. Beloborodov^{122b,122a}, K. Belotskiy¹¹², N.L. Belyaev¹¹², D. Benchekroun^{35a}, N. Benekos¹⁰, Y. Benhammou¹⁶¹, D.P. Benjamin⁶, M. Benoit⁵⁴, J.R. Bensinger²⁶, S. Bentvelsen¹²⁰, L. Beresford¹³⁵, M. Bernetta⁵¹, D. Berge¹⁹, E. Bergeaas Kuutmann¹⁷², N. Berger⁵, B. Bergmann¹⁴², L.J. Bergsten²⁶, J. Beringer¹⁸, S. Berlendis⁷, G. Bernardi¹³⁶, C. Bernius¹⁵³, F.U. Bernlochner²⁴, T. Berry⁹⁴, P. Berta¹⁰⁰, C. Bertella^{15a}, I.A. Bertram⁹⁰, O. Bessidskaia Bylund¹⁸², N. Besson¹⁴⁵, A. Bethani¹⁰¹, S. Bethke¹¹⁵, A. Betti⁴², A.J. Bevan⁹³, J. Beyer¹¹⁵, D.S. Bhattacharya¹⁷⁷, P. Bhattarai²⁶, R. Bi¹³⁹, R.M. Bianchi¹³⁹, O. Biebel¹¹⁴, D. Biedermann¹⁹, R. Bielski³⁶, K. Bierwagen¹⁰⁰, N.V. Biesuz^{72a,72b}, M. Biglietti^{75a},

T.R.V. Billoud¹¹⁰, M. Bindi⁵³, A. Bingul^{12d}, C. Bini^{73a,73b}, S. Biondi^{23b,23a}, M. Birman¹⁸⁰, T. Bisanz⁵³, J.P. Biswal³, D. Biswas^{181,i}, A. Bitadze¹⁰¹, C. Bittrich⁴⁸, K. Bjørke¹³⁴, T. Blazek^{28a}, I. Bloch⁴⁶, C. Blocker²⁶, A. Blue⁵⁷, U. Blumenschein⁹³, G.J. Bobbink¹²⁰, V.S. Bobrovnikov^{122b,122a}, S.S. Bocchetta⁹⁷, A. Bocci⁴⁹, D. Boerner⁴⁶, D. Bogavac¹⁴, A.G. Bogdanchikov^{122b,122a}, C. Boehm^{45a}, V. Boisvert⁹⁴, P. Bokan^{53,172}, T. Bold^{84a}, A.E. Bolz^{61b}, M. Bomben¹³⁶, M. Bona⁹³, J.S. Bonilla¹³², M. Boonekamp¹⁴⁵, C.D. Booth⁹⁴, H.M. Borecka-Bielska⁹¹, L.S. Borgna⁹⁵, A. Borisov¹²³, G. Borissov⁹⁰, J. Bortfeldt³⁶, D. Bortoletto¹³⁵, D. Boscherini^{23b}, M. Bosman¹⁴, J.D. Bossio Sola¹⁰⁴, K. Bouaouda^{35a}, J. Boudreau¹³⁹, E.V. Bouhova-Thacker⁹⁰, D. Boumediene³⁸, S.K. Boutle⁵⁷, A. Boveia¹²⁷, J. Boyd³⁶, D. Boye^{33c,al}, I.R. Boyko⁸⁰, A.J. Bozson⁹⁴, J. Bracinik²¹, N. Brahimi¹⁰², G. Brandt¹⁸², O. Brandt³², F. Braren⁴⁶, B. Brau¹⁰³, J.E. Brau¹³², W.D. Breaden Madden⁵⁷, K. Brendlinger⁴⁶, L. Brenner⁴⁶, R. Brenner¹⁷², S. Bressler¹⁸⁰, B. Brickwedde¹⁰⁰, D.L. Briglin²¹, D. Britton⁵⁷, D. Britzger¹¹⁵, I. Brock²⁴, R. Brock¹⁰⁷, G. Brooijmans³⁹, W.K. Brooks^{147d}, E. Brost²⁹, J.H. Broughton²¹, P.A. Bruckman de Renstrom⁸⁵, D. Bruncko^{28b}, A. Bruni^{23b}, G. Bruni^{23b}, L.S. Bruni¹²⁰, S. Bruno^{74a,74b}, M. Bruschi^{23b}, N. Brusino^{73a,73b}, P. Bryant³⁷, L. Bryngemark⁹⁷, T. Buanes¹⁷, Q. Buat³⁶, P. Buchholz¹⁵¹, A.G. Buckley⁵⁷, I.A. Budagov⁸⁰, M.K. Bugge¹³⁴, F. Bühner⁵², O. Bulekov¹¹², T.J. Burch¹²¹, S. Burdin⁹¹, C.D. Burgard¹²⁰, A.M. Burger¹³⁰, B. Burghgrave⁸, J.T.P. Burr⁴⁶, C.D. Burton¹¹, J.C. Burzynski¹⁰³, V. Büscher¹⁰⁰, E. Buschmann⁵³, P.J. Bussey⁵⁷, J.M. Butler²⁵, C.M. Buttar⁵⁷, J.M. Butterworth⁹⁵, P. Butti³⁶, W. Buttinger³⁶, C.J. Buxo Vazquez¹⁰⁷, A. Buzatu¹⁵⁸, A.R. Buzykaev^{122b,122a}, G. Cabras^{23b,23a}, S. Cabrera Urbán¹⁷⁴, D. Caforio⁵⁶, H. Cai¹⁷³, V.M.M. Cairo¹⁵³, O. Cakir^{4a}, N. Calace³⁶, P. Calafiura¹⁸, A. Calandri¹⁰², G. Calderini¹³⁶, P. Calfayan⁶⁶, G. Callea⁵⁷, L.P. Caloba^{81b}, A. Caltabiano^{74a,74b}, S. Calvente Lopez⁹⁹, D. Calvet³⁸, S. Calvet³⁸, T.P. Calvet¹⁵⁵, M. Calvetti^{72a,72b}, R. Camacho Toro¹³⁶, S. Camarda³⁶, D. Camarero Munoz⁹⁹, P. Camarri^{74a,74b}, D. Cameron¹³⁴, C. Camincher³⁶, S. Campana³⁶, M. Campanelli⁹⁵, A. Camplani⁴⁰, A. Campoverde¹⁵¹, V. Canale^{70a,70b}, A. Canesse¹⁰⁴, M. Cano Bret^{60c}, J. Cantero¹³⁰, T. Cao¹⁶¹, Y. Cao¹⁷³, M.D.M. Capeans Garrido³⁶, M. Capua^{41b,41a}, R. Cardarelli^{74a}, F. Cardillo¹⁴⁹, G. Carducci^{41b,41a}, I. Carli¹⁴³, T. Carli³⁶, G. Carlino^{70a}, B.T. Carlson¹³⁹, L. Carminati^{69a,69b}, R.M.D. Carney¹⁵³, S. Caron¹¹⁹, E. Carquin^{147d}, S. Carrá⁴⁶, J.W.S. Carter¹⁶⁷, M.P. Casado^{14,e}, A.F. Casha¹⁶⁷, R. Castelijns¹²⁰, F.L. Castillo¹⁷⁴, L. Castillo Garcia¹⁴, V. Castillo Gimenez¹⁷⁴, N.F. Castro^{140a,140e}, A. Catinaccio³⁶, J.R. Catmore¹³⁴, A. Cattai³⁶, V. Cavaliere²⁹, E. Cavallaro¹⁴, M. Cavalli-Sforza¹⁴, V. Cavasinni^{72a,72b}, E. Celebi^{12b}, L. Cerda Alberich¹⁷⁴, K. Cerny¹³¹, A.S. Cerqueira^{81a}, A. Cerri¹⁵⁶, L. Cerrito^{74a,74b}, F. Cerutti¹⁸, A. Cervelli^{23b,23a}, S.A. Cetin^{12b}, Z. Chadi^{35a}, D. Chakraborty¹²¹, J. Chan¹⁸¹, W.S. Chan¹²⁰, W.Y. Chan⁹¹, J.D. Chapman³², B. Chargeishvili^{159b}, D.G. Charlton²¹, T.P. Charman⁹³, C.C. Chau³⁴, S. Che¹²⁷, S. Chekanov⁶, S.V. Chekulaev^{168a}, G.A. Chelkov⁸⁰, B. Chen⁷⁹, C. Chen^{60a}, C.H. Chen⁷⁹, H. Chen²⁹, J. Chen^{60a}, J. Chen³⁹, J. Chen²⁶, S. Chen¹³⁷, S.J. Chen^{15c}, X. Chen^{15b}, Y.-H. Chen⁴⁶, H.C. Cheng^{63a}, H.J. Cheng^{15a}, A. Cheplakov⁸⁰, E. Cheremushkina¹²³, R. Cherkaoui El Moursli^{35e}, E. Cheu⁷, K. Cheung⁶⁴, T.J.A. Chevaléras¹⁴⁵, L. Chevalier¹⁴⁵, V. Chiarella⁵¹, G. Chiarelli^{72a}, G. Chiodini^{68a}, A.S. Chisholm²¹, A. Chitan^{27b}, I. Chiu¹⁶³, Y.H. Chiu¹⁷⁶, M.V. Chizhov⁸⁰, K. Choi¹¹, A.R. Chomont^{73a,73b}, S. Chouridou¹⁶², Y.S. Chow¹²⁰, M.C. Chu^{63a}, X. Chu^{15a,15d}, J. Chudoba¹⁴¹, J.J. Chwastowski⁸⁵, L. Chytka¹³¹, D. Cieri¹¹⁵, K.M. Ciesla⁸⁵, D. Cinca⁴⁷, V. Cindro⁹², I.A. Cioară^{27b}, A. Ciocio¹⁸, F. Ciotto^{70a,70b}, Z.H. Citron^{180,j}, M. Citterio^{69a}, D.A. Ciubotaru^{27b}, B.M. Ciungu¹⁶⁷, A. Clark⁵⁴, M.R. Clark³⁹, P.J. Clark⁵⁰, C. Clement^{45a,45b}, Y. Coadou¹⁰², M. Cobal^{67a,67c}, A. Coccaro^{55b}, J. Cochran⁷⁹, R. Coelho Lopes De Sa¹⁰³, H. Cohen¹⁶¹, A.E.C. Coimbra³⁶, B. Cole³⁹, A.P. Colijn¹²⁰, J. Collot⁵⁸, P. Conde Muiño^{140a,140h}, S.H. Connell^{33c}, I.A. Connelly⁵⁷, S. Constantinescu^{27b}, F. Conventi^{70a,ap}, A.M. Cooper-Sarkar¹³⁵, F. Cormier¹⁷⁵, K.J.R. Cormier¹⁶⁷, L.D. Corpe⁹⁵, M. Corradi^{73a,73b}, E.E. Corrigan⁹⁷, F. Corriveau^{104,ad}, A. Cortes-Gonzalez³⁶, M.J. Costa¹⁷⁴, F. Costanza⁵, D. Costanzo¹⁴⁹, G. Cowan⁹⁴, J.W. Cowley³², J. Crane¹⁰¹, K. Cranmer¹²⁵, S.J. Crawley⁵⁷, R.A. Creager¹³⁷, S. Crépe-Renaudin⁵⁸, F. Crescioli¹³⁶, M. Cristinziani²⁴, V. Croft¹⁷⁰, G. Crosetti^{41b,41a}, A. Cueto⁵, T. Cuhadar Donszelmann¹⁴⁹, A.R. Cukierman¹⁵³, W.R. Cunningham⁵⁷, S. Czekierda⁸⁵, P. Czodrowski³⁶, M.J. Da Cunha Sargedas De Sousa^{60b}, J.V. Da Fonseca Pinto^{81b}, C. Da Via¹⁰¹, W. Dabrowski^{84a}, F. Dachs³⁶, T. Dado^{28a}, S. Dahbi^{33e}, T. Dai¹⁰⁶, C. Dallapiccola¹⁰³, M. Dam⁴⁰, G. D'amen²⁹, V. D'Amico^{75a,75b}, J. Damp¹⁰⁰, J.R. Dandoy¹³⁷, M.F. Daneri³⁰, N.S. Dann¹⁰¹, M. Danninger¹⁵², V. Dao³⁶, G. Darbo^{55b}, O. Dartsis⁵, A. Dattagupta¹³², T. Daubney⁴⁶, S. D'Auria^{69a,69b}, C. David^{168b}, T. Davidek¹⁴³, D.R. Davis⁴⁹, I. Dawson¹⁴⁹, K. De⁸, R. De Asmundis^{70a}, M. De Beurs¹²⁰, S. De Castro^{23b,23a}, S. De Cecco^{73a,73b}, N. De Groot¹¹⁹, P. de Jong¹²⁰, H. De la Torre¹⁰⁷, A. De Maria^{15c}, D. De Pedis^{73a},

A. De Salvo ^{73a}, U. De Sanctis ^{74a,74b}, M. De Santis ^{74a,74b}, A. De Santo ¹⁵⁶, K. De Vasconcelos Corga ¹⁰²,
 J.B. De Vivie De Regie ⁶⁵, C. Debenedetti ¹⁴⁶, D.V. Dedovich ⁸⁰, A.M. Deiana ⁴², J. Del Peso ⁹⁹,
 Y. Delabat Diaz ⁴⁶, D. Delgove ⁶⁵, F. Deliot ^{145,q}, C.M. Delitzsch ⁷, M. Della Pietra ^{70a,70b}, D. Della Volpe ⁵⁴,
 A. Dell'Acqua ³⁶, L. Dell'Asta ^{74a,74b}, M. Delmastro ⁵, C. Delporte ⁶⁵, P.A. Delsart ⁵⁸, D.A. DeMarco ¹⁶⁷,
 S. Demers ¹⁸³, M. Demichev ⁸⁰, G. Demontigny ¹¹⁰, S.P. Denisov ¹²³, L. D'Eramo ¹³⁶, D. Derendarz ⁸⁵,
 J.E. Derkaoui ^{35d}, F. Derue ¹³⁶, P. Dervan ⁹¹, K. Desch ²⁴, C. Deterre ⁴⁶, K. Dette ¹⁶⁷, C. Deutsch ²⁴,
 M.R. Devesa ³⁰, P.O. Deviveiros ³⁶, F.A. Di Bello ^{73a,73b}, A. Di Ciaccio ^{74a,74b}, L. Di Ciaccio ⁵,
 W.K. Di Clemente ¹³⁷, C. Di Donato ^{70a,70b}, A. Di Girolamo ³⁶, G. Di Gregorio ^{72a,72b}, B. Di Micco ^{75a,75b},
 R. Di Nardo ^{75a,75b}, K.F. Di Petrillo ⁵⁹, R. Di Sipio ¹⁶⁷, C. Diaconu ¹⁰², F.A. Dias ⁴⁰, T. Dias Do Vale ^{140a},
 M.A. Diaz ^{147a}, J. Dickinson ¹⁸, E.B. Diehl ¹⁰⁶, J. Dietrich ¹⁹, S. Díez Cornell ⁴⁶, A. Dimitrievska ¹⁸,
 W. Ding ^{15b}, J. Dingfelder ²⁴, F. Dittus ³⁶, F. Djama ¹⁰², T. Djobava ^{159b}, J.I. Djuvsland ¹⁷, M.A.B. Do Vale ^{81c},
 M. Dobre ^{27b}, D. Dodsworth ²⁶, C. Doglioni ⁹⁷, J. Dolejsi ¹⁴³, Z. Dolezal ¹⁴³, M. Donadelli ^{81d}, B. Dong ^{60c},
 J. Donini ³⁸, A. D'onofrio ^{15c}, M. D'Onofrio ⁹¹, J. Dopke ¹⁴⁴, A. Doria ^{70a}, M.T. Dova ⁸⁹, A.T. Doyle ⁵⁷,
 E. Drechsler ¹⁵², E. Dreyer ¹⁵², T. Dreyer ⁵³, A.S. Drobac ¹⁷⁰, D. Du ^{60b}, Y. Duan ^{60b}, F. Dubinin ¹¹¹,
 M. Dubovsky ^{28a}, A. Dubreuil ⁵⁴, E. Duchovni ¹⁸⁰, G. Duckeck ¹¹⁴, A. Ducourthial ¹³⁶, O.A. Ducu ¹¹⁰,
 D. Duda ¹¹⁵, A. Dudarev ³⁶, A.C. Dudder ¹⁰⁰, E.M. Duffield ¹⁸, L. Duflost ⁶⁵, M. Dührssen ³⁶, C. Dülsen ¹⁸²,
 M. Dumancic ¹⁸⁰, A.E. Dumitriu ^{27b}, A.K. Duncan ⁵⁷, M. Dunford ^{61a}, A. Duperrin ¹⁰², H. Duran Yildiz ^{4a},
 M. Düren ⁵⁶, A. Durglishvili ^{159b}, D. Duschinger ⁴⁸, B. Dutta ⁴⁶, D. Duvnjak ¹, G.I. Dyckes ¹³⁷, M. Dyndal ³⁶,
 S. Dysch ¹⁰¹, B.S. Dziedzic ⁸⁵, K.M. Ecker ¹¹⁵, M.G. Eggleston ⁴⁹, T. Eifert ⁸, G. Eigen ¹⁷, K. Einsweiler ¹⁸,
 T. Ekelof ¹⁷², H. El Jarrari ^{35e}, R. El Kosseifi ¹⁰², V. Ellajosyula ¹⁷², M. Ellert ¹⁷², F. Ellinghaus ¹⁸²,
 A.A. Elliot ⁹³, N. Ellis ³⁶, J. Elmsheuser ²⁹, M. Elsing ³⁶, D. Emelianov ¹⁴⁴, A. Emerman ³⁹, Y. Enari ¹⁶³,
 M.B. Epland ⁴⁹, J. Erdmann ⁴⁷, A. Ereditato ²⁰, P.A. Erland ⁸⁵, M. Errenst ³⁶, M. Escalier ⁶⁵, C. Escobar ¹⁷⁴,
 O. Estrada Pastor ¹⁷⁴, E. Etzion ¹⁶¹, H. Evans ⁶⁶, A. Ezhilov ¹³⁸, F. Fabbri ⁵⁷, L. Fabbri ^{23b,23a}, V. Fabiani ¹¹⁹,
 G. Facini ¹⁷⁸, R.M. Faisca Rodrigues Pereira ^{140a}, R.M. Fakhruddinov ¹²³, S. Falciano ^{73a}, P.J. Falke ⁵,
 S. Falke ⁵, J. Faltova ¹⁴³, Y. Fang ^{15a}, Y. Fang ^{15a}, G. Fanourakis ⁴⁴, M. Fanti ^{69a,69b}, M. Faraj ^{67a,67c,s},
 A. Farbin ⁸, A. Farilla ^{75a}, E.M. Farina ^{71a,71b}, T. Farooque ¹⁰⁷, S.M. Farrington ⁵⁰, P. Farthouat ³⁶, F. Fassi ^{35e},
 P. Fassnacht ³⁶, D. Fassouliotis ⁹, M. Fauci Giannelli ⁵⁰, W.J. Fawcett ³², L. Fayard ⁶⁵, O.L. Fedin ^{138,o},
 W. Fedorko ¹⁷⁵, A. Fehr ²⁰, M. Feickert ¹⁷³, L. Feligioni ¹⁰², A. Fell ¹⁴⁹, C. Feng ^{60b}, M. Feng ⁴⁹,
 M.J. Fenton ¹⁷¹, A.B. Fenyuk ¹²³, S.W. Ferguson ⁴³, J. Ferrando ⁴⁶, A. Ferrante ¹⁷³, A. Ferrari ¹⁷²,
 P. Ferrari ¹²⁰, R. Ferrari ^{71a}, D.E. Ferreira de Lima ^{61b}, A. Ferrer ¹⁷⁴, D. Ferrere ⁵⁴, C. Ferretti ¹⁰⁶,
 F. Fiedler ¹⁰⁰, A. Filipčič ⁹², F. Filthaut ¹¹⁹, K.D. Finelli ²⁵, M.C.N. Fiolhais ^{140a,140c,a}, L. Fiorini ¹⁷⁴,
 F. Fischer ¹¹⁴, W.C. Fisher ¹⁰⁷, I. Fleck ¹⁵¹, P. Fleischmann ¹⁰⁶, T. Flick ¹⁸², B.M. Flierl ¹¹⁴, L. Flores ¹³⁷,
 L.R. Flores Castillo ^{63a}, F.M. Follega ^{76a,76b}, N. Fomin ¹⁷, J.H. Foo ¹⁶⁷, G.T. Forcolin ^{76a,76b}, A. Formica ¹⁴⁵,
 F.A. Förster ¹⁴, A.C. Forti ¹⁰¹, A.G. Foster ²¹, M.G. Foti ¹³⁵, D. Fournier ⁶⁵, H. Fox ⁹⁰, P. Francavilla ^{72a,72b},
 S. Francescato ^{73a,73b}, M. Franchini ^{23b,23a}, S. Franchino ^{61a}, D. Francis ³⁶, L. Franconi ²⁰, M. Franklin ⁵⁹,
 A.N. Fray ⁹³, P.M. Freeman ²¹, B. Freund ¹¹⁰, W.S. Freund ^{81b}, E.M. Freundlich ⁴⁷, D.C. Frizzell ¹²⁹,
 D. Froidevaux ³⁶, J.A. Frost ¹³⁵, C. Fukunaga ¹⁶⁴, E. Fullana Torregrosa ¹⁷⁴, T. Fusayasu ¹¹⁶, J. Fuster ¹⁷⁴,
 A. Gabrielli ^{23b,23a}, A. Gabrielli ¹⁸, S. Gadatsch ⁵⁴, P. Gadow ¹¹⁵, G. Gagliardi ^{55b,55a}, L.G. Gagnon ¹¹⁰,
 B. Galhardo ^{140a}, G.E. Gallardo ¹³⁵, E.J. Gallas ¹³⁵, B.J. Gallop ¹⁴⁴, G. Galster ⁴⁰, R. Gamboa Goni ⁹³,
 K.K. Gan ¹²⁷, S. Ganguly ¹⁸⁰, J. Gao ^{60a}, Y. Gao ⁵⁰, Y.S. Gao ^{31,l}, C. García ¹⁷⁴, J.E. García Navarro ¹⁷⁴,
 J.A. García Pascual ^{15a}, C. Garcia-Argos ⁵², M. Garcia-Sciveres ¹⁸, R.W. Gardner ³⁷, N. Garelli ¹⁵³,
 S. Gargiulo ⁵², C.A. Garner ¹⁶⁷, V. Garonne ¹³⁴, S.J. Gasiorowski ¹⁴⁸, P. Gaspar ^{81b}, A. Gaudiello ^{55b,55a},
 G. Gaudio ^{71a}, I.L. Gavrilenko ¹¹¹, A. Gavrilyuk ¹²⁴, C. Gay ¹⁷⁵, G. Gaycken ⁴⁶, E.N. Gazis ¹⁰, A.A. Geanta ^{27b},
 C.M. Gee ¹⁴⁶, C.N.P. Gee ¹⁴⁴, J. Geisen ⁹⁷, M. Geisen ¹⁰⁰, C. Gemme ^{55b}, M.H. Genest ⁵⁸, C. Geng ¹⁰⁶,
 S. Gentile ^{73a,73b}, S. George ⁹⁴, T. Gerialis ⁴⁴, L.O. Gerlach ⁵³, P. Gessinger-Befurt ¹⁰⁰, G. Gessner ⁴⁷,
 S. Ghasemi ¹⁵¹, M. Ghasemi Bostanabad ¹⁷⁶, M. Ghneimat ¹⁵¹, A. Ghosh ⁶⁵, A. Ghosh ⁷⁸, B. Giacobbe ^{23b},
 S. Giagu ^{73a,73b}, N. Giangiacomi ^{23b,23a}, P. Giannetti ^{72a}, A. Giannini ^{70a,70b}, G. Giannini ¹⁴, S.M. Gibson ⁹⁴,
 M. Gignac ¹⁴⁶, D. Gillberg ³⁴, G. Gilles ¹⁸², D.M. Gingrich ^{3,ao}, M.P. Giordani ^{67a,67c}, P.F. Giraud ¹⁴⁵,
 G. Giugliarelli ^{67a,67c}, D. Giugni ^{69a}, F. Giuli ^{74a,74b}, S. Gkaitatzis ¹⁶², I. Gkialas ^{9,g}, E.L. Gkoukousis ¹⁴,
 P. Gkoutoumis ¹⁰, L.K. Gladilin ¹¹³, C. Glasman ⁹⁹, J. Glatzer ¹⁴, P.C.F. Glaysher ⁴⁶, A. Glazov ⁴⁶,
 G.R. Gledhill ¹³², M. Goblirsch-Kolb ²⁶, D. Godin ¹¹⁰, S. Goldfarb ¹⁰⁵, T. Golling ⁵⁴, D. Golubkov ¹²³,
 A. Gomes ^{140a,140b}, R. Goncalves Gama ⁵³, R. Gonçalves ^{140a}, G. Gonella ¹³², L. Gonella ²¹, A. Gongadze ⁸⁰,
 F. Gonnella ²¹, J.L. Gonski ³⁹, S. González de la Hoz ¹⁷⁴, S. Gonzalez Fernandez ¹⁴, S. Gonzalez-Sevilla ⁵⁴,

G.R. Gonzalvo Rodriguez¹⁷⁴, L. Goossens³⁶, N.A. Gorasia²¹, P.A. Gorbounov¹²⁴, H.A. Gordon²⁹, B. Gorini³⁶, E. Gorini^{68a,68b}, A. Gorišek⁹², A.T. Goshaw⁴⁹, M.I. Gostkin⁸⁰, C.A. Gottardo¹¹⁹, M. Gouighri^{35b}, A.G. Goussiou¹⁴⁸, N. Govender^{33c}, C. Goy⁵, E. Gozani¹⁶⁰, I. Grabowska-Bold^{84a}, E.C. Graham⁹¹, J. Gramling¹⁷¹, E. Gramstad¹³⁴, S. Grancagnolo¹⁹, M. Grandi¹⁵⁶, V. Gratchev¹³⁸, P.M. Gravila^{27f}, F.G. Gravili^{68a,68b}, C. Gray⁵⁷, H.M. Gray¹⁸, C. Greife²⁴, K. Gregersen⁹⁷, I.M. Gregor⁴⁶, P. Grenier¹⁵³, K. Grevtsov⁴⁶, C. Grieco¹⁴, N.A. Grieser¹²⁹, A.A. Grillo¹⁴⁶, K. Grimm^{31,k}, S. Grinstein^{14,y}, J.-F. Grivaz⁶⁵, S. Groh¹⁰⁰, E. Gross¹⁸⁰, J. Grosse-Knetter⁵³, Z.J. Grout⁹⁵, C. Grud¹⁰⁶, A. Grummer¹¹⁸, L. Guan¹⁰⁶, W. Guan¹⁸¹, C. Gubbels¹⁷⁵, J. Guenther³⁶, A. Guerguichon⁶⁵, J.G.R. Guerrero Rojas¹⁷⁴, F. Guescini¹¹⁵, D. Guest¹⁷¹, R. Gugel⁵², T. Guillemin⁵, S. Guindon³⁶, U. Gul⁵⁷, J. Guo^{60c}, W. Guo¹⁰⁶, Y. Guo^{60a}, Z. Guo¹⁰², R. Gupta⁴⁶, S. Gurbuz^{12c}, G. Gustavino¹²⁹, M. Guth⁵², P. Gutierrez¹²⁹, C. Gutsche⁹⁵, C. Guyot¹⁴⁵, C. Gwenlan¹³⁵, C.B. Gwilliam⁹¹, A. Haas¹²⁵, C. Haber¹⁸, H.K. Hadavand⁸, A. Hadeef^{60a}, M. Haleem¹⁷⁷, J. Haley¹³⁰, G. Halladjian¹⁰⁷, G.D. Hallewell¹⁰², K. Hamacher¹⁸², P. Hamal¹³¹, K. Hamano¹⁷⁶, H. Hamdaoui^{35e}, M. Hamer²⁴, G.N. Hamity⁵⁰, K. Han^{60a,x}, L. Han^{60a}, S. Han^{15a}, Y.F. Han¹⁶⁷, K. Hanagaki^{82,v}, M. Hance¹⁴⁶, D.M. Handl¹¹⁴, B. Haney¹³⁷, R. Hankache¹³⁶, E. Hansen⁹⁷, J.B. Hansen⁴⁰, J.D. Hansen⁴⁰, M.C. Hansen²⁴, P.H. Hansen⁴⁰, E.C. Hanson¹⁰¹, K. Hara¹⁶⁹, T. Harenberg¹⁸², S. Harkusha¹⁰⁸, P.F. Harrison¹⁷⁸, N.M. Hartmann¹¹⁴, Y. Hasegawa¹⁵⁰, A. Hasib⁵⁰, S. Hassani¹⁴⁵, S. Haug²⁰, R. Hauser¹⁰⁷, L.B. Havener³⁹, M. Havranek¹⁴², C.M. Hawkes²¹, R.J. Hawking³⁶, D. Hayden¹⁰⁷, C. Hayes¹⁰⁶, R.L. Hayes¹⁷⁵, C.P. Hays¹³⁵, J.M. Hays⁹³, H.S. Hayward⁹¹, S.J. Haywood¹⁴⁴, F. He^{60a}, M.P. Heath⁵⁰, V. Hedberg⁹⁷, S. Heer²⁴, K.K. Heidegger⁵², W.D. Heidorn⁷⁹, J. Heilman³⁴, S. Heim⁴⁶, T. Heim¹⁸, B. Heinemann^{46,am}, J.J. Heinrich¹³², L. Heinrich³⁶, J. Hejbal¹⁴¹, L. Helary^{61b}, A. Held¹²⁵, S. Hellesund¹³⁴, C.M. Helling¹⁴⁶, S. Hellman^{45a,45b}, C. Helsens³⁶, R.C.W. Henderson⁹⁰, Y. Heng¹⁸¹, L. Henkelmann^{61a}, S. Henkelmann¹⁷⁵, A.M. Henriques Correia³⁶, H. Herde²⁶, V. Herget¹⁷⁷, Y. Hernández Jiménez^{33e}, H. Herr¹⁰⁰, M.G. Herrmann¹¹⁴, T. Herrmann⁴⁸, G. Herten⁵², R. Hertenberger¹¹⁴, L. Hervas³⁶, T.C. Herwig¹³⁷, G.G. Hesketh⁹⁵, N.P. Hessey^{168a}, A. Higashida¹⁶³, S. Higashino⁸², E. Higón-Rodríguez¹⁷⁴, K. Hildebrand³⁷, J.C. Hill³², K.K. Hill²⁹, K.H. Hiller⁴⁶, S.J. Hillier²¹, M. Hils⁴⁸, I. Hinchliffe¹⁸, F. Hinterkeuser²⁴, M. Hirose¹³³, S. Hirose⁵², D. Hirschbuehl¹⁸², B. Hiti⁹², O. Hladik¹⁴¹, D.R. Hlaluku^{33e}, J. Hobbs¹⁵⁵, N. Hod¹⁸⁰, M.C. Hodgkinson¹⁴⁹, A. Hoecker³⁶, D. Hohn⁵², D. Hohov⁶⁵, T. Holm²⁴, T.R. Holmes³⁷, M. Holzbock¹¹⁴, L.B.A.H. Hommels³², S. Honda¹⁶⁹, T.M. Hong¹³⁹, J.C. Honig⁵², A. Hönle¹¹⁵, B.H. Hooberman¹⁷³, W.H. Hopkins⁶, Y. Horii¹¹⁷, P. Horn⁴⁸, L.A. Horyn³⁷, S. Hou¹⁵⁸, A. Hoummada^{35a}, J. Howarth¹⁰¹, J. Hoya⁸⁹, M. Hrabovsky¹³¹, J. Hrdinka⁷⁷, I. Hristova¹⁹, J. Hrivnac⁶⁵, A. Hrynevich¹⁰⁹, T. Hryn'ova⁵, P.J. Hsu⁶⁴, S.-C. Hsu¹⁴⁸, Q. Hu²⁹, S. Hu^{60c}, Y.F. Hu^{15a,15d}, D.P. Huang⁹⁵, Y. Huang^{60a}, Y. Huang^{15a}, Z. Hubacek¹⁴², F. Hubaut¹⁰², M. Huebner²⁴, F. Huegging²⁴, T.B. Huffman¹³⁵, M. Huhtinen³⁶, R.F.H. Hunter³⁴, P. Huo¹⁵⁵, N. Huseynov^{80,ae}, J. Huston¹⁰⁷, J. Huth⁵⁹, R. Hyneman¹⁰⁶, S. Hyrych^{28a}, G. Iacobucci⁵⁴, G. Iakovidis²⁹, I. Ibragimov¹⁵¹, L. Iconomidou-Fayard⁶⁵, P. Iengo³⁶, R. Ignazzi⁴⁰, O. Igonkina^{120,aa,*}, R. Iguchi¹⁶³, T. Iizawa⁵⁴, Y. Ikegami⁸², M. Ikeno⁸², D. Iliadis¹⁶², N. Ilic^{119,167,ad}, F. Iltzsche⁴⁸, G. Introzzi^{71a,71b}, M. Iodice^{75a}, K. Iordanidou^{168a}, V. Ippolito^{73a,73b}, M.F. Isacson¹⁷², M. Ishino¹⁶³, W. Islam¹³⁰, C. Issever^{19,46}, S. Istin¹⁶⁰, F. Ito¹⁶⁹, J.M. Iturbe Ponce^{63a}, R. Iuppa^{76a,76b}, A. Ivina¹⁸⁰, H. Iwasaki⁸², J.M. Izen⁴³, V. Izzo^{70a}, P. Jacka¹⁴¹, P. Jackson¹, R.M. Jacobs²⁴, B.P. Jaeger¹⁵², V. Jain², G. Jäkel¹⁸², K.B. Jakobi¹⁰⁰, K. Jakobs⁵², T. Jakoubek¹⁴¹, J. Jamieson⁵⁷, K.W. Janas^{84a}, R. Jansky⁵⁴, M. Janus⁵³, P.A. Janus^{84a}, G. Jarlskog⁹⁷, N. Javadov^{80,ae}, T. Javůrek³⁶, M. Javurkova¹⁰³, F. Jeanneau¹⁴⁵, L. Jeanty¹³², J. Jejelava^{159a}, A. Jelinskas¹⁷⁸, P. Jenni^{52,b}, N. Jeong⁴⁶, S. Jézéquel⁵, H. Ji¹⁸¹, J. Jia¹⁵⁵, H. Jiang⁷⁹, Y. Jiang^{60a}, Z. Jiang^{153,p}, S. Jiggins⁵², F.A. Jimenez Morales³⁸, J. Jimenez Pena¹¹⁵, S. Jin^{15c}, A. Jinaru^{27b}, O. Jinnouchi¹⁶⁵, H. Jivan^{33e}, P. Johansson¹⁴⁹, K.A. Johns⁷, C.A. Johnson⁶⁶, R.W.L. Jones⁹⁰, S.D. Jones¹⁵⁶, S. Jones⁷, T.J. Jones⁹¹, J. Jongmanns^{61a}, P.M. Jorge^{140a}, J. Jovicevic³⁶, X. Ju¹⁸, J.J. Junggeburth¹¹⁵, A. Juste Rozas^{14,y}, A. Kaczmarska⁸⁵, M. Kado^{73a,73b}, H. Kagan¹²⁷, M. Kagan¹⁵³, A. Kahn³⁹, C. Kahra¹⁰⁰, T. Kaji¹⁷⁹, E. Kajomovitz¹⁶⁰, C.W. Kalderon²⁹, A. Kaluza¹⁰⁰, A. Kamenshchikov¹²³, M. Kaneda¹⁶³, N.J. Kang¹⁴⁶, S. Kang⁷⁹, L. Kanjir⁹², Y. Kano¹¹⁷, J. Kanzaki⁸², L.S. Kaplan¹⁸¹, D. Kar^{33e}, K. Karava¹³⁵, M.J. Kareem^{168b}, S.N. Karpov⁸⁰, Z.M. Karpova⁸⁰, V. Kartvelishvili⁹⁰, A.N. Karyukhin¹²³, A. Kastanas^{45a,45b}, C. Kato^{60d,60c}, J. Katzy⁴⁶, K. Kawade¹⁵⁰, K. Kawagoe⁸⁸, T. Kawaguchi¹¹⁷, T. Kawamoto¹⁴⁵, G. Kawamura⁵³, E.F. Kay¹⁷⁶, V.F. Kazanin^{122b,122a}, R. Keeler¹⁷⁶, R. Kehoe⁴², J.S. Keller³⁴, E. Kellermann⁹⁷, D. Kelsey¹⁵⁶, J.J. Kempster²¹, J. Kendrick²¹, K.E. Kennedy³⁹, O. Kepka¹⁴¹, S. Kersten¹⁸², B.P. Kerševan⁹², S. Ketabchi Haghighat¹⁶⁷, M. Khader¹⁷³, F. Khalil-Zada¹³,

M. Khandoga¹⁴⁵, A. Khanov¹³⁰, A.G. Kharlamov^{122b,122a}, T. Kharlamova^{122b,122a}, E.E. Khoda¹⁷⁵,
 A. Khodinov¹⁶⁶, T.J. Khoo⁵⁴, E. Khramov⁸⁰, J. Khubua^{159b}, S. Kido⁸³, M. Kiehn⁵⁴, C.R. Kilby⁹⁴,
 E. Kim¹⁶⁵, Y.K. Kim³⁷, N. Kimura⁹⁵, O.M. Kind¹⁹, B.T. King^{91,*}, D. Kirchmeier⁴⁸, J. Kirk¹⁴⁴,
 A.E. Kiryunin¹¹⁵, T. Kishimoto¹⁶³, D.P. Kisliuk¹⁶⁷, V. Kitali⁴⁶, O. Kivernyk⁵, T. Klapdor-Kleingrothaus⁵²,
 M. Klassen^{61a}, C. Klein³², M.H. Klein¹⁰⁶, M. Klein⁹¹, U. Klein⁹¹, K. Kleinknecht¹⁰⁰, P. Klimek¹²¹,
 A. Klimentov²⁹, T. Klingl²⁴, T. Klioutchnikova³⁶, F.F. Klitzner¹¹⁴, P. Kluit¹²⁰, S. Kluth¹¹⁵, E. Kneringer⁷⁷,
 E.B.F.G. Knoop¹⁰², A. Knue⁵², D. Kobayashi⁸⁸, T. Kobayashi¹⁶³, M. Kobel⁴⁸, M. Kocian¹⁵³,
 T. Kodama¹⁶³, P. Kodys¹⁴³, P.T. Koenig²⁴, T. Koffas³⁴, N.M. Köhler³⁶, M. Kolb¹⁴⁵, I. Koletsou⁵,
 T. Komarek¹³¹, T. Kondo⁸², K. Köneke⁵², A.X.Y. Kong¹, A.C. König¹¹⁹, T. Kono¹²⁶, V. Konstantinides⁹⁵,
 N. Konstantinidis⁹⁵, B. Konya⁹⁷, R. Kopeliansky⁶⁶, S. Koperny^{84a}, K. Korcyl⁸⁵, K. Kordas¹⁶², G. Koren¹⁶¹,
 A. Korn⁹⁵, I. Korolkov¹⁴, E.V. Korolkova¹⁴⁹, N. Korotkova¹¹³, O. Kortner¹¹⁵, S. Kortner¹¹⁵, T. Kosek¹⁴³,
 V.V. Kostyukhin^{149,166}, A. Kotskechagia⁶⁵, A. Kotwal⁴⁹, A. Koulouris¹⁰,
 A. Kourkoumeli-Charalampidi^{71a,71b}, C. Kourkoumelis⁹, E. Kourlitis¹⁴⁹, V. Kouskoura²⁹,
 A.B. Kowalewska⁸⁵, R. Kowalewski¹⁷⁶, W. Kozanecki¹⁰¹, A.S. Kozhin¹²³, V.A. Kramarenko¹¹³,
 G. Kramberger⁹², D. Krasnopevtsev^{60a}, M.W. Krasny¹³⁶, A. Krasznahorkay³⁶, D. Krauss¹¹⁵,
 J.A. Kremer^{84a}, J. Kretschmar⁹¹, P. Krieger¹⁶⁷, F. Krieter¹¹⁴, A. Krishnan^{61b}, K. Krizka¹⁸,
 K. Kroeninger⁴⁷, H. Kroha¹¹⁵, J. Kroll¹⁴¹, J. Kroll¹³⁷, K.S. Krowpman¹⁰⁷, U. Kruchonak⁸⁰, H. Krüger²⁴,
 N. Krumnack⁷⁹, M.C. Kruse⁴⁹, J.A. Krzysiak⁸⁵, T. Kubota¹⁰⁵, O. Kuchinskaia¹⁶⁶, S. Kudah^{4b},
 J.T. Kuechler⁴⁶, S. Kuehn³⁶, A. Kugel^{61a}, T. Kuhl⁴⁶, V. Kukhtin⁸⁰, R. Kukla¹⁰², Y. Kulchitsky^{108,ag},
 S. Kuleshov^{147d}, Y.P. Kulinich¹⁷³, M. Kuna⁵⁸, T. Kunigo⁸⁶, A. Kupco¹⁴¹, T. Kupfer⁴⁷, O. Kuprash⁵²,
 H. Kurashige⁸³, L.L. Kurchaninov^{168a}, Y.A. Kurochkin¹⁰⁸, A. Kurova¹¹², M.G. Kurth^{15a,15d}, E.S. Kuwertz³⁶,
 M. Kuze¹⁶⁵, A.K. Kvam¹⁴⁸, J. Kvita¹³¹, T. Kwan¹⁰⁴, L. La Rotonda^{41b,41a}, F. La Ruffa^{41b,41a}, C. Lacasta¹⁷⁴,
 F. Lacava^{73a,73b}, D.P.J. Lack¹⁰¹, H. Lacker¹⁹, D. Lacour¹³⁶, E. Ladygin⁸⁰, R. Lafaye⁵, B. Laforge¹³⁶,
 T. Lagouri^{147b}, S. Lai⁵³, I.K. Lakomic^{84a}, S. Lammers⁶⁶, W. Lampl⁷, C. Lampoudis¹⁶², E. Lançon²⁹,
 U. Landgraf⁵², M.P.J. Landon⁹³, M.C. Lanfermann⁵⁴, V.S. Lang⁴⁶, J.C. Lange⁵³, R.J. Langenberg¹⁰³,
 A.J. Lankford¹⁷¹, F. Lanni²⁹, K. Lantzsch²⁴, A. Lanza^{71a}, A. Lapertosa^{55b,55a}, S. Laplace¹³⁶, J.F. Laporte¹⁴⁵,
 T. Lari^{69a}, F. Lasagni Manghi^{23b,23a}, M. Lassnig³⁶, T.S. Lau^{63a}, A. Laudrain⁶⁵, A. Laurier³⁴,
 M. Lavorgna^{70a,70b}, S.D. Lawlor⁹⁴, M. Lazzaroni^{69a,69b}, B. Le¹⁰⁵, E. Le Guirriec¹⁰², A. Lebedev⁷⁹,
 M. LeBlanc⁷, T. LeCompte⁶, F. Ledroit-Guillon⁵⁸, A.C.A. Lee⁹⁵, C.A. Lee²⁹, G.R. Lee¹⁷, L. Lee⁵⁹,
 S.C. Lee¹⁵⁸, S. Lee⁷⁹, B. Lefebvre^{168a}, H.P. Lefebvre⁹⁴, M. Lefebvre¹⁷⁶, C. Leggett¹⁸, K. Lehmann¹⁵²,
 N. Lehmann¹⁸², G. Lehmann Miotto³⁶, W.A. Leight⁴⁶, A. Leisos^{162,w}, M.A.L. Leite^{81d}, C.E. Leitgeb¹¹⁴,
 R. Leitner¹⁴³, D. Lellouch^{180,*}, K.J.C. Leney⁴², T. Lenz²⁴, R. Leone⁷, S. Leone^{72a}, C. Leonidopoulos⁵⁰,
 A. Leopold¹³⁶, C. Leroy¹¹⁰, R. Les¹⁶⁷, C.G. Lester³², M. Levchenko¹³⁸, J. Levêque⁵, D. Levin¹⁰⁶,
 L.J. Levinson¹⁸⁰, D.J. Lewis²¹, B. Li^{15b}, B. Li¹⁰⁶, C-Q. Li^{60a}, F. Li^{60c}, H. Li^{60a}, H. Li^{60b}, J. Li^{60c}, K. Li¹⁴⁸,
 L. Li^{60c}, M. Li^{15a,15d}, Q. Li^{15a,15d}, Q.Y. Li^{60a}, S. Li^{60d,60c}, X. Li⁴⁶, Y. Li⁴⁶, Z. Li^{60b}, Z. Li¹⁰⁴, Z. Liang^{15a},
 B. Liberti^{74a}, A. Liblong¹⁶⁷, K. Lie^{63c}, S. Lim²⁹, C.Y. Lin³², K. Lin¹⁰⁷, T.H. Lin¹⁰⁰, R.A. Linck⁶⁶,
 J.H. Lindon²¹, A.L. Lioni⁵⁴, E. Lipeles¹³⁷, A. Lipniacka¹⁷, T.M. Liss^{173,an}, A. Lister¹⁷⁵, J.D. Little⁸,
 B. Liu⁷⁹, B.L. Liu⁶, H.B. Liu²⁹, H. Liu¹⁰⁶, J.B. Liu^{60a}, J.K.K. Liu³⁷, K. Liu^{60d}, M. Liu^{60a}, P. Liu^{15a}, Y. Liu⁴⁶,
 Y. Liu^{15a,15d}, Y.L. Liu¹⁰⁶, Y.W. Liu^{60a}, M. Livan^{71a,71b}, A. Lleres⁵⁸, J. Llorente Merino¹⁵², S.L. Lloyd⁹³,
 C.Y. Lo^{63b}, E.M. Lobodzinska⁴⁶, P. Loch⁷, S. Loffredo^{74a,74b}, T. Lohse¹⁹, K. Lohwasser¹⁴⁹, M. Lokajicek¹⁴¹,
 J.D. Long¹⁷³, R.E. Long⁹⁰, L. Longo³⁶, K.A. Looper¹²⁷, J.A. Lopez^{147d}, I. Lopez Paz¹⁰¹, A. Lopez Solis¹⁴⁹,
 J. Lorenz¹¹⁴, N. Lorenzo Martinez⁵, A.M. Lory¹¹⁴, M. Losada^{22a}, P.J. Lösel¹¹⁴, A. Lösle⁵², X. Lou⁴⁶,
 X. Lou^{15a}, A. Lounis⁶⁵, J. Love⁶, P.A. Love⁹⁰, J.J. Lozano Bahilo¹⁷⁴, M. Lu^{60a}, Y.J. Lu⁶⁴, H.J. Lubatti¹⁴⁸,
 C. Luci^{73a,73b}, A. Lucotte⁵⁸, C. Luedtke⁵², F. Luehring⁶⁶, I. Luise¹³⁶, L. Luminari^{73a}, B. Lund-Jensen¹⁵⁴,
 M.S. Lutz¹⁰³, D. Lynn²⁹, H. Lyons⁹¹, R. Lysak¹⁴¹, E. Lytken⁹⁷, F. Lyu^{15a}, V. Lyubushkin⁸⁰,
 T. Lyubushkina⁸⁰, H. Ma²⁹, L.L. Ma^{60b}, Y. Ma^{60b}, G. Maccarrone⁵¹, A. Macchiolo¹¹⁵, C.M. Macdonald¹⁴⁹,
 J. Machado Miguens¹³⁷, D. Madaffari¹⁷⁴, R. Madar³⁸, W.F. Mader⁴⁸, M. Madugoda Ralalage Don¹³⁰,
 N. Madysa⁴⁸, J. Maeda⁸³, T. Maeno²⁹, M. Maerker⁴⁸, V. Magerl⁵², N. Magini⁷⁹, J. Magro^{67a,67c,s},
 D.J. Mahon³⁹, C. Maidantchik^{81b}, T. Maier¹¹⁴, A. Maio^{140a,140b,140d}, K. Maj^{84a}, O. Majersky^{28a},
 S. Majewski¹³², Y. Makida⁸², N. Makovec⁶⁵, B. Malaescu¹³⁶, Pa. Malecki⁸⁵, V.P. Maleev¹³⁸, F. Malek⁵⁸,
 U. Mallik⁷⁸, D. Malon⁶, C. Malone³², S. Maltezos¹⁰, S. Malyukov⁸⁰, J. Mamuzic¹⁷⁴, G. Mancini⁵¹,
 I. Mandić⁹², L. Manhaes de Andrade Filho^{81a}, I.M. Maniatis¹⁶², J. Manjarres Ramos⁴⁸, K.H. Mankinen⁹⁷,
 A. Mann¹¹⁴, A. Manousos⁷⁷, B. Mansoulie¹⁴⁵, I. Manthos¹⁶², S. Manzoni¹²⁰, A. Marantis¹⁶²,

G. Marceca³⁰, L. Marchese¹³⁵, G. Marchiori¹³⁶, M. Marcisovsky¹⁴¹, L. Marcoccia^{74a,74b}, C. Marcon⁹⁷, C.A. Marin Tobon³⁶, M. Marjanovic¹²⁹, Z. Marshall¹⁸, M.U.F. Martensson¹⁷², S. Marti-Garcia¹⁷⁴, C.B. Martin¹²⁷, T.A. Martin¹⁷⁸, V.J. Martin⁵⁰, B. Martin dit Latour¹⁷, L. Martinelli^{75a,75b}, M. Martinez^{14,y}, V.I. Martinez Outschoorn¹⁰³, S. Martin-Haugh¹⁴⁴, V.S. Martoiu^{27b}, A.C. Martyniuk⁹⁵, A. Marzin³⁶, S.R. Maschek¹¹⁵, L. Masetti¹⁰⁰, T. Mashimo¹⁶³, R. Mashinistov¹¹¹, J. Masik¹⁰¹, A.L. Maslennikov^{122b,122a}, L. Massa^{23b,23a}, P. Massarotti^{70a,70b}, P. Mastrandrea^{72a,72b}, A. Mastroberardino^{41b,41a}, T. Masubuchi¹⁶³, D. Matakias²⁹, A. Matic¹¹⁴, N. Matsuzawa¹⁶³, P. Mättig²⁴, J. Maurer^{27b}, B. Maček⁹², D.A. Maximov^{122b,122a}, R. Mazini¹⁵⁸, I. Maznas¹⁶², S.M. Mazza¹⁴⁶, S.P. Mc Kee¹⁰⁶, T.G. McCarthy¹¹⁵, W.P. McCormack¹⁸, E.F. McDonald¹⁰⁵, J.A. Mcfayden³⁶, G. Mchedlidze^{159b}, M.A. McKay⁴², K.D. McLean¹⁷⁶, S.J. McMahon¹⁴⁴, P.C. McNamara¹⁰⁵, C.J. McNicol¹⁷⁸, R.A. McPherson^{176,ad}, J.E. Mdhului^{33e}, Z.A. Meadows¹⁰³, S. Meehan³⁶, T. Megy⁵², S. Mehlhase¹¹⁴, A. Mehta⁹¹, T. Meideck⁵⁸, B. Meirose⁴³, D. Melini¹⁶⁰, B.R. Mellado Garcia^{33e}, J.D. Mellenthin⁵³, M. Melo^{28a}, F. Meloni⁴⁶, A. Melzer²⁴, S.B. Menary¹⁰¹, E.D. Mendes Gouveia^{140a,140e}, L. Meng³⁶, X.T. Meng¹⁰⁶, S. Menke¹¹⁵, E. Meoni^{41b,41a}, S. Mergelmeyer¹⁹, S.A.M. Merkt¹³⁹, C. Merlassino¹³⁵, P. Mermod⁵⁴, L. Merola^{70a,70b}, C. Meroni^{69a}, G. Merz¹⁰⁶, O. Meshkov^{113,111}, J.K.R. Meshreki¹⁵¹, A. Messina^{73a,73b}, J. Metcalfe⁶, A.S. Mete⁶, C. Meyer⁶⁶, J-P. Meyer¹⁴⁵, H. Meyer Zu Theenhausen^{61a}, F. Miano¹⁵⁶, M. Michetti¹⁹, R.P. Middleton¹⁴⁴, L. Mijović⁵⁰, G. Mikenberg¹⁸⁰, M. Mikestikova¹⁴¹, M. Mikuž⁹², H. Mildner¹⁴⁹, M. Milesi¹⁰⁵, A. Milic¹⁶⁷, D.A. Millar⁹³, D.W. Miller³⁷, A. Milov¹⁸⁰, D.A. Milstead^{45a,45b}, R.A. Mina¹⁵³, A.A. Minaenko¹²³, M. Miñano Moya¹⁷⁴, I.A. Minashvili^{159b}, A.I. Mincer¹²⁵, B. Mindur^{84a}, M. Mineev⁸⁰, Y. Minegishi¹⁶³, L.M. Mir¹⁴, A. Mirto^{68a,68b}, K.P. Mistry¹³⁷, T. Mitani¹⁷⁹, J. Mitrevski¹¹⁴, V.A. Mitsou¹⁷⁴, M. Mittal^{60c}, O. Miu¹⁶⁷, A. Miucci²⁰, P.S. Miyagawa¹⁴⁹, A. Mizukami⁸², J.U. Mjörnmark⁹⁷, T. Mkrtchyan^{61a}, M. Mlynarikova¹⁴³, T. Moa^{45a,45b}, K. Mochizuki¹¹⁰, P. Mogg⁵², S. Mohapatra³⁹, R. Moles-Valls²⁴, M.C. Mondragon¹⁰⁷, K. Mönig⁴⁶, J. Monk⁴⁰, E. Monnier¹⁰², A. Montalbano¹⁵², J. Montejo Berlingen³⁶, M. Montella⁹⁵, F. Monticelli⁸⁹, S. Monzani^{69a}, N. Morange⁶⁵, D. Moreno^{22a}, M. Moreno Llácer¹⁷⁴, C. Moreno Martinez¹⁴, P. Morettini^{55b}, M. Morgenstern¹⁶⁰, S. Morgenstern⁴⁸, D. Mori¹⁵², M. Morii⁵⁹, M. Morinaga¹⁷⁹, V. Morisbak¹³⁴, A.K. Morley³⁶, G. Mornacchi³⁶, A.P. Morris⁹⁵, L. Morvaj¹⁵⁵, P. Moschovakos³⁶, B. Moser¹²⁰, M. Mosidze^{159b}, T. Moskalets¹⁴⁵, H.J. Moss¹⁴⁹, J. Moss^{31,m}, E.J.W. Moyse¹⁰³, S. Muanza¹⁰², J. Mueller¹³⁹, R.S.P. Mueller¹¹⁴, D. Muenstermann⁹⁰, G.A. Mullier⁹⁷, D.P. Mungo^{69a,69b}, J.L. Munoz Martinez¹⁴, F.J. Munoz Sanchez¹⁰¹, P. Murin^{28b}, W.J. Murray^{178,144}, A. Murrone^{69a,69b}, M. Muškinja¹⁸, C. Mwewa^{33a}, A.G. Myagkov^{123,ai}, A.A. Myers¹³⁹, J. Myers¹³², M. Myska¹⁴², B.P. Nachman¹⁸, O. Nackenhorst⁴⁷, A. Nag Nag⁴⁸, K. Nagai¹³⁵, K. Nagano⁸², Y. Nagasaka⁶², J.L. Nagle²⁹, E. Nagy¹⁰², A.M. Nairz³⁶, Y. Nakahama¹¹⁷, K. Nakamura⁸², T. Nakamura¹⁶³, I. Nakano¹²⁸, H. Nanjo¹³³, F. Napolitano^{61a}, R.F. Naranjo Garcia⁴⁶, R. Narayan⁴², I. Naryshkin¹³⁸, T. Naumann⁴⁶, G. Navarro^{22a}, P.Y. Nechaeva¹¹¹, F. Nechansky⁴⁶, T.J. Neep²¹, A. Negri^{71a,71b}, M. Negrini^{23b}, C. Nellist¹¹⁹, M.E. Nelson^{45a,45b}, S. Nemecek¹⁴¹, M. Nessi^{36,d}, M.S. Neubauer¹⁷³, F. Neuhaus¹⁰⁰, M. Neumann¹⁸², R. Newhouse¹⁷⁵, P.R. Newman²¹, C.W. Ng¹³⁹, Y.S. Ng¹⁹, Y.W.Y. Ng¹⁷¹, B. Ngair^{35e}, H.D.N. Nguyen¹⁰², T. Nguyen Manh¹¹⁰, E. Nibigira³⁸, R.B. Nickerson¹³⁵, R. Nicolaidou¹⁴⁵, D.S. Nielsen⁴⁰, J. Nielsen¹⁴⁶, N. Nikiforou¹¹, V. Nikolaenko^{123,ai}, I. Nikolic-Audit¹³⁶, K. Nikolopoulos²¹, P. Nilsson²⁹, H.R. Nindhito⁵⁴, Y. Ninomiya⁸², A. Nisati^{73a}, N. Nishu^{60c}, R. Nisius¹¹⁵, I. Nitsche⁴⁷, T. Nitta¹⁷⁹, T. Nobe¹⁶³, Y. Noguchi⁸⁶, I. Nomidis¹³⁶, M.A. Nomura²⁹, M. Nordberg³⁶, T. Novak⁹², O. Novgorodova⁴⁸, R. Novotny¹⁴², L. Nozka¹³¹, K. Ntekas¹⁷¹, E. Nurse⁹⁵, F.G. Oakham^{34,ao}, H. Oberlack¹¹⁵, J. Ocariz¹³⁶, A. Ochi⁸³, I. Ochoa³⁹, J.P. Ochoa-Ricoux^{147a}, K. O'Connor²⁶, S. Oda⁸⁸, S. Odaka⁸², S. Oerdek⁵³, A. Ogrodnik^{84a}, A. Oh¹⁰¹, S.H. Oh⁴⁹, C.C. Ohm¹⁵⁴, H. Oide¹⁶⁵, M.L. Ojeda¹⁶⁷, H. Okawa¹⁶⁹, Y. Okazaki⁸⁶, M.W. O'Keefe⁹¹, Y. Okumura¹⁶³, T. Okuyama⁸², A. Olariu^{27b}, L.F. Oleiro Seabra^{140a}, S.A. Olivares Pino^{147a}, D. Oliveira Damazio²⁹, J.L. Oliver¹, M.J.R. Olsson¹⁷¹, A. Olszewski⁸⁵, J. Olszowska⁸⁵, D.C. O'Neil¹⁵², A.P. O'Neill¹³⁵, A. Onofre^{140a,140e}, P.U.E. Onyisi¹¹, H. Oppen¹³⁴, M.J. Oreglia³⁷, G.E. Orellana⁸⁹, D. Orestano^{75a,75b}, N. Orlando¹⁴, R.S. Orr¹⁶⁷, V. O'Shea⁵⁷, R. Ospanov^{60a}, G. Otero y Garzon³⁰, H. Otono⁸⁸, P.S. Ott^{61a}, M. Ouchrif^{35d}, J. Ouellette²⁹, F. Ould-Saada¹³⁴, A. Ouraou¹⁴⁵, Q. Ouyang^{15a}, M. Owen⁵⁷, R.E. Owen²¹, V.E. Ozcan^{12c}, N. Ozturk⁸, J. Pacalt¹³¹, H.A. Pacey³², K. Pachal⁴⁹, A. Pacheco Pages¹⁴, C. Padilla Aranda¹⁴, S. Pagan Griso¹⁸, M. Paganini¹⁸³, G. Palacino⁶⁶, S. Palazzo⁵⁰, S. Palestini³⁶, M. Palka^{84b}, D. Pallin³⁸, P. Palni^{84a}, I. Panagoulas¹⁰, C.E. Pandini³⁶, J.G. Panduro Vazquez⁹⁴, P. Pani⁴⁶, G. Panizzo^{67a,67c}, L. Paolozzi⁵⁴, C. Papadatos¹¹⁰, K. Papageorgiou^{9,g}, S. Parajuli⁴², A. Paramonov⁶, D. Paredes Hernandez^{63b},

S.R. Paredes Saenz ¹³⁵, B. Parida ¹⁶⁶, T.H. Park ¹⁶⁷, A.J. Parker ³¹, M.A. Parker ³², F. Parodi ^{55b,55a}, E.W. Parrish ¹²¹, J.A. Parsons ³⁹, U. Parzefall ⁵², L. Pascual Dominguez ¹³⁶, V.R. Pascuzzi ¹⁶⁷, J.M.P. Pasner ¹⁴⁶, F. Pasquali ¹²⁰, E. Pasqualucci ^{73a}, S. Passaggio ^{55b}, F. Pastore ⁹⁴, P. Pasuwan ^{45a,45b}, S. Pataraiia ¹⁰⁰, J.R. Pater ¹⁰¹, A. Pathak ^{181,i}, J. Patton ⁹¹, T. Pauly ³⁶, J. Pearkes ¹⁵³, B. Pearson ¹¹⁵, M. Pedersen ¹³⁴, L. Pedraza Diaz ¹¹⁹, R. Pedro ^{140a}, T. Peiffer ⁵³, S.V. Peleganchuk ^{122b,122a}, O. Penc ¹⁴¹, H. Peng ^{60a}, B.S. Peralva ^{81a}, M.M. Perego ⁶⁵, A.P. Pereira Peixoto ^{140a}, D.V. Perepelitsa ²⁹, F. Peri ¹⁹, L. Perini ^{69a,69b}, H. Pernegger ³⁶, S. Perrella ^{140a}, A. Perrevoort ¹²⁰, K. Peters ⁴⁶, R.F.Y. Peters ¹⁰¹, B.A. Petersen ³⁶, T.C. Petersen ⁴⁰, E. Petit ¹⁰², A. Petridis ¹, C. Petridou ¹⁶², P. Petroff ⁶⁵, M. Petrov ¹³⁵, F. Petrucci ^{75a,75b}, M. Pettee ¹⁸³, N.E. Pettersson ¹⁰³, K. Petukhova ¹⁴³, A. Peyaud ¹⁴⁵, R. Pezoa ^{147d}, L. Pezzotti ^{71a,71b}, T. Pham ¹⁰⁵, F.H. Phillips ¹⁰⁷, P.W. Phillips ¹⁴⁴, M.W. Phipps ¹⁷³, G. Piacquadio ¹⁵⁵, E. Pianori ¹⁸, A. Picazio ¹⁰³, R.H. Pickles ¹⁰¹, R. Piegaia ³⁰, D. Pietreanu ^{27b}, J.E. Pilcher ³⁷, A.D. Pilkington ¹⁰¹, M. Pinamonti ^{67a,67c}, J.L. Pinfold ³, M. Pitt ¹⁶¹, L. Pizzimento ^{74a,74b}, M.-A. Pleier ²⁹, V. Pleskot ¹⁴³, E. Plotnikova ⁸⁰, P. Podberezko ^{122b,122a}, R. Poettgen ⁹⁷, R. Poggi ⁵⁴, L. Poggioli ¹³⁶, I. Pogrebnyak ¹⁰⁷, D. Pohl ²⁴, I. Pokharel ⁵³, G. Polesello ^{71a}, A. Poley ¹⁸, A. Policicchio ^{73a,73b}, R. Polifka ¹⁴³, A. Polini ^{23b}, C.S. Pollard ⁴⁶, V. Polychronakos ²⁹, D. Ponomarenko ¹¹², L. Pontecorvo ³⁶, S. Popa ^{27a}, G.A. Popeneciu ^{27d}, L. Portales ⁵, D.M. Portillo Quintero ⁵⁸, S. Pospisil ¹⁴², K. Potamianos ⁴⁶, I.N. Potrap ⁸⁰, C.J. Potter ³², H. Potti ¹¹, T. Poulsen ⁹⁷, J. Poveda ³⁶, T.D. Powell ¹⁴⁹, G. Pownall ⁴⁶, M.E. Pozo Astigarraga ³⁶, P. Pralavorio ¹⁰², S. Prell ⁷⁹, D. Price ¹⁰¹, M. Primavera ^{68a}, S. Prince ¹⁰⁴, M.L. Proffitt ¹⁴⁸, N. Proklova ¹¹², K. Prokofiev ^{63c}, F. Prokoshin ⁸⁰, S. Protopopescu ²⁹, J. Proudfoot ⁶, M. Przybycien ^{84a}, D. Pudzha ¹³⁸, A. Puri ¹⁷³, P. Puzo ⁶⁵, J. Qian ¹⁰⁶, Y. Qin ¹⁰¹, A. Quadt ⁵³, M. Queitsch-Maitland ³⁶, A. Qureshi ¹, M. Racko ^{28a}, F. Ragusa ^{69a,69b}, G. Rahal ⁹⁸, J.A. Raine ⁵⁴, S. Rajagopalan ²⁹, A. Ramirez Morales ⁹³, K. Ran ^{15a,15d}, T. Rashid ⁶⁵, S. Raspopov ⁵, D.M. Rauch ⁴⁶, F. Rauscher ¹¹⁴, S. Rave ¹⁰⁰, B. Ravina ¹⁴⁹, I. Ravinovich ¹⁸⁰, J.H. Rawling ¹⁰¹, M. Raymond ³⁶, A.L. Read ¹³⁴, N.P. Readioff ⁵⁸, M. Reale ^{68a,68b}, D.M. Rebuffi ^{71a,71b}, A. Redelbach ¹⁷⁷, G. Redlinger ²⁹, K. Reeves ⁴³, L. Rehnisch ¹⁹, J. Reichert ¹³⁷, D. Reikher ¹⁶¹, A. Reiss ¹⁰⁰, A. Rej ¹⁵¹, C. Rembser ³⁶, A. Renardi ⁴⁶, M. Renda ^{27b}, M. Rescigno ^{73a}, S. Resconi ^{69a}, E.D. Resseguie ¹⁸, S. Rettie ⁹⁵, B. Reynolds ¹²⁷, E. Reynolds ²¹, O.L. Rezanova ^{122b,122a}, P. Reznicek ¹⁴³, E. Ricci ^{76a,76b}, R. Richter ¹¹⁵, S. Richter ⁴⁶, E. Richter-Was ^{84b}, O. Ricken ²⁴, M. Ridel ¹³⁶, P. Rieck ¹¹⁵, O. Rifki ⁴⁶, M. Rijssenbeek ¹⁵⁵, A. Rimoldi ^{71a,71b}, M. Rimoldi ⁴⁶, L. Rinaldi ^{23b}, G. Ripellino ¹⁵⁴, I. Riu ¹⁴, J.C. Rivera Vergara ¹⁷⁶, F. Rizatdinova ¹³⁰, E. Rizvi ⁹³, C. Rizzi ³⁶, R.T. Roberts ¹⁰¹, S.H. Robertson ^{104,ad}, M. Robin ⁴⁶, D. Robinson ³², C.M. Robles Gajardo ^{147d}, M. Robles Manzano ¹⁰⁰, A. Robson ⁵⁷, A. Rocchi ^{74a,74b}, E. Rocco ¹⁰⁰, C. Roda ^{72a,72b}, S. Rodriguez Bosca ¹⁷⁴, A. Rodriguez Perez ¹⁴, D. Rodriguez Rodriguez ¹⁷⁴, A.M. Rodríguez Vera ^{168b}, S. Roe ³⁶, O. Röhne ¹³⁴, R. Röhrig ¹¹⁵, R.A. Rojas ^{147d}, B. Roland ⁵², C.P.A. Roland ⁶⁶, J. Roloff ²⁹, A. Romaniouk ¹¹², M. Romano ^{23b,23a}, N. Rompotis ⁹¹, M. Ronzani ¹²⁵, L. Roos ¹³⁶, S. Rosati ^{73a}, G. Rosin ¹⁰³, B.J. Rosser ¹³⁷, E. Rossi ⁴⁶, E. Rossi ^{75a,75b}, E. Rossi ^{70a,70b}, L.P. Rossi ^{55b}, L. Rossini ^{69a,69b}, R. Rosten ¹⁴, M. Rotaru ^{27b}, J. Rothberg ¹⁴⁸, B. Rottler ⁵², D. Rousseau ⁶⁵, G. Rovelli ^{71a,71b}, A. Roy ¹¹, D. Roy ^{33e}, A. Rozanov ¹⁰², Y. Rozen ¹⁶⁰, X. Ruan ^{33e}, F. Rühr ⁵², A. Ruiz-Martinez ¹⁷⁴, A. Rummler ³⁶, Z. Rurikova ⁵², N.A. Rusakovich ⁸⁰, H.L. Russell ¹⁰⁴, L. Rustige ^{38,47}, J.P. Rutherford ⁷, E.M. Rüttinger ¹⁴⁹, M. Rybar ³⁹, G. Rybkin ⁶⁵, E.B. Rye ¹³⁴, A. Ryzhov ¹²³, J.A. Sabater Iglesias ⁴⁶, P. Sabatini ⁵³, G. Sabato ¹²⁰, S. Sacerdoti ⁶⁵, H.F.-W. Sadrozinski ¹⁴⁶, R. Sadykov ⁸⁰, F. Safai Tehrani ^{73a}, B. Safarzadeh Samani ¹⁵⁶, M. Safdari ¹⁵³, P. Saha ¹²¹, S. Saha ¹⁰⁴, M. Sahinsoy ^{61a}, A. Sahu ¹⁸², M. Saimpert ⁴⁶, M. Saito ¹⁶³, T. Saito ¹⁶³, H. Sakamoto ¹⁶³, D. Salamani ⁵⁴, G. Salamanna ^{75a,75b}, J.E. Salazar Loyola ^{147d}, A. Salnikov ¹⁵³, J. Salt ¹⁷⁴, D. Salvatore ^{41b,41a}, F. Salvatore ¹⁵⁶, A. Salvucci ^{63a,63b,63c}, A. Salzburger ³⁶, J. Samarati ³⁶, D. Sammel ⁵², D. Sampsonidis ¹⁶², D. Sampsonidou ¹⁶², J. Sánchez ¹⁷⁴, A. Sanchez Pineda ^{67a,36,67c}, H. Sandaker ¹³⁴, C.O. Sander ⁴⁶, I.G. Sanderswood ⁹⁰, M. Sandhoff ¹⁸², C. Sandoval ^{22a}, D.P.C. Sankey ¹⁴⁴, M. Sannino ^{55b,55a}, Y. Sano ¹¹⁷, A. Sansoni ⁵¹, C. Santoni ³⁸, H. Santos ^{140a,140b}, S.N. Santpur ¹⁸, A. Santra ¹⁷⁴, A. Saprionov ⁸⁰, J.G. Saraiva ^{140a,140d}, O. Sasaki ⁸², K. Sato ¹⁶⁹, F. Sauerburger ⁵², E. Sauvan ⁵, P. Savard ^{167,ao}, R. Sawada ¹⁶³, C. Sawyer ¹⁴⁴, L. Sawyer ^{96,ah}, C. Sbarra ^{23b}, A. Sbrizzi ^{23a}, T. Scanlon ⁹⁵, J. Schaarschmidt ¹⁴⁸, P. Schacht ¹¹⁵, B.M. Schachtner ¹¹⁴, D. Schaefer ³⁷, L. Schaefer ¹³⁷, J. Schaeffer ¹⁰⁰, S. Schaepe ³⁶, U. Schäfer ¹⁰⁰, A.C. Schaffer ⁶⁵, D. Schaile ¹¹⁴, R.D. Schamberger ¹⁵⁵, N. Scharmberg ¹⁰¹, V.A. Schegelsky ¹³⁸, D. Scheirich ¹⁴³, F. Schenck ¹⁹, M. Schernau ¹⁷¹, C. Schiavi ^{55b,55a}, L.K. Schildgen ²⁴, Z.M. Schillaci ²⁶, E.J. Schioppa ³⁶, M. Schioppa ^{41b,41a}, K.E. Schleicher ⁵², S. Schlenker ³⁶, K.R. Schmidt-Sommerfeld ¹¹⁵, K. Schmieden ³⁶, C. Schmitt ¹⁰⁰, S. Schmitt ⁴⁶, S. Schmitz ¹⁰⁰, J.C. Schmoeckel ⁴⁶, L. Schoeffel ¹⁴⁵,

A. Schoening^{61b}, P.G. Scholer⁵², E. Schopf¹³⁵, M. Schott¹⁰⁰, J.F.P. Schouwenberg¹¹⁹, J. Schovancova³⁶,
 S. Schramm⁵⁴, F. Schroeder¹⁸², A. Schulte¹⁰⁰, H-C. Schultz-Coulon^{61a}, M. Schumacher^{52,aq},
 B.A. Schumm¹⁴⁶, Ph. Schune¹⁴⁵, A. Schwartzman¹⁵³, T.A. Schwarz¹⁰⁶, Ph. Schwemling¹⁴⁵,
 R. Schwienhorst¹⁰⁷, A. Sciandra¹⁴⁶, G. Sciolla²⁶, M. Scodreggio⁴⁶, M. Scornajenghi^{41b,41a}, F. Scuri^{72a},
 F. Scutti¹⁰⁵, L.M. Scyboz¹¹⁵, C.D. Sebastiani^{73a,73b}, P. Seema¹⁹, S.C. Seidel¹¹⁸, A. Seiden¹⁴⁶,
 B.D. Seidlitz²⁹, T. Seiss³⁷, J.M. Seixas^{81b}, G. Sekhniaidze^{70a}, S.J. Sekula⁴², N. Semprini-Cesari^{23b,23a},
 S. Sen⁴⁹, C. Serfon⁷⁷, L. Serin⁶⁵, L. Serkin^{67a,67b}, M. Sessa^{60a}, H. Severini¹²⁹, S. Sevova¹⁵³, T. Šfligoj⁹²,
 F. Sforza^{55b,55a}, A. Sfyrla⁵⁴, E. Shabalina⁵³, J.D. Shahinian¹⁴⁶, N.W. Shaikh^{45a,45b}, D. Shaked Renous¹⁸⁰,
 L.Y. Shan^{15a}, M. Shapiro¹⁸, A. Sharma¹³⁵, A.S. Sharma¹, P.B. Shatalov¹²⁴, K. Shaw¹⁵⁶, S.M. Shaw¹⁰¹,
 M. Shehade¹⁸⁰, Y. Shen¹²⁹, A.D. Sherman²⁵, P. Sherwood⁹⁵, L. Shi¹⁵⁸, S. Shimizu⁸², C.O. Shimmin¹⁸³,
 Y. Shimogama¹⁷⁹, M. Shimojima¹¹⁶, I.P.J. Shipsey¹³⁵, S. Shirabe¹⁶⁵, M. Shiyakova^{80,ab}, J. Shlomi¹⁸⁰,
 A. Shmeleva¹¹¹, M.J. Shochet³⁷, J. Shojaii¹⁰⁵, D.R. Shope¹²⁹, S. Shrestha¹²⁷, E.M. Shrif^{33e}, E. Shulga¹⁸⁰,
 P. Sicho¹⁴¹, A.M. Sickles¹⁷³, P.E. Sidebo¹⁵⁴, E. Sideras Haddad^{33e}, O. Sidiropoulou³⁶, A. Sidoti^{23b,23a},
 F. Siegert⁴⁸, Dj. Sijacki¹⁶, M.Jr. Silva¹⁸¹, M.V. Silva Oliveira^{81a}, S.B. Silverstein^{45a}, S. Simion⁶⁵,
 R. Simoniello¹⁰⁰, S. Simsek^{12b}, P. Sinervo¹⁶⁷, V. Sinetckii¹¹³, S. Singh¹⁵², M. Sioli^{23b,23a}, I. Siral¹³²,
 S.Yu. Sivoklokov¹¹³, J. Sjölin^{45a,45b}, E. Skorda⁹⁷, P. Skubic¹²⁹, M. Slawinska⁸⁵, K. Sliwa¹⁷⁰, R. Slovak¹⁴³,
 V. Smakhtin¹⁸⁰, B.H. Smart¹⁴⁴, J. Smiesko^{28b}, N. Smirnov¹¹², S.Yu. Smirnov¹¹², Y. Smirnov¹¹²,
 L.N. Smirnova^{113,t}, O. Smirnova⁹⁷, J.W. Smith⁵³, M. Smizanska⁹⁰, K. Smolek¹⁴², A. Smykiewicz⁸⁵,
 A.A. Snesev¹¹¹, H.L. Snoek¹²⁰, I.M. Snyder¹³², S. Snyder²⁹, R. Sobie^{176,ad}, A. Soffer¹⁶¹, A. Søgaard⁵⁰,
 F. Sohns⁵³, C.A. Solans Sanchez³⁶, E.Yu. Soldatov¹¹², U. Soldevila¹⁷⁴, A.A. Solodkov¹²³, A. Soloshenko⁸⁰,
 O.V. Solovyanov¹²³, V. Solovyev¹³⁸, P. Sommer¹⁴⁹, H. Son¹⁷⁰, W. Song¹⁴⁴, W.Y. Song^{168b}, A. Sopczak¹⁴²,
 A.L. Soppio⁹⁵, F. Sopkova^{28b}, C.L. Sotiropoulou^{72a,72b}, S. Sottocornola^{71a,71b}, R. Soualah^{67a,67c,f},
 A.M. Soukharev^{122b,122a}, D. South⁴⁶, S. Spagnolo^{68a,68b}, M. Spalla¹¹⁵, M. Spangenberg¹⁷⁸, F. Spanò⁹⁴,
 D. Sperlich⁵², T.M. Spieker^{61a}, G. Spigo³⁶, M. Spina¹⁵⁶, D.P. Spiteri⁵⁷, M. Spousta¹⁴³, A. Stabile^{69a,69b},
 B.L. Stamas¹²¹, R. Stamen^{61a}, M. Stamenkovic¹²⁰, E. Stanecka⁸⁵, B. Stanislaus¹³⁵, M.M. Stanitzki⁴⁶,
 M. Stankaityte¹³⁵, B. Stapf¹²⁰, E.A. Starchenko¹²³, G.H. Stark¹⁴⁶, J. Stark⁵⁸, P. Staroba¹⁴¹,
 P. Starovoitov^{61a}, S. Stärz¹⁰⁴, R. Staszewski⁸⁵, G. Stavropoulos⁴⁴, M. Stegler⁴⁶, P. Steinberg²⁹,
 A.L. Steinhebel¹³², B. Stelzer¹⁵², H.J. Stelzer¹³⁹, O. Stelzer-Chilton^{168a}, H. Stenzel⁵⁶, T.J. Stevenson¹⁵⁶,
 G.A. Stewart³⁶, M.C. Stockton³⁶, G. Stoicea^{27b}, M. Stolarski^{140a}, S. Stonjek¹¹⁵, A. Straessner⁴⁸,
 J. Strandberg¹⁵⁴, S. Strandberg^{45a,45b}, M. Strauss¹²⁹, P. Strizenec^{28b}, R. Ströhmer¹⁷⁷, D.M. Strom¹³²,
 R. Stroynowski⁴², A. Strubig⁵⁰, S.A. Stucci²⁹, B. Stugu¹⁷, J. Stupak¹²⁹, N.A. Styles⁴⁶, D. Su¹⁵³, W. Su^{60c},
 S. Suchek^{61a}, V.V. Sulin¹¹¹, M.J. Sullivan⁹¹, D.M.S. Sultan⁵⁴, S. Sultansoy^{4c}, T. Sumida⁸⁶, S. Sun¹⁰⁶,
 X. Sun¹⁰¹, K. Suruliz¹⁵⁶, C.J.E. Suster¹⁵⁷, M.R. Sutton¹⁵⁶, S. Suzuki⁸², M. Svatos¹⁴¹, M. Swiatlowski³⁷,
 S.P. Swift², T. Swirski¹⁷⁷, A. Sydorenko¹⁰⁰, I. Sykora^{28a}, M. Sykora¹⁴³, T. Sykora¹⁴³, D. Ta¹⁰⁰,
 K. Tackmann^{46,z}, J. Taenzer¹⁶¹, A. Taffard¹⁷¹, R. Tafirout^{168a}, R. Takashima⁸⁷, K. Takeda⁸³,
 T. Takeshita¹⁵⁰, E.P. Takeva⁵⁰, Y. Takubo⁸², M. Talby¹⁰², A.A. Talyshev^{122b,122a}, N.M. Tamir¹⁶¹,
 J. Tanaka¹⁶³, M. Tanaka¹⁶⁵, R. Tanaka⁶⁵, S. Tapia Araya¹⁷³, S. Tapprogge¹⁰⁰,
 A. Tarek Abouelfadl Mohamed¹³⁶, S. Tarem¹⁶⁰, K. Tariq^{60b}, G. Tarna^{27b,c}, G.F. Tartarelli^{69a}, P. Tas¹⁴³,
 M. Tasevsky¹⁴¹, T. Tashiro⁸⁶, E. Tassi^{41b,41a}, A. Tavares Delgado^{140a}, Y. Tayalati^{35e}, A.J. Taylor⁵⁰,
 G.N. Taylor¹⁰⁵, W. Taylor^{168b}, A.S. Tee⁹⁰, R. Teixeira De Lima¹⁵³, P. Teixeira-Dias⁹⁴, H. Ten Kate³⁶,
 J.J. Teoh¹²⁰, S. Terada⁸², K. Terashi¹⁶³, J. Terron⁹⁹, S. Terzo¹⁴, M. Testa⁵¹, R.J. Teuscher^{167,ad},
 S.J. Thais¹⁸³, T. Theveneaux-Pelzer⁴⁶, F. Thiele⁴⁰, D.W. Thomas⁹⁴, J.O. Thomas⁴², J.P. Thomas²¹,
 P.D. Thompson²¹, L.A. Thomsen¹⁸³, E. Thomson¹³⁷, E.J. Thorpe⁹³, R.E. Ticse Torres⁵³,
 V.O. Tikhomirov^{111,qj}, Yu.A. Tikhonov^{122b,122a}, S. Timoshenko¹¹², P. Tipton¹⁸³, S. Tisserant¹⁰²,
 K. Todome^{23b,23a}, S. Todorova-Nova¹⁴³, S. Todt⁴⁸, J. Tojo⁸⁸, S. Tokár^{28a}, K. Tokushuku⁸², E. Tolley¹²⁷,
 K.G. Tomiwa^{33e}, M. Tomoto¹¹⁷, L. Tompkins^{153,p}, B. Tong⁵⁹, P. Tornambe¹⁰³, E. Torrence¹³², H. Torres⁴⁸,
 E. Torró Pastor¹⁴⁸, C. Toscirci¹³⁵, J. Toth^{102,ac}, D.R. Tovey¹⁴⁹, A. Traet¹⁷, C.J. Treado¹²⁵, T. Trefzger¹⁷⁷,
 F. Tresoldi¹⁵⁶, A. Tricoli²⁹, I.M. Trigger^{168a}, S. Trincaz-Duvold¹³⁶, D.T. Trischuk¹⁷⁵, W. Trischuk¹⁶⁷,
 B. Trocmé⁵⁸, A. Trofymov¹⁴⁵, C. Troncon^{69a}, F. Trovato¹⁵⁶, L. Truong^{33c}, M. Trzebinski⁸⁵, A. Trzupek⁸⁵,
 F. Tsai⁴⁶, J.C-L. Tseng¹³⁵, P.V. Tsiarehka^{108,ag}, A. Tsirigotis^{162,w}, V. Tsiskaridze¹⁵⁵, E.G. Tskhadadze^{159a},
 M. Tsopoulou¹⁶², I.I. Tsukerman¹²⁴, V. Tsulaia¹⁸, S. Tsuno⁸², D. Tsybychev¹⁵⁵, Y. Tu^{63b}, A. Tudorache^{27b},
 V. Tudorache^{27b}, T.T. Tulbure^{27a}, A.N. Tuna⁵⁹, S. Turchikhin⁸⁰, D. Turgeman¹⁸⁰, I. Turk Cakir^{4b,u},
 R.J. Turner²¹, R.T. Turra^{69a}, P.M. Tuts³⁹, S. Tzamarias¹⁶², E. Tzovara¹⁰⁰, G. Ucchielli⁴⁷, K. Uchida¹⁶³,

F. Ukegawa¹⁶⁹, G. Unal³⁶, A. Undrus²⁹, G. Unel¹⁷¹, F.C. Ungaro¹⁰⁵, Y. Unno⁸², K. Uno¹⁶³, J. Urban^{28b}, P. Urquijo¹⁰⁵, G. Usai⁸, Z. Uysal^{12d}, V. Vacek¹⁴², B. Vachon¹⁰⁴, K.O.H. Vadla¹³⁴, A. Vaidya⁹⁵, C. Valderanis¹¹⁴, E. Valdes Santurio^{45a,45b}, M. Valente⁵⁴, S. Valentinetti^{23b,23a}, A. Valero¹⁷⁴, L. Valéry⁴⁶, R.A. Vallance²¹, A. Vallier³⁶, J.A. Valls Ferrer¹⁷⁴, T.R. Van Daalen¹⁴, P. Van Gemmeren⁶, I. Van Vulpen¹²⁰, M. Vanadia^{74a,74b}, W. Vandelli³⁶, M. Vandenbroucke¹⁴⁵, E.R. Vandewall¹³⁰, A. Vaniachine¹⁶⁶, D. Vannicola^{73a,73b}, R. Vari^{73a}, E.W. Varnes⁷, C. Varni^{55b,55a}, T. Varol¹⁵⁸, D. Varouchas⁶⁵, K.E. Varvell¹⁵⁷, M.E. Vasile^{27b}, G.A. Vasquez¹⁷⁶, F. Vazeille³⁸, D. Vazquez Furelos¹⁴, T. Vazquez Schroeder³⁶, J. Veatch⁵³, V. Vecchio^{75a,75b}, M.J. Veen¹²⁰, L.M. Veloce¹⁶⁷, F. Veloso^{140a,140c}, S. Veneziano^{73a}, A. Ventura^{68a,68b}, N. Venturi³⁶, A. Verbitskyi¹¹⁵, V. Vercesi^{71a}, M. Verducci^{72a,72b}, C.M. Vergel Infante⁷⁹, C. Vergis²⁴, W. Verkerke¹²⁰, A.T. Vermeulen¹²⁰, J.C. Vermeulen¹²⁰, M.C. Vetterli^{152,ao}, N. Viaux Maira^{147d}, M. Vicente Barreto Pinto⁵⁴, T. Vickey¹⁴⁹, O.E. Vickey Boeriu¹⁴⁹, G.H.A. Viehhauser¹³⁵, L. Vigani^{61b}, M. Villa^{23b,23a}, M. Villaplana Perez³, E. Vilucchi⁵¹, M.G. Vincter³⁴, G.S. Virdee²¹, A. Vishwakarma⁴⁶, C. Vittori^{23b,23a}, I. Vivarelli¹⁵⁶, M. Vogel¹⁸², P. Vokac¹⁴², S.E. von Buddenbrock^{33e}, E. Von Toerne²⁴, V. Vorobel¹⁴³, K. Vorobev¹¹², M. Vos¹⁷⁴, J.H. Vosseveld⁹¹, M. Vozak¹⁰¹, N. Vranjes¹⁶, M. Vranjes Milosavljevic¹⁶, V. Vrba¹⁴², M. Vreeswijk¹²⁰, R. Vuillermet³⁶, I. Vukotic³⁷, P. Wagner²⁴, W. Wagner¹⁸², J. Wagner-Kuhr¹¹⁴, S. Wahdan¹⁸², H. Wahlberg⁸⁹, V.M. Walbrecht¹¹⁵, J. Walder⁹⁰, R. Walker¹¹⁴, S.D. Walker⁹⁴, W. Walkowiak¹⁵¹, V. Wallangen^{45a,45b}, A.M. Wang⁵⁹, A.Z. Wang¹⁸¹, C. Wang^{60c}, F. Wang¹⁸¹, H. Wang¹⁸, H. Wang³, J. Wang^{63a}, J. Wang^{61b}, P. Wang⁴², Q. Wang¹²⁹, R.-J. Wang¹⁰⁰, R. Wang^{60a}, R. Wang⁶, S.M. Wang¹⁵⁸, W.T. Wang^{60a}, W. Wang^{15c}, W.X. Wang^{60a}, Y. Wang^{60a}, Z. Wang^{60c}, C. Wanotayaraj⁴⁶, A. Warburton¹⁰⁴, C.P. Ward³², D.R. Wardrope⁹⁵, N. Warrack⁵⁷, A. Washbrook⁵⁰, A.T. Watson²¹, M.F. Watson²¹, G. Watts¹⁴⁸, B.M. Waugh⁹⁵, A.F. Webb¹¹, S. Webb¹⁰⁰, C. Weber¹⁸³, M.S. Weber²⁰, S.A. Weber³⁴, S.M. Weber^{61a}, A.R. Weidberg¹³⁵, J. Weingarten⁴⁷, M. Weirich¹⁰⁰, C. Weiser⁵², P.S. Wells³⁶, T. Wenaus²⁹, T. Wengler³⁶, S. Wenig³⁶, N. Wermes²⁴, M.D. Werner⁷⁹, M. Wessels^{61a}, T.D. Weston²⁰, K. Whalen¹³², N.L. Whallon¹⁴⁸, A.M. Wharton⁹⁰, A.S. White¹⁰⁶, A. White⁸, M.J. White¹, D. Whiteson¹⁷¹, B.W. Whitmore⁹⁰, W. Wiedenmann¹⁸¹, C. Wiel⁴⁸, M. Wielers¹⁴⁴, N. Wieseotte¹⁰⁰, C. Wiglesworth⁴⁰, L.A.M. Wiik-Fuchs⁵², H.G. Wilkens³⁶, L.J. Wilkins⁹⁴, H.H. Williams¹³⁷, S. Williams³², C. Willis¹⁰⁷, S. Willocq¹⁰³, I. Wingerter-Seez⁵, E. Winkels¹⁵⁶, F. Winklmeier¹³², O.J. Winston¹⁵⁶, B.T. Winter⁵², M. Wittgen¹⁵³, M. Wobisch⁹⁶, A. Wolf¹⁰⁰, T.M.H. Wolf¹²⁰, R. Wolff¹⁰², R. Wölker¹³⁵, J. Wollrath⁵², M.W. Wolter⁸⁵, H. Wolters^{140a,140c}, V.W.S. Wong¹⁷⁵, N.L. Woods¹⁴⁶, S.D. Worm⁴⁶, B.K. Wosiek⁸⁵, K.W. Woźniak⁸⁵, K. Wraight⁵⁷, S.L. Wu¹⁸¹, X. Wu⁵⁴, Y. Wu^{60a}, T.R. Wyatt¹⁰¹, B.M. Wynne⁵⁰, S. Xella⁴⁰, Z. Xi¹⁰⁶, L. Xia¹⁷⁸, X. Xiao¹⁰⁶, I. Xiotidis¹⁵⁶, D. Xu^{15a}, H. Xu^{60a}, H. Xu^{60a}, L. Xu²⁹, T. Xu¹⁴⁵, W. Xu¹⁰⁶, Z. Xu^{60b}, Z. Xu¹⁵³, B. Yabsley¹⁵⁷, S. Yacoub^{33a}, K. Yajima¹³³, D.P. Yallup⁹⁵, N. Yamaguchi⁸⁸, Y. Yamaguchi¹⁶⁵, A. Yamamoto⁸², M. Yamatani¹⁶³, T. Yamazaki¹⁶³, Y. Yamazaki⁸³, Z. Yan²⁵, H.J. Yang^{60c,60d}, H.T. Yang¹⁸, S. Yang^{60a}, T. Yang^{63c}, X. Yang^{60b,58}, Y. Yang¹⁶³, W.-M. Yao¹⁸, Y.C. Yap⁴⁶, Y. Yasu⁸², E. Yatsenko^{60c,60d}, H. Ye^{15c}, J. Ye⁴², S. Ye²⁹, I. Yeletsikh⁸⁰, M.R. Yexley⁹⁰, E. Yigitbasi²⁵, K. Yorita¹⁷⁹, K. Yoshihara¹³⁷, C.J.S. Young³⁶, C. Young¹⁵³, J. Yu⁷⁹, R. Yuan^{60b,h}, X. Yue^{61a}, M. Zaazoua^{35e}, B. Zabinski⁸⁵, G. Zacharis¹⁰, E. Zaffaroni⁵⁴, J. Zahreddine¹³⁶, A.M. Zaitsev^{123,ai}, T. Zakareishvili^{159b}, N. Zakharchuk³⁴, S. Zambito⁵⁹, D. Zanzi³⁶, D.R. Zaripovas⁵⁷, S.V. Zeiřner⁴⁷, C. Zeitnitz¹⁸², G. Zemaityte¹³⁵, J.C. Zeng¹⁷³, O. Zenin¹²³, T. Ženiř^{28a}, D. Zerwas⁶⁵, M. Zgubič¹³⁵, B. Zhang^{15c}, D.F. Zhang^{15b}, G. Zhang^{15b}, H. Zhang^{15c}, J. Zhang⁶, L. Zhang^{15c}, L. Zhang^{60a}, M. Zhang¹⁷³, R. Zhang¹⁸¹, S. Zhang¹⁰⁶, X. Zhang^{60b}, Y. Zhang^{15a,15d}, Z. Zhang^{63a}, Z. Zhang⁶⁵, P. Zhao⁴⁹, Z. Zhao^{60a}, A. Zhemchugov⁸⁰, Z. Zheng¹⁰⁶, D. Zhong¹⁷³, B. Zhou¹⁰⁶, C. Zhou¹⁸¹, M.S. Zhou^{15a,15d}, M. Zhou¹⁵⁵, N. Zhou^{60c}, Y. Zhou⁷, C.G. Zhu^{60b}, C. Zhu^{15a,15d}, H.L. Zhu^{60a}, H. Zhu^{15a}, J. Zhu¹⁰⁶, Y. Zhu^{60a}, X. Zhuang^{15a}, K. Zhukov¹¹¹, V. Zhulanov^{122b,122a}, D. Ziemska⁶⁶, N.I. Zimine⁸⁰, S. Zimmermann⁵², Z. Zinonos¹¹⁵, M. Ziolkowski¹⁵¹, L. Živković¹⁶, G. Zobernig¹⁸¹, A. Zoccoli^{23b,23a}, K. Zoch⁵³, T.G. Zorbas¹⁴⁹, R. Zou³⁷, L. Zwalinski³⁶

¹ Department of Physics, University of Adelaide, Adelaide; Australia

² Physics Department, SUNY Albany, Albany NY; United States of America

³ Department of Physics, University of Alberta, Edmonton AB; Canada

⁴ (a) Department of Physics, Ankara University, Ankara; (b) Istanbul Aydin University, Istanbul; (c) Division of Physics, TOBB University of Economics and Technology, Ankara; Turkey

⁵ LAPP, Université Grenoble Alpes, Université Savoie Mont Blanc, CNRS/IN2P3, Annecy; France

⁶ High Energy Physics Division, Argonne National Laboratory, Argonne IL; United States of America

⁷ Department of Physics, University of Arizona, Tucson AZ; United States of America

⁸ Department of Physics, University of Texas at Arlington, Arlington TX; United States of America

- ⁹ Physics Department, National and Kapodistrian University of Athens, Athens; Greece
- ¹⁰ Physics Department, National Technical University of Athens, Zografou; Greece
- ¹¹ Department of Physics, University of Texas at Austin, Austin TX; United States of America
- ¹² (a) Bahcesehir University, Faculty of Engineering and Natural Sciences, Istanbul; (b) Istanbul Bilgi University, Faculty of Engineering and Natural Sciences, Istanbul; (c) Department of Physics, Bogazici University, Istanbul; (d) Department of Physics Engineering, Gaziantep University, Gaziantep; Turkey
- ¹³ Institute of Physics, Azerbaijan Academy of Sciences, Baku; Azerbaijan
- ¹⁴ Institut de Física d'Altes Energies (IFAE), Barcelona Institute of Science and Technology, Barcelona; Spain
- ¹⁵ (a) Institute of High Energy Physics, Chinese Academy of Sciences, Beijing; (b) Physics Department, Tsinghua University, Beijing; (c) Department of Physics, Nanjing University, Nanjing; (d) University of Chinese Academy of Science (UCAS), Beijing; China
- ¹⁶ Institute of Physics, University of Belgrade, Belgrade; Serbia
- ¹⁷ Department for Physics and Technology, University of Bergen, Bergen; Norway
- ¹⁸ Physics Division, Lawrence Berkeley National Laboratory and University of California, Berkeley CA; United States of America
- ¹⁹ Institut für Physik, Humboldt Universität zu Berlin, Berlin; Germany
- ²⁰ Albert Einstein Center for Fundamental Physics and Laboratory for High Energy Physics, University of Bern, Bern; Switzerland
- ²¹ School of Physics and Astronomy, University of Birmingham, Birmingham; United Kingdom
- ²² (a) Facultad de Ciencias y Centro de Investigaciones, Universidad Antonio Nariño, Bogotá; (b) Departamento de Física, Universidad Nacional de Colombia, Bogotá; Colombia
- ²³ (a) INFN Bologna and Università di Bologna, Dipartimento di Fisica; (b) INFN Sezione di Bologna; Italy
- ²⁴ Physikalisches Institut, Universität Bonn, Bonn; Germany
- ²⁵ Department of Physics, Boston University, Boston MA; United States of America
- ²⁶ Department of Physics, Brandeis University, Waltham MA; United States of America
- ²⁷ (a) Transilvania University of Brasov, Brasov; (b) Horia Hulubei National Institute of Physics and Nuclear Engineering, Bucharest; (c) Department of Physics, Alexandru Ioan Cuza University of Iasi, Iasi; (d) National Institute for Research and Development of Isotopic and Molecular Technologies, Physics Department, Cluj-Napoca; (e) University Politehnica Bucharest, Bucharest; (f) West University in Timisoara, Timisoara; Romania
- ²⁸ (a) Faculty of Mathematics, Physics and Informatics, Comenius University, Bratislava; (b) Department of Subnuclear Physics, Institute of Experimental Physics of the Slovak Academy of Sciences, Kosice; Slovak Republic
- ²⁹ Physics Department, Brookhaven National Laboratory, Upton NY; United States of America
- ³⁰ Departamento de Física, Universidad de Buenos Aires, Buenos Aires; Argentina
- ³¹ California State University, CA; United States of America
- ³² Cavendish Laboratory, University of Cambridge, Cambridge; United Kingdom
- ³³ (a) Department of Physics, University of Cape Town, Cape Town; (b) iThemba Labs, Western Cape; (c) Department of Mechanical Engineering Science, University of Johannesburg, Johannesburg; (d) University of South Africa, Department of Physics, Pretoria; (e) School of Physics, University of the Witwatersrand, Johannesburg; South Africa
- ³⁴ Department of Physics, Carleton University, Ottawa ON; Canada
- ³⁵ (a) Faculté des Sciences Ain Chock, Réseau Universitaire de Physique des Hautes Energies - Université Hassan II, Casablanca; (b) Faculté des Sciences, Université Ibn-Tofail, Kénitra; (c) Faculté des Sciences Semlalia, Université Cadi Ayyad, LPHEA-Marrakech; (d) Faculté des Sciences, Université Mohamed Premier and LPTPM, Oujda; (e) Faculté des sciences, Université Mohammed V, Rabat; Morocco
- ³⁶ CERN, Geneva; Switzerland
- ³⁷ Enrico Fermi Institute, University of Chicago, Chicago IL; United States of America
- ³⁸ LPC, Université Clermont Auvergne, CNRS/IN2P3, Clermont-Ferrand; France
- ³⁹ Nevis Laboratory, Columbia University, Irvington NY; United States of America
- ⁴⁰ Niels Bohr Institute, University of Copenhagen, Copenhagen; Denmark
- ⁴¹ (a) Dipartimento di Fisica, Università della Calabria, Rende; (b) INFN Gruppo Collegato di Cosenza, Laboratori Nazionali di Frascati; Italy
- ⁴² Physics Department, Southern Methodist University, Dallas TX; United States of America
- ⁴³ Physics Department, University of Texas at Dallas, Richardson TX; United States of America
- ⁴⁴ National Centre for Scientific Research "Demokritos", Agia Paraskevi; Greece
- ⁴⁵ (a) Department of Physics, Stockholm University; (b) Oskar Klein Centre, Stockholm; Sweden
- ⁴⁶ Deutsches Elektronen-Synchrotron DESY, Hamburg and Zeuthen; Germany
- ⁴⁷ Lehrstuhl für Experimentelle Physik IV, Technische Universität Dortmund, Dortmund; Germany
- ⁴⁸ Institut für Kern- und Teilchenphysik, Technische Universität Dresden, Dresden; Germany
- ⁴⁹ Department of Physics, Duke University, Durham NC; United States of America
- ⁵⁰ SUPA - School of Physics and Astronomy, University of Edinburgh, Edinburgh; United Kingdom
- ⁵¹ INFN e Laboratori Nazionali di Frascati, Frascati; Italy
- ⁵² Physikalisches Institut, Albert-Ludwigs-Universität Freiburg, Freiburg; Germany
- ⁵³ II. Physikalisches Institut, Georg-August-Universität Göttingen, Göttingen; Germany
- ⁵⁴ Département de Physique Nucléaire et Corpusculaire, Université de Genève, Genève; Switzerland
- ⁵⁵ (a) Dipartimento di Fisica, Università di Genova, Genova; (b) INFN Sezione di Genova; Italy
- ⁵⁶ II. Physikalisches Institut, Justus-Liebig-Universität Giessen, Giessen; Germany
- ⁵⁷ SUPA - School of Physics and Astronomy, University of Glasgow, Glasgow; United Kingdom
- ⁵⁸ LPSC, Université Grenoble Alpes, CNRS/IN2P3, Grenoble INP, Grenoble; France
- ⁵⁹ Laboratory for Particle Physics and Cosmology, Harvard University, Cambridge MA; United States of America
- ⁶⁰ (a) Department of Modern Physics and State Key Laboratory of Particle Detection and Electronics, University of Science and Technology of China, Hefei; (b) Institute of Frontier and Interdisciplinary Science and Key Laboratory of Particle Physics and Particle Irradiation (MOE), Shandong University, Qingdao; (c) School of Physics and Astronomy, Shanghai Jiao Tong University, KLPPAC-MoE, SKLPPC, Shanghai; (d) Tsung-Dao Lee Institute, Shanghai; China
- ⁶¹ (a) Kirchhoff-Institut für Physik, Ruprecht-Karls-Universität Heidelberg, Heidelberg; (b) Physikalisches Institut, Ruprecht-Karls-Universität Heidelberg, Heidelberg; Germany
- ⁶² Faculty of Applied Information Science, Hiroshima Institute of Technology, Hiroshima; Japan
- ⁶³ (a) Department of Physics, Chinese University of Hong Kong, Shatin, N.T., Hong Kong; (b) Department of Physics, University of Hong Kong, Hong Kong; (c) Department of Physics and Institute for Advanced Study, Hong Kong University of Science and Technology, Clear Water Bay, Kowloon, Hong Kong; China
- ⁶⁴ Department of Physics, National Tsing Hua University, Hsinchu; Taiwan
- ⁶⁵ IJCLab, Université Paris-Saclay, CNRS/IN2P3, 91405, Orsay; France
- ⁶⁶ Department of Physics, Indiana University, Bloomington IN; United States of America
- ⁶⁷ (a) INFN Gruppo Collegato di Udine, Sezione di Trieste, Udine; (b) ICTP, Trieste; (c) Dipartimento Politecnico di Ingegneria e Architettura, Università di Udine, Udine; Italy
- ⁶⁸ (a) INFN Sezione di Lecce; (b) Dipartimento di Matematica e Fisica, Università del Salento, Lecce; Italy
- ⁶⁹ (a) INFN Sezione di Milano; (b) Dipartimento di Fisica, Università di Milano, Milano; Italy
- ⁷⁰ (a) INFN Sezione di Napoli; (b) Dipartimento di Fisica, Università di Napoli, Napoli; Italy
- ⁷¹ (a) INFN Sezione di Pavia; (b) Dipartimento di Fisica, Università di Pavia, Pavia; Italy
- ⁷² (a) INFN Sezione di Pisa; (b) Dipartimento di Fisica E. Fermi, Università di Pisa, Pisa; Italy
- ⁷³ (a) INFN Sezione di Roma; (b) Dipartimento di Fisica, Sapienza Università di Roma, Roma; Italy
- ⁷⁴ (a) INFN Sezione di Roma Tor Vergata; (b) Dipartimento di Fisica, Università di Roma Tor Vergata, Roma; Italy
- ⁷⁵ (a) INFN Sezione di Roma Tre; (b) Dipartimento di Matematica e Fisica, Università Roma Tre, Roma; Italy
- ⁷⁶ (a) INFN-TIFPA; (b) Università degli Studi di Trento, Trento; Italy
- ⁷⁷ Institut für Astro- und Teilchenphysik, Leopold-Franzens-Universität, Innsbruck; Austria

- 78 University of Iowa, Iowa City IA; United States of America
 79 Department of Physics and Astronomy, Iowa State University, Ames IA; United States of America
 80 Joint Institute for Nuclear Research, Dubna; Russia
 81 ^(a) Departamento de Engenharia Elétrica, Universidade Federal de Juiz de Fora (UFJF), Juiz de Fora; ^(b) Universidade Federal do Rio De Janeiro COPPE/EE/IF, Rio de Janeiro;
^(c) Universidade Federal de São João del Rei (UFSJ), São João del Rei; ^(d) Instituto de Física, Universidade de São Paulo, São Paulo; Brazil
 82 KEK, High Energy Accelerator Research Organization, Tsukuba; Japan
 83 Graduate School of Science, Kobe University, Kobe; Japan
 84 ^(a) AGH University of Science and Technology, Faculty of Physics and Applied Computer Science, Krakow; ^(b) Marian Smoluchowski Institute of Physics, Jagiellonian University, Krakow; Poland
 85 Institute of Nuclear Physics Polish Academy of Sciences, Krakow; Poland
 86 Faculty of Science, Kyoto University, Kyoto; Japan
 87 Kyoto University of Education, Kyoto; Japan
 88 Research Center for Advanced Particle Physics and Department of Physics, Kyushu University, Fukuoka; Japan
 89 Instituto de Física La Plata, Universidad Nacional de La Plata and CONICET, La Plata; Argentina
 90 Physics Department, Lancaster University, Lancaster; United Kingdom
 91 Oliver Lodge Laboratory, University of Liverpool, Liverpool; United Kingdom
 92 Department of Experimental Particle Physics, Jožef Stefan Institute and Department of Physics, University of Ljubljana, Ljubljana; Slovenia
 93 School of Physics and Astronomy, Queen Mary University of London, London; United Kingdom
 94 Department of Physics, Royal Holloway University of London, Egham; United Kingdom
 95 Department of Physics and Astronomy, University College London, London; United Kingdom
 96 Louisiana Tech University, Ruston LA; United States of America
 97 Fysiska institutionen, Lunds universitet, Lund; Sweden
 98 Centre de Calcul de l'Institut National de Physique Nucléaire et de Physique des Particules (IN2P3), Villeurbanne; France
 99 Departamento de Física Teórica C-15 and CIAFF, Universidad Autónoma de Madrid, Madrid; Spain
 100 Institut für Physik, Universität Mainz, Mainz; Germany
 101 School of Physics and Astronomy, University of Manchester, Manchester; United Kingdom
 102 CPPM, Aix-Marseille Université, CNRS/IN2P3, Marseille; France
 103 Department of Physics, University of Massachusetts, Amherst MA; United States of America
 104 Department of Physics, McGill University, Montreal QC; Canada
 105 School of Physics, University of Melbourne, Victoria; Australia
 106 Department of Physics, University of Michigan, Ann Arbor MI; United States of America
 107 Department of Physics and Astronomy, Michigan State University, East Lansing MI; United States of America
 108 B.I. Stepanov Institute of Physics, National Academy of Sciences of Belarus, Minsk; Belarus
 109 Research Institute for Nuclear Problems of Byelorussian State University, Minsk; Belarus
 110 Group of Particle Physics, University of Montreal, Montreal QC; Canada
 111 P.N. Lebedev Physical Institute of the Russian Academy of Sciences, Moscow; Russia
 112 National Research Nuclear University MEPhI, Moscow; Russia
 113 D.V. Skobel'syn Institute of Nuclear Physics, M.V. Lomonosov Moscow State University, Moscow; Russia
 114 Fakultät für Physik, Ludwig-Maximilians-Universität München, München; Germany
 115 Max-Planck-Institut für Physik (Werner-Heisenberg-Institut), München; Germany
 116 Nagasaki Institute of Applied Science, Nagasaki; Japan
 117 Graduate School of Science and Kobayashi-Maskawa Institute, Nagoya University, Nagoya; Japan
 118 Department of Physics and Astronomy, University of New Mexico, Albuquerque NM; United States of America
 119 Institute for Mathematics, Astrophysics and Particle Physics, Radboud University Nijmegen/Nikhef, Nijmegen; Netherlands
 120 Nikhef National Institute for Subatomic Physics and University of Amsterdam, Amsterdam; Netherlands
 121 Department of Physics, Northern Illinois University, DeKalb IL; United States of America
 122 ^(a) Budker Institute of Nuclear Physics and NSU, SB RAS, Novosibirsk; ^(b) Novosibirsk State University Novosibirsk; Russia
 123 Institute for High Energy Physics of the National Research Centre Kurchatov Institute, Protvino; Russia
 124 Institute for Theoretical and Experimental Physics named by A.I. Alikhanov of National Research Centre "Kurchatov Institute", Moscow; Russia
 125 Department of Physics, New York University, New York NY; United States of America
 126 Ochanomizu University, Otsuka, Bunkyo-ku, Tokyo; Japan
 127 Ohio State University, Columbus OH; United States of America
 128 Faculty of Science, Okayama University, Okayama; Japan
 129 Homer L. Dodge Department of Physics and Astronomy, University of Oklahoma, Norman OK; United States of America
 130 Department of Physics, Oklahoma State University, Stillwater OK; United States of America
 131 Palacký University, RCPTM, Joint Laboratory of Optics, Olomouc; Czech Republic
 132 Center for High Energy Physics, University of Oregon, Eugene OR; United States of America
 133 Graduate School of Science, Osaka University, Osaka; Japan
 134 Department of Physics, University of Oslo, Oslo; Norway
 135 Department of Physics, Oxford University, Oxford; United Kingdom
 136 LPNHE, Sorbonne Université, Université de Paris, CNRS/IN2P3, Paris; France
 137 Department of Physics, University of Pennsylvania, Philadelphia PA; United States of America
 138 Konstantinov Nuclear Physics Institute of National Research Centre "Kurchatov Institute", PNPI, St. Petersburg; Russia
 139 Department of Physics and Astronomy, University of Pittsburgh, Pittsburgh PA; United States of America
 140 ^(a) Laboratório de Instrumentação e Física Experimental de Partículas - LIP, Lisboa; ^(b) Departamento de Física, Faculdade de Ciências, Universidade de Lisboa, Lisboa; ^(c) Departamento de Física, Universidade de Coimbra, Coimbra; ^(d) Centro de Física Nuclear da Universidade de Lisboa, Lisboa; ^(e) Departamento de Física, Universidade do Minho, Braga; ^(f) Departamento de Física Teórica y del Cosmos, Universidad de Granada, Granada (Spain); ^(g) Dep Física and CEFITEC of Faculdade de Ciências e Tecnologia, Universidade Nova de Lisboa, Caparica;
^(h) Instituto Superior Técnico, Universidade de Lisboa, Lisboa; Portugal
 141 Institute of Physics of the Czech Academy of Sciences, Prague; Czech Republic
 142 Czech Technical University in Prague, Prague; Czech Republic
 143 Charles University, Faculty of Mathematics and Physics, Prague; Czech Republic
 144 Particle Physics Department, Rutherford Appleton Laboratory, Didcot; United Kingdom
 145 IRFU, CEA, Université Paris-Saclay, Gif-sur-Yvette; France
 146 Santa Cruz Institute for Particle Physics, University of California Santa Cruz, Santa Cruz CA; United States of America
 147 ^(a) Departamento de Física, Pontificia Universidad Católica de Chile, Santiago; ^(b) Universidad Andres Bello, Department of Physics, Santiago; ^(c) Instituto de Alta Investigación, Universidad de Tarapacá; ^(d) Departamento de Física, Universidad Técnica Federico Santa María, Valparaíso; Chile
 148 Department of Physics, University of Washington, Seattle WA; United States of America
 149 Department of Physics and Astronomy, University of Sheffield, Sheffield; United Kingdom
 150 Department of Physics, Shinshu University, Nagano; Japan
 151 Department Physik, Universität Siegen, Siegen; Germany

- 152 Department of Physics, Simon Fraser University, Burnaby BC; Canada
 153 SLAC National Accelerator Laboratory, Stanford CA; United States of America
 154 Physics Department, Royal Institute of Technology, Stockholm; Sweden
 155 Departments of Physics and Astronomy, Stony Brook University, Stony Brook NY; United States of America
 156 Department of Physics and Astronomy, University of Sussex, Brighton; United Kingdom
 157 School of Physics, University of Sydney, Sydney; Australia
 158 Institute of Physics, Academia Sinica, Taipei; Taiwan
 159 ^(a) E. Andronikashvili Institute of Physics, Iv. Javakishvili Tbilisi State University, Tbilisi; ^(b) High Energy Physics Institute, Tbilisi State University, Tbilisi; Georgia
 160 Department of Physics, Technion, Israel Institute of Technology, Haifa; Israel
 161 Raymond and Beverly Sackler School of Physics and Astronomy, Tel Aviv University, Tel Aviv; Israel
 162 Department of Physics, Aristotle University of Thessaloniki, Thessaloniki; Greece
 163 International Center for Elementary Particle Physics and Department of Physics, University of Tokyo, Tokyo; Japan
 164 Graduate School of Science and Technology, Tokyo Metropolitan University, Tokyo; Japan
 165 Department of Physics, Tokyo Institute of Technology, Tokyo; Japan
 166 Tomsk State University, Tomsk; Russia
 167 Department of Physics, University of Toronto, Toronto ON; Canada
 168 ^(a) TRIUMF, Vancouver BC; ^(b) Department of Physics and Astronomy, York University, Toronto ON; Canada
 169 Division of Physics and Tomonaga Center for the History of the Universe, Faculty of Pure and Applied Sciences, University of Tsukuba, Tsukuba; Japan
 170 Department of Physics and Astronomy, Tufts University, Medford MA; United States of America
 171 Department of Physics and Astronomy, University of California Irvine, Irvine CA; United States of America
 172 Department of Physics and Astronomy, University of Uppsala, Uppsala; Sweden
 173 Department of Physics, University of Illinois, Urbana IL; United States of America
 174 Instituto de Física Corpuscular (IFIC), Centro Mixto Universidad de Valencia - CSIC, Valencia; Spain
 175 Department of Physics, University of British Columbia, Vancouver BC; Canada
 176 Department of Physics and Astronomy, University of Victoria, Victoria BC; Canada
 177 Fakultät für Physik und Astronomie, Julius-Maximilians-Universität Würzburg, Würzburg; Germany
 178 Department of Physics, University of Warwick, Coventry; United Kingdom
 179 Waseda University, Tokyo; Japan
 180 Department of Particle Physics, Weizmann Institute of Science, Rehovot; Israel
 181 Department of Physics, University of Wisconsin, Madison WI; United States of America
 182 Fakultät für Mathematik und Naturwissenschaften, Fachgruppe Physik, Bergische Universität Wuppertal, Wuppertal; Germany
 183 Department of Physics, Yale University, New Haven CT; United States of America

^a Also at Borough of Manhattan Community College, City University of New York, New York NY; United States of America.

^b Also at CERN, Geneva; Switzerland.

^c Also at CPPM, Aix-Marseille Université, CNRS/IN2P3, Marseille; France.

^d Also at Département de Physique Nucléaire et Corpusculaire, Université de Genève, Genève; Switzerland.

^e Also at Departament de Física de la Universitat Autònoma de Barcelona, Barcelona; Spain.

^f Also at Department of Applied Physics and Astronomy, University of Sharjah, Sharjah; United Arab Emirates.

^g Also at Department of Financial and Management Engineering, University of the Aegean, Chios; Greece.

^h Also at Department of Physics and Astronomy, Michigan State University, East Lansing MI; United States of America.

ⁱ Also at Department of Physics and Astronomy, University of Louisville, Louisville, KY; United States of America.

^j Also at Department of Physics, Ben Gurion University of the Negev, Beer Sheva; Israel.

^k Also at Department of Physics, California State University, East Bay; United States of America.

^l Also at Department of Physics, California State University, Fresno; United States of America.

^m Also at Department of Physics, California State University, Sacramento; United States of America.

ⁿ Also at Department of Physics, King's College London, London; United Kingdom.

^o Also at Department of Physics, St. Petersburg State Polytechnical University, St. Petersburg; Russia.

^p Also at Department of Physics, Stanford University, Stanford CA; United States of America.

^q Also at Department of Physics, University of Adelaide, Adelaide; Australia.

^r Also at Department of Physics, University of Fribourg, Fribourg; Switzerland.

^s Also at Dipartimento di Matematica, Informatica e Fisica, Università di Udine, Udine; Italy.

^t Also at Faculty of Physics, M.V. Lomonosov Moscow State University, Moscow; Russia.

^u Also at Giresun University, Faculty of Engineering, Giresun; Turkey.

^v Also at Graduate School of Science, Osaka University, Osaka; Japan.

^w Also at Hellenic Open University, Patras; Greece.

^x Also at IJCLab, Université Paris-Saclay, CNRS/IN2P3, 91405, Orsay; France.

^y Also at Institutio Catalana de Recerca i Estudis Avancats, ICREA, Barcelona; Spain.

^z Also at Institut für Experimentalphysik, Universität Hamburg, Hamburg; Germany.

^{aa} Also at Institute for Mathematics, Astrophysics and Particle Physics, Radboud University Nijmegen/Nikhef, Nijmegen; Netherlands.

^{ab} Also at Institute for Nuclear Research and Nuclear Energy (INRNE) of the Bulgarian Academy of Sciences, Sofia; Bulgaria.

^{ac} Also at Institute for Particle and Nuclear Physics, Wigner Research Centre for Physics, Budapest; Hungary.

^{ad} Also at Institute of Particle Physics (IPP), Vancouver; Canada.

^{ae} Also at Institute of Physics, Azerbaijan Academy of Sciences, Baku; Azerbaijan.

^{af} Also at Instituto de Física Teórica, IFT-UAM/CSIC, Madrid; Spain.

^{ag} Also at Joint Institute for Nuclear Research, Dubna; Russia.

^{ah} Also at Louisiana Tech University, Ruston LA; United States of America.

^{ai} Also at Moscow Institute of Physics and Technology State University, Dolgoprudny; Russia.

^{aj} Also at National Research Nuclear University MEPhI, Moscow; Russia.

^{ak} Also at Physics Department, An-Najah National University, Nablus; Palestine.

^{al} Also at Physics Dept, University of South Africa, Pretoria; South Africa.

^{am} Also at Physikalisches Institut, Albert-Ludwigs-Universität Freiburg, Freiburg; Germany.

^{an} Also at The City College of New York, New York NY; United States of America.

^{ao} Also at TRIUMF, Vancouver BC; Canada.

^{ap} Also at Università di Napoli Parthenope, Napoli; Italy.

^{aq} Also Weston Visiting Professor at Department of Particle Physics, Weizmann Institute of Science; Rehovot; Israel.

* Deceased.